Engineering Persistent Interleukin-2 for Cancer Immunotherapy

by

Shuning Gai

B.S. Chemical Engineering
Stanford University, 2004

ARCHIVES
MASSACHUSETTS INSTITUTE OF TECHNOLOGY
JUL 19 2012
LIBRARIES

Submitted to the Department of Chemical Engineering
in partial fulfillment of the requirements for the degree of

Doctor of Philosophy in Chemical Engineering

at the

MASSACHUSETTS INSTITUTE OF TECHNOLOGY

June 2012

© 2012 Massachusetts Institute of Technology.
All rights reserved.

Signature of Author: .....
Department of Chemical Engineering
May 22, 2012

Certified by: .....
K. Dane Wittrup
C.P. Dubbs Professor of Chemical Engineering and Biological Engineering
Thesis Supervisor

Accepted by: .....
Patrick S. Doyle
Professor of Chemical Engineering
Chairman, Committee for Graduate Students

Engineering Persistent Interleukin-2 for Cancer Immunotherapy

by

Shuning Gai

Submitted to the Department of Chemical Engineering on May 22, 2012
in partial fulfillment of the requirements for the degree of
Doctor of Philosophy in Chemical Engineering

Abstract

Mobilizing the immune system to recognize and destroy tumor cells is a promising strategy for treating cancer. In contrast to standard therapeutic approaches such as surgery, radiation, and chemotherapy, immunotherapy offers the possibility of systemic yet tumor-specific cell killing as well as long-lasting cancer protection. A significant mode of tumor rejection is direct tumor cell killing by immune cells, such as cytotoxic T lymphocytes (CTLs) and natural killer (NK) cells. These cell types are stimulated to proliferate by the cytokine interleukin-2 (IL-2). Consequently, IL-2 has been actively pursued as an agent for immunotherapy, either alone or in combination with other therapeutic strategies.

IL-2 is characterized by rapid systemic clearance, with a fast-phase serum half-life of 13 minutes and a slow-phase half-life of 85 minutes. We hypothesized that prolonging the persistence of IL-2 at the cell surface or extending its circulation lifetime would increase its immunostimulatory potency. Therefore, we evolved murine IL-2 to bind the alpha subunit of its receptor, known as IL-2Rα or CD25, with 500-fold higher affinity; tethered IL-2 to the surface of T cells via streptavidin sandwiches; and fused IL-2 to the antibody Fc fragment, designated Fc/IL-2, which extended the slow-phase serum half-life by 15 hours.

Compared to free IL-2, Fc/IL-2 fusions induced superior control of solid tumors in mice. Interestingly, combining Fc/IL-2 with an anti-tumor antibody led to potent suppression of tumor growth during treatment. Furthermore, combination therapy protected two of three mice

from subsequent tumor re-challenge. Depletion of CTLs or NK cells completely or partially, respectively, abrogated treatment efficacy, suggesting these immune cell types contribute to the anti-tumor response. In the context of Fc fusion, increasing the affinity of IL-2 for CD25 did not further improve efficacy. Ablation of CD25 binding, however, significantly reduced efficacy and also increased treatment toxicity.

Since we employed a mutant Fc with disrupted FcγR binding, and hence reduced effector function, and fused IL-2 to mutant Fc monovalently, the significant therapeutic benefit of Fc/IL-2 over free IL-2 likely results from the extension of IL-2 circulation lifetime. We hypothesize that long-circulating IL-2 would potently synergize with other anti-tumor antibodies for effective cancer immunotherapy.

Thesis Supervisor: K. Dane Wittrup

Title: C.P. Dubbs Professor of Chemical Engineering and Biological Engineering

Acknowledgements

Many people contributed to the completion of this work, and for all of their help and support, I am incredibly grateful.

My advisor, Dane Wittrup, provided guidance throughout, and his suggestions were instrumental to the exciting result described in Chapter 4. At times of excitement and disappointment alike, I was motivated by his dedication, optimism, and enthusiasm, and I was often humbled by the intellectual leaps and connections he made that propelled the project forward. I am very grateful for the opportunity to work on this project and to train in his lab.

My thesis committee members, Arup Chakraborty and Jianzhu Chen, encouraged me to think critically about the fundamental assumptions of our approach and provided important immunological insights for interpreting results and designing experiments. Darrell Irvine and Brandon Kwong likewise contributed substantial scientific input.

Matthias Stephan and Pete Bak taught me techniques for mouse work from point zero, and, along with Eileen Higham, were responsive, knowledgeable, and dependable collaborators on several animal experiments. Vladimir Voynov kindly instructed me in using the HEK293 cell protein expression system. Jebrell Glover provided advice on insect cell protein expression.

I thoroughly enjoyed working in the Wittrup Lab and would like to thank all of its members, past and present. In particular: Bala Rao oriented me to the lab and the IL-2 project; Wai Lau, Ginger Chao, Steve Sazinsky, and Ben Hackel generously shared their wealth of expertise on protein engineering and protein production. Margie Ackerman, Mike Schmidt, Kelly Davis Orcutt, David Liu, John Rhoden, and Byron Kwan helped at many other steps along the way. Jordi Mata-Fink, Jamie Spangler, Tiffany Chen, Xiaosai Yao, Cary Opel, and Alice Tzeng readily

shared many protocols and reagents and contributed significantly to the smooth operation of the lab.

The work of the staff of the Koch Institute Swanson Biotechnology Center and animal facility significantly accelerated the rate of experimental progress. I would especially like to thank the core facilities Applied Therapeutics & Whole Animal Imaging, Biopolymers & Proteomics, Flow Cytometry, Histology, and Microscopy. Roderick Bronson, in particular, patiently examined and interpreted many histology slides.

In addition, I am grateful for the financial support of the National Science Foundation Graduate Research Fellowship Program.

During my time as a graduate student, I lived in the graduate residence Sidney-Pacific, which greatly enriched my life and recharged me for the challenges in lab. I am especially grateful to the housemasters, Roger and Dottie Mark, and Roland Tang and Annette Kim, for all of their care and attention.

Finally, my family has been a wellspring of comfort and support, and I can hardly find the words to express my gratitude. My parents overcame many obstacles to provide me with opportunities to pursue my interests, and with their steadfast confidence in me, buoyed me through this and many other endeavors. My sisters, Linda and Lisa, brought me countless causes for joy and pride. My boyfriend, Matt, motivated and sustained me through research and writing. I am so thankful to have had his company on this adventure.

To

Skip, Cammy, and Tai

Table of Contents

1. Background and Motivation

1.1. Cancer Immunotherapy

Since its proposal at the beginning of the 20th century, the concept of immunotherapy for cancer has often been the subject of skepticism, and even mockery (1, 2). However, there is now compelling evidence, from both the laboratory and the clinic, that the immune system can be mobilized to sustain a therapeutic effect against established tumors (3). Moreover, in contrast to standard therapeutic approaches such as surgery, radiation, and chemotherapy, immunotherapy offers the promise of tumor-specific cell killing systemically and the possibility of establishing long-lasting cancer protection.

A significant mode of tumor rejection is mediated by tumor-reactive T cells (4). Consequently, many strategies for boosting their anti-tumor activities are currently being explored. These strategies include active vaccination against cancer antigens; administration of stimulatory cytokines, inhibition of lymphocyte regulatory mechanisms, and adoptive transfer of tumor-reactive lymphocytes. While results from these treatments are promising, complete regression after treatment is still rare. These approaches, therefore, do not yet adequately address the full assortment of mechanisms by which tumors can escape immune destruction. Improvements and/or novel strategies are therefore necessary to fully utilize the immune system's potential to efficiently and specifically eliminate tumors.

Two factors that may contribute to tumor escape are (1) insufficient number of tumor-specific T cells and (2) inadequate function of the cells present. Indeed, several studies have shown that elevated numbers of tumor-infiltrating $CD8^+$ T lymphocytes is associated with favorable prognosis in human cancers (5-7). In addition, the efficacy of adoptive transfer treatments correlates directly with the number of tumor-reactive cells administered (8). Merely high numbers of tumor-specific lymphocytes is not sufficient, however, since tumor eradication requires effective exertion of tumoricidal activity (9, 10). Predictably, lymphocytes in progressive tumors are often functionally unresponsive (11, 12), and adoptive transfer efficacy

strongly correlates with the infused cells' anti-tumor reactivity, (e.g. antigen-specific lysis and interferon-γ secretion) (8).

The insufficient number and inadequate function of tumor-specific T cells at sites of malignancy may be due to suppressive networks orchestrated by the tumor as well as regulatory mechanisms inherent to the immune system. The tumor microenvironment engages in various tactics to limit anti-tumor immune responses, including inhibition of dendritic cell (DC) maturation, production of lymphocyte-suppressive factors, and recruitment of regulatory T (T_{reg}) cells, all of which can contribute to the inadequate numbers and functions of potentially tumor-reactive T cells (13). In addition, these T cells may be limited by the immune system's measures for ensuring self-tolerance. Specifically, many tumor antigens are expressed by normal peripheral tissues, such that the majority of potentially tumor-reactive T cells are purged from the repertoire by thymic selection. Of the cells that escape deletion, those possessing T cell receptors (TCRs) with low antigen affinity are unlikely to be effectively triggered, either by self or the tumor. Those that express TCRs with higher affinity, while potentially useful in tumor therapy, may already be rendered unresponsive (by *e.g.* antigen engagement without co-stimulation, antigen persistence, T_{reg} cells) to minimize their potential to injure self (14, 15).

In this setting, the task of improving T-cell anti-tumor reactivity is a daunting one. Nonetheless, significant inroads have been made, particularly by employing cytokines. Cytokines bind to specific receptors on target cells to trigger signal-transduction pathways, leading to altered gene expression profiles in those cells. Through this process, cytokines regulate processes such as lymphocyte homeostasis and differentiation, thereby significantly influencing the intensity and duration of the overall immune response.

1.2. Interleukin-2

One cytokine that has shown particular aptitude as a cancer immunotherapy agent is interleukin-2 (IL-2). While IL-2 participates in a variety of immunoregulatory processes, its most notable effect is the expansion of T lymphocytes after their activation by antigen. As such, in the three decades since its discovery, it has exhibited anti-tumor efficacy both as a single agent and

as a complement to other therapeutic approaches. Used alone, high-dose IL-2 injections have mediated regression of metastatic melanomas and renal cell carcinomas (16-19). Generally, 15 to 20 percent of IL-2-treated patients show an objective response (total tumor reduction by at least 50 percent), half of whom show complete and durable cancer regression. These results led to FDA approval of IL-2, in 1992, for the treatment of these diseases. IL-2 is also being used in conjunction with adoptive cell transfer therapy, which involves the expansion of highly active tumor-specific lymphocytes *ex vivo* and their subsequent transfer back into the autologous cancer hosts. In such treatments, IL-2 is used for both the *ex vivo* expansion as well as the *in vivo* persistence of the tumor-reactive cells. The adoptive transfer technique has yielded the greatest success so far, with half of the patients showing objective responses (20). Importantly, IL-2 does not directly inhibit tumor growth, so its *in vivo* impact on cancers is due to its ability to expand tumor-reactive lymphocytes.

Mature human IL-2 is a 133 amino acid protein, which folds into a four α-helical bundle and has one essential disulfide bond (21-23), as shown in Figure 1-1. IL-2 is produced primarily by $CD4^+$ T cells after TCR engagement and co-stimulation, although its expression has also been detected in $CD8^+$ T cells and thymocytes, as well as B cells and DCs (24-29).

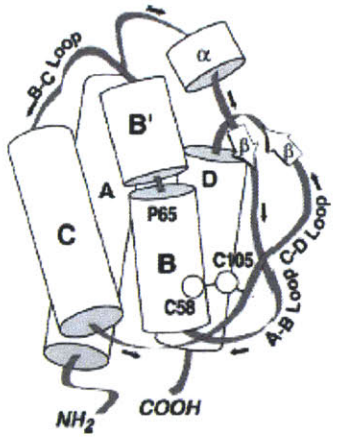

Figure 1-1: Structure of human IL-2. (30)

The effects of IL-2 are initiated through interactions with its receptors on the surface of lymphocytes. The IL-2 receptor consists of three distinct subunits, which associate in various combinations to form receptors of different affinities and signal transduction capabilities, as shown in Figure 1-2. The low-affinity IL-2 receptor, with equilibrium dissociation constant (K_d) ~ 10 nM, consists of only the α chain (IL-2Rα or CD25), a 55-kDa protein with no signaling capacity. The intermediate-affinity receptor, with K_d ~ 1 nM, consists of the 75-kDa IL-2 receptor β chain (IL-2Rβ) and the 65-kDa common γ chain (γ_c), which are together sufficient for effective signal transduction. The high-affinity receptor, with K_d ~ 10 pM, consists of all three subunits (IL-2R$\alpha\beta\gamma_c$) and also signals effectively. IL-2Rβ alone has a very low affinity for IL-2, with K_d ~ 100 nM, and γ_c alone has no detectable affinity. (31)

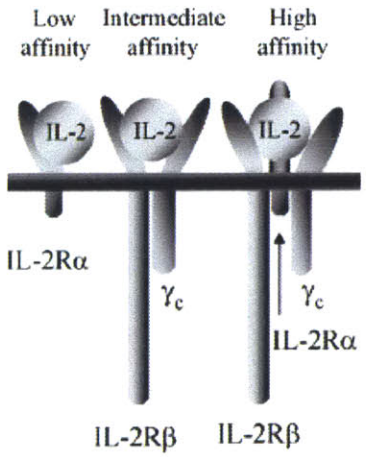

Figure 1-2: Forms of the IL-2 receptor. (32)

The form of the IL-2 receptor present at the cell surface is dictated by the expression level of each receptor subunit. The common γ chain is expressed constitutively by lymphoid cells and also serves as an integral receptor component for several other cytokines, including IL-4, IL-7, IL-9, IL-15, and IL-21 (32). IL-2Rβ is expressed at low to moderate levels on resting cells of several lymphoid subsets, notably T cells and NK cells, and its expression is further

induced upon activation (31). Similar to γ_c, IL-2Rβ is not exclusive to the IL-2 receptor, being employed also in the receptor for IL-15. IL-2Rα, by contrast, is specific for IL-2 and is expressed on mature T cells only after activation, as well as by naturally occurring T_{reg} cells constitutively (33).

The signaling events resulting from IL-2 stimulation, shown in Figure 1-3, are initiated by ligand-induced oligomerization of the receptor subunits (34, 35). In particular, the α, β, and γ_c chains recognize distinct sites on IL-2 and associate with IL-2 in a stepwise manner, with IL-2Rα binding IL-2 leading to subsequent recruitment of IL-2Rβ and γ_c (31). Following receptor subunit oligomerization, Janus kinases 1 and 3 (Jak1; Jak3) associated with the cytoplasmic tails of IL-2Rβ and γ_c, respectively, phosphorylate key tyrosine residues on IL-2Rβ and γ_c, as well as themselves. These phosphorylated tyrosines then enable docking of the adaptor molecule Shc and the transcription factors Stat3 and Stat5.

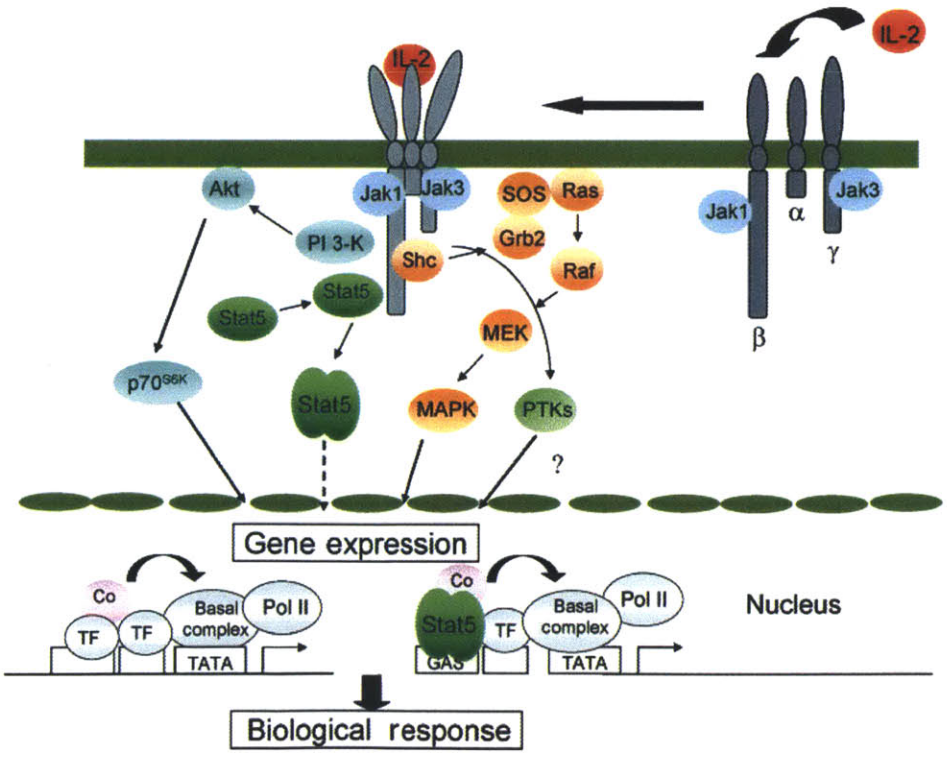

Figure 1-3: Major signal transduction pathways activated by IL-2. Abbreviations: protein tyrosine kinases (PTKs) activated by IL-2 (*e.g.* Syk, Pyk2, $p56^{lck}$, $p53/p56^{lyn}$, $p59^{fyn}$); transcription factor (TF); coactivator (Co); RNA polymerase II (Pol II); interferon-γ activated site (GAS). (32)

The recruitment of Shc to the IL-2 receptor complex links IL-2 binding to several signal transduction pathways that promote proliferation and cell survival. One is that of mitogen-activated protein kinase (MAPK), which becomes engaged via Shc recruitment of the adaptor molecule Grb2 and the nucleotide exchange factor SOS, which subsequently activates Ras. The consequences of triggering MAPK include induction of protooncogenes such *c-fos* and *c-jun*, upregulation of anti-apototic factors such as Bcl-2 and Bcl-x_L, and regulation of the proapoptotic mediator Bad. IL-2 stimulation also activates phosphatidylinositol-3-kinase (PI3K), which is implicated in proliferative and anti-apoptotic outcomes as well. For instance, PI3K regulates the transcriptional activity of E2F, which controls various genes governing cell cycle progression, and activates Akt, which also participates in the regulation of Bad. (36)

The recruitment of Stat3 and Stat5 to the IL-2 receptor complex leads to their phosphorylation, enabling their dimerization and translocation to the nucleus. There, they initiate the transcription of various target genes that affect both cellular proliferation and survival. One of the most important targets is the gene for IL-2Rα, whose expression permits the formation of the high-affinity IL-2 receptor. (36) However, as is generally the case for Jak-Stat pathways, activation of this pathway is transient and subject to negative-feedback regulation. For instance, Stat5 has also been shown to induce expression of the cytokine-signaling suppressor CIS1 and the apoptosis-mediator Fas ligand (37, 38).

The stimulation of the above processes through administration of exogenous IL-2 has been important for enhancing anti-tumor responses. However, the outcomes of systemic IL-2 administration are far from ideal. While 15 to 20 percent of patients respond objectively to high-dose IL-2, the great majority does not, and many suffer severe, life-threatening side effects, including nausea, confusion, hypotension, and septic shock (18). The severe toxicity associated with IL-2 treatment is largely attributable to the activity of natural killer (NK) cells (39). As alluded to above, NK cells express the intermediate-affinity receptor, IL-2R$\beta\gamma_c$. As such, they are stimulated at nanomolar concentrations of IL-2, which do in fact result in patient sera during high-dose of IL-2 therapy (10). Attempts to reduce serum concentration, and hence selectively stimulate IL-2R$\alpha\beta\gamma_c$-bearing cells, by reducing dose and adjusting dosing regimen have been tried. However, while less toxic, such treatments were also less efficacious (40).

One probable cause for this is the difficulty of maintaining IL-2 concentration within the therapeutic picomolar range *in vivo*. When administered as an intravenous bolus, IL-2 has an initial half-life of 12.9 minutes followed a slower-phase half-life of 85 minutes; when administered via intravenous infusion, IL-2 has a clearance rate of 120 minutes (41). A method of selectively stimulating IL-2R$\alpha\beta\gamma_c$-bearing T cells at sub-picomolar concentrations would widen the therapeutic window and reduce NK-cell-associated side effects, thereby leading, potentially, to more efficacious therapy.

The technique of adoptive cell transfer overcomes some of the challenges confronting non-selective immune stimulation methods like high-dose IL-2. In adoptive transfer, effector T cells with desired characteristics, such as avid tumor-antigen specificity, high cytokine secretion, and cytotoxicity, are specifically selected for expansion *ex vivo*. Besides selectively amplifying the desired tumor-specific cells, this approach also circumvents the *in vivo* regulatory mechanisms of the immune system and the tumor microenvironment. In addition, non-myeoblative, but lymphodepleting, chemotherapy may be applied to the patient prior to administration of the tumor-reactive cells, which has been shown to generate an environment more conducive to the functioning of the transferred cells (42). The benefit of such chemotherapy may be due to the elimination of T_{reg} cells, which may suppress effector T cells, and/or the elimination of host lymphocytes, which may compete with transferred cells for homeostatic cytokines (43).

A limitation for adoptive transfer therapy, however, has been the lack of *in vivo* persistence of transferred tumor-reactive cells, which has correlated with poor patient response (44-46). One strategy with demonstrable benefit is the use of IL-2. For instance, co-administration of high-dose IL-2 with tumor-reactive cells or transducing these cells with IL-2-encoding retroviral vectors have both been shown to prolong *in vivo* persistence (47-49). Nonetheless, the use of high-dose IL-2 still causes systemic toxicity, limiting its administration to 2 to 3 days (20). A method of improving *in vivo* persistence without severe side effects would therefore be valuable.

Besides T cell number, adoptive transfer therapy is also limited by the availability of functional tumor-reactive T cells (20). As discussed earlier, potentially tumor-reactive T cells are

often tolerized to the relevant tumor antigens. Fortunately, the phenotype of T cells can frequently be influenced by manipulating the cytokine milieu of their *in vitro* culture. IL-2 has already been shown to improve the function of transferred cells in human patients (20). In experimental murine models, the cytokine IL-15 has also shown effectiveness. Specifically, IL-15 has been demonstrated to restore function to tolerized self-specific $CD8^+$ T cells, enabling their subsequent treatment of leukemia upon adoptive transfer (50). In addition, *in vitro* stimulation of $CD8^+$ T cells with IL-15 has been shown to bias differentiation toward the central memory phenotype, which was found to be more effective than its effector memory counterpart in eradicating established murine tumors (51, 52).

The cytokine IL-15 is closely related to IL-2. Like IL-2, it is a four α-helical bundle protein and uses IL-2Rβ and γ_c for signal transduction, interacting with IL-2R$\beta\gamma_c$ through comparable affinity (53, 54). Furthermore, the IL-15 receptor complex includes an analogous private α chain (IL-15Rα), which bears structural resemblance to IL-2Rα. Thus, IL-15R forms a series of receptor complexes analogous to those of IL-2R (55). However, the affinity between IL-15 and IL-15Rα, with $K_d \sim 10$ pM, is 1000-fold higher than that between IL-2 and IL-2Rα (55). While signaling capacity has been reported for IL-15Rα, its importance is still controversial (56-58). Indeed, most evidence to date suggests that the interaction of IL-2 and IL-15 with their respective receptor complexes leads to similar, if not identical, signal transduction events (59).

In light of these similarities, the ability to restore function to tolerized T cells and to direct T cell differentiation toward the central memory phenotype should not be exclusive to IL-15. In fact, high-dose IL-2 was found to trigger proliferation of tolerant cells as well (50). Several mechanisms have been proposed to account for the disparities between IL-2 and IL-15 effects, including IL-15R$\alpha\beta\gamma_c$'s ability to present IL-15 to other cells in *trans* and IL-15's ability to recycle with IL-15Rα following endocytosis (60). However, *trans* presentation has also been reported for IL-2 (61). And, while IL-2 is rapidly degraded following receptor-mediated endocytosis, the lack of IL-2 recycling with IL-2Rα is likely due to their low-affinity interaction (62). Improving this affinity may, therefore, lead to IL-2 recycling and enable IL-2 to effectively execute the favorable T-cell functional changes shown to be achievable with IL-15. A significant advantage of this strategy over using IL-15 is the ability to retain T-cell specificity. IL-15Rα is

expressed on multiple tissues and cell types and, even more, another unrelated receptor for IL-15, designated IL-15RX, has been identified on the surface of mast cells (63, 64). As such, when *in vivo*, IL-15 may trigger undesired responses from these other cell types leading to side effects.

The challenges described above, namely, reducing IL-2 systemic toxicity, prolonging *in vivo* persistence of adoptively transferred tumor-reactive T cells, and restoring function to tolerized tumor-specific T cells, may all be addressed elegantly with IL-2 variants engineered for higher IL-2Rα binding affinity. Specifically, such molecules would selectively target IL-2R$\alpha\beta\gamma_c$-expressing cells at sub-picomolar concentrations, thereby reducing systemic toxicity derived from stimulation of IL-2R$\beta\gamma_c$-bearing NK cells. In addition, increasing IL-2's affinity for IL-2Rα may enable its recycling to the cell surface after endocytosis, thereby prolonging IL-2 signaling. This will likely enhance effects already observed for IL-2 stimulation, such as promotion of *in vivo* persistence, and also lead to T-cell functional changes induced by IL-15. Thus, such molecules may possess great therapeutic value.

1.3. Thesis Overview

In the following chapters, I describe our efforts to increase the potency of IL-2 for use in cancer immunotherapy.

We set out first to engineer mutants of murine IL-2 with high binding affinity for IL-2Rα (also known as CD25), and then characterized their effects on T-cell growth and function *in vitro* and *in vivo*. As described in Chapter 2, directed evolution by yeast surface display yielded murine IL-2 mutants with 500-fold higher affinity than wild-type. However, while a high-affinity mutant, named QQ 6.2-10, potently stimulated T-cell growth *in vitro*, we were unable to detect significant T-cell proliferation or functional advantage *in vivo*. Extending the circulation lifetime of this high-affinity mutant through Fc fusion did not improve its *in vivo* T-cell stimulatory capacity over its wild-type counterpart either. Consequently, we examined the possibility of attaching IL-2 directly to the T-cell surface. Using streptavidin to tether biotinylated IL-2 onto biotinylated T cells, we found IL-2-tethered cells to exhibit prolonged

survival *in vitro*. Importantly, modification of cell-surface primary amines did not interfere with subsequent T-cell homing to antigenic sites *in vivo*. Therefore, cell-surface tethering of IL-2 may be a viable means of increasing the persistence of IL-2 on the T-cell surface for promoting T-cell growth.

The lack of detectable *in vivo* benefit from the high-affinity CD25-binding mutant QQ 6.2-10 and a recent report suggesting that CD25 engagement actually promotes IL-2 toxicity and interferes with IL-2 efficacy (65) led us to directly examine the effect of CD25 binding affinity on the immunostimulatory capacity and systemic toxicity of IL-2. As described in Chapter 3, we first engineered non-CD25 binding IL-2 mutants by rational design, thereby completing an affinity series of IL-2 in CD25 binding, consisting also of wild-type IL-2 and high-affinity mutant QQ 6.2-10. To prolong the circulation lifetime of these cytokines, we fused each monovalently to a non-lytic mutant of antibody Fc. In wild-type C57BL/6 mice treated with a single intravenous bolus, we found the non-CD25 binding mutant, called E76G, to significantly expand the $CD8^+$ T and NK cell populations. However, disruption of CD25 binding also increased toxicity, as inferred from whole animal body weight and pulmonary wet weight after treatment.

The significant expansion of $CD8^+$ T cells and NK cells by Fc/E76G prompted us to evaluate its efficacy in controlling solid syngeneic tumors in mice. In particular, we hypothesized that the increased numbers of NK cells could be mobilized for tumor-cell killing by antibody-dependent cell-mediated cytotoxicity (ADCC). As described in Chapter 4, we first established a tolerable dosing regimen for Fc/IL-2 and its mutants in C57BL/6 mice bearing subcutaneous B16-F10 melanomas. Surprisingly, Fc/IL-2, more than Fc/E76G, synergized with the anti-tumor antibody TA99 to potently suppress tumor growth during treatment. Furthermore, combination therapy with Fc/IL-2 and TA99 protected two of three mice from subsequent tumor re-challenge. Depletion of $CD8^+$ T cells or NK cells completely or partially, respectively, abrogated treatment efficacy, suggesting these immune cell types contribute to the anti-tumor response. In the context of Fc fusion, increasing the affinity of IL-2 for CD25 did not significantly affect efficacy. Ablation of CD25 binding, by contrast, significantly reduced efficacy while also increasing treatment toxicity.

Since we employed a mutant Fc with disrupted FcγR binding, and hence reduced effector function, and fused IL-2 to mutant Fc monovalently, the significant therapeutic benefit of Fc/IL-2 over free IL-2 in combination therapy likely results from the extension of IL-2 circulation lifetime. We hypothesize that long-circulating IL-2 would potently synergize with other anti-tumor antibodies for effective cancer immunotherapy.

2. Engineering Murine IL-2 for High-Affinity Binding to CD25

2.1. Introduction

2.1.1. High-affinity CD25-binding mutants of human IL-2

Recently, Rao *et al.* generated mutants of human IL-2 with high affinity for human CD25 (66-68). These mutants were found to persist longer on the surface of Kit225 cells (an IL-2 dependent human T cell line that constitutively expresses CD25) and to stimulate their proliferation potently (66-69). Furthermore, when used to culture F15R-Kit cells (a human T cell line that expresses comparable levels of CD25 and IL-15Rα), IL-2 mutants with CD25 binding affinity approaching that of IL-15 for IL-15Rα stimulated growth responses comparably to IL-15 (60, 68).

These studies demonstrated that, *in vitro*, high-affinity CD25-binding IL-2 mutants possess superior bioactivity and can induce T-cell responses comparably to IL-15. Improving the CD25 binding affinity of IL-2 therefore seemed to be a promising strategy for improving IL-2 function and endowing it the ability to promote the favorable T-cell phenotype changes associated with IL-15. Consequently, we sought to investigate the effects of such molecules further, in the more clinically relevant setting of intact animals.

One of the most common pre-clinical animal models is the lab mouse. While the murine immune system does not mirror the human one perfectly, it is nevertheless a good experimental model and has yielded important insights into human immune functions (70). Wild-type human IL-2 stimulates the proliferation of murine T lymphocytes and is often used in experiments with murine models (71). However, the high-affinity human IL-2 mutants engineered by Rao *et al.* do not bind to murine CD25 with higher affinity (Rao and Gai, unpublished observations). In order to evaluate their effects *in vivo*, we therefore employed the approach of Rao *et al.* to affinity mature murine IL-2 for murine CD25 using yeast surface display.

2.1.2. *Protein engineering by yeast surface display*

As Rao *et al.*, we engineered murine IL-2 by directed evolution. The strategy of directed evolution circumvents our still limited understanding of the relationship between protein sequence and structure and between protein structure and function. The directed evolution process, consisting of generating a diverse collection of mutants from which to select clones of the desirable phenotype, and then screening the collection to isolate those clones possessing the desirable phenotype, can be accomplished by yeast surface display.

Yeast surface display is a protein engineering method that, since its development in 1997 (72), has been used to improve the function of many proteins (73). In yeast surface display, the protein of interest is tethered to the cell wall of *Saccharomyces cerevisiae* yeast, for facile interrogation of its phenotype by flow cytometry. The genetic information encoding that protein is maintained on plasmid inside the cell, thereby linking any favorable phenotypes to their genetic basis. (72)

The surface tethering of the protein of interest is accomplished by expressing the protein as a fusion to the yeast protein Aga2p. Aga2p is one of two subunits of the yeast protein a-agglutinin, which mediates cell-cell adhesion as a prelude to yeast cell mating. The other subunit of a-agglutinin, Aga1p, is covalently linked to β-glucans of the yeast cell wall. Upon being secreted from the yeast cell, Aga2p attaches to Aga1p via two disulfide bonds, and thereby becomes anchored to the cell surface. The protein of interest, as a fusion to Aga2p, then becomes "displayed" on the surface of yeast.

The cassette encoding Aga2p and the protein of interest is contained in the yeast display vector pCTCON2 and its expression is driven by the galactose-inducible GAL1-10 promoter. Expression of Aga1p is likewise induced by galactose, although Aga1p is encoded in the genome of the yeast display strain EBY100. Display of the protein of interest, therefore, is accomplished by transforming the display vector encoding the protein into the EBY100 strain, followed by cell growth and galactose induction.

In the surface-displayed fusion protein, the protein of interest is flanked by the epitope tags HA and c-myc. When the protein of interest is fused C-terminal to Aga2p, detection of the HA tag indicates successful display of Aga2p and detection of the c-myc tag indicates successful

display of the protein of interest. Once displayed, at approximately 50,000 identical copies per cell, the protein of interest can be evaluated for desirable properties, such as high-affinity binding, by flow cytometry through the use of fluorescently labeled soluble reagents. (72)

As a platform for directed evolution, yeast surface display is compatible with diversity generation by error-prone PCR and library screening by fluorescence-activated cell sorting (FACS). Yeast display libraries commonly contain 10^7 to 10^8 mutants, the display of which are subject to the quality control mechanisms of yeast eukaryotic secretory system. Screening by FACS enables fine, quantitative discrimination between mutants. In addition, the plasmid encoding the mutant of interest can be retrieved and sequenced to identify the mutations underlying any phenotype improvement. (74)

2.2. Materials and Methods

2.2.1. *Yeast surface display of murine IL-2*

A plasmid containing the coding sequence of murine IL-2, pORF-mIL2, was purchased from InvivoGen. The IL-2 coding sequence was amplified by PCR using primers with flanking NheI and BamHI restriction sites (MWG Biotech) and cloned into pCTCON2 by ligation. The resulting plasmid, pCT-mIL2, was transformed into EBY100 using the Frozen-EZ Yeast Transformation II Kit (Zymo Research) according to manufacturer's instructions.

Transformed yeast were grown in SD-CAA, pH 4.5 (20 g/L dextrose, 6.7 g/L yeast nitrogen base without amino acids, 5 g/L casamino acids, 10.4 g/L sodium citrate, 7.4 g/L citric acid monohydrate) at 30°C to logarithmic phase, pelleted, and resuspended to 10^7 cells/ml in SG-CAA, pH 6.0 (20 g/L galactose, 6.7 g/L yeast nitrogen base without amino acids, 5 g/L casamino acids, 5.4 g/L Na_2HPO_4, 8.56 g/L $NaH_2PO_4 \cdot H_2O$) to induce protein expression. Cells were induced at 30°C for 16 to 20 hours. IL-2 display was verified by staining with biotinylated rat anti-HA IgG Fab fragments, clone 3F10 (Roche), followed by streptavidin-phycoerythrin (PE), and chicken anti-c-myc IgY, followed by Alexa Fluor 488- or 647-conjugated goat anti-chicken IgG (Invitrogen), in PBS with 0.1% (w/v) BSA (Sigma-Aldrich), pH 7.4, on ice. Proper IL-2 folding was confirmed by labeling with His-tagged recombinant mouse IL-2Rα / CD25

(R&D Systems) and rabbit polyclonal anti-6xHis tag antibody (Abcam), labeled with Alexa Fluor 647 using Invitrogen's Monoclonal Antibody Labeling Kit.

The equilibrium dissociation constant, K_d, for the interaction between yeast-displayed IL-2 and soluble CD25 was determined essentially as described (74). Briefly, induced cells were labeled with soluble CD25 at concentrations ranging from 1 nM to 250 nM in PBS with 0.1% (w/v) BSA at 37°C. At each concentration, the number of cells and the volume of the labeling reaction were selected to ensure at least 10-fold excess of soluble CD25 relative to yeast-displayed IL-2. The K_d was determined by fitting the total measured mean fluorescence and CD25 concentrations to a monovalent binding isotherm, by minimizing the sum of squared errors:

$$MFU_{tot} = MFU_{min} + (MFU_{range} \times [CD25]) / ([CD25] + K_d), \quad (2.1)$$

where MFU_{tot} is the total measured mean fluorescence, [CD25] is the concentration of CD25, assumed to be constant for each reaction, and MFU_{min}, MFU_{range}, and K_d are constant free parameters to be fitted.

2.2.2. *IL-2 affinity maturation*

The homology model of the murine IL-2 / IL-2 receptor complex was built using SWISS-MODEL (75), by threading the mouse IL-2 and IL-2 receptor protein sequences into the crystal structure the human IL-2 / IL-2 receptor complex (76).

In general, affinity maturation of IL-2 was performed as previously described (74). Briefly, the IL-2 coding sequence was mutagenized by error-prone PCR under conditions predicted to yield predominantly mutants with one or two amino acid changes per protein. These conditions (nucleotide analogue concentration and number of mutagenic PCR cycles) were determined by Ben Hackel, using a model described in his thesis (77). Specifically, to a 50 µl reaction containing 1x polymerase reaction buffer, 5 ng pCT-mIL2 template, 0.5 µM each of the forward and reverse primers recommended for library generation in pCTCON2 (74), 200 µM dNTPs, and 5 U Taq Polymerase (New England Biolabs), 2 µM each of the nucleotide

analogues 8-oxo-dGTP and dPTP were added. In a thermal cycler, the mixture was denatured for 3 min at 94°C and mutagenized by ten amplification cycles of 45 sec at 94°C, 30 sec at 55°C, and 45 sec at 72°C, followed by a final extension of 10 min at 72°C. The mutagenized PCR products were then gel-purified and amplified by thermal cycling at the above conditions, but without nucleotide analogues, and with 1 M betaine and 1.5% DMSO, for 35 cycles.

PCR amplified IL-2 library inserts and linearized pCTCON2 backbone, digested with NheI, BamHI, and SalI (New England Biolabs), were gel-purified and concentrated using PelletPaint (Novagen) and transformed into competent EBY100 by electroporation. Specifically, multiple aliquots of 50 μl electrocompetent EBY100 were mixed with 2 μg linearized pCTCON2 backbone and 10 μg IL-2 inserts, in 5 μl water, and pulsed at 0.54 kV and 25 μF in 0.2 mm electroporation cuvettes (VWR International) using a Gene Pulser unit (Bio-Rad Laboratories). Electroporated cells were grown in YPD at 30°C for 1 hour, allowing intact plasmids to form through homologous recombination of backbone with IL-2 inserts. Cells were then pelleted, resuspended in SD-CAA, and grown at 30°C. Maximal library diversity was determined by plating serial dilutions of the library onto SD-CAA plates immediately after YPD outgrowth. The library was passaged to SD-CAA at least once to reduce the number of untransformed cells. At least 10-fold the maximum library diversity was passaged each time to reduce the probability of losing unique clones. To determine the DNA sequences of the library's clones, plasmids were retrieved from the yeast library using the Zymoprep Yeast Plasmid Miniprep I Kit (Zymo Research); single clones were obtained after transformation into *E. coli* strain XL1-Blue (Strategene).

FACS screening of the library was performed six times with near-equilibrium labeling of soluble CD25, at successively decreasing concentrations of 7.7 nM to 1 nM. As before, CD25 binding was detected by Alexa Fluor 647-conjugated rabbit anti-6xHis. Display of Aga2p/IL-2 fusion protein was concurrently determined by staining with biotinylated rat anti-HA followed by streptavidin-phycoerythrin. At each sort, clones with higher CD25-binding signal, for a given level of expression, as compared with wild-type IL-2, were collected into SD-CAA, pH 4.5, with penicillin-streptomycin and kanamycin (Invitrogen). DNA sequences and CD25 binding affinities of individual clones were determined as above.

To further improve IL-2 affinity for CD25, five additional libraries were successively generated by error-prone PCR. The second mutagenized IL-2 library[1], library 2.0, was generated using the DNA of libraries 1.4 and 1.6 and clones 1.4-1 and 1.4-14 as templates for mutagenesis, and screened twice by FACS with soluble CD25 labeling at 2 nM and 1 nM, respectively. Clone 1.4-14 was used as the reference for setting the sort gate. Subsequent libraries were generated by mutagenizing the twice-sorted population of the previous mutagenesis library, and each newly mutagenized library was screened twice using the previous twice-sorted population to set the sort gate. FACS screening of libraries through 5.1 was conducted with near-equilibrium labeling of soluble CD25, at concentrations successively decreasing to 0.2 nM. FACS screening of libraries 6.0 and 6.1 were conducted with kinetic competition from library 5.2 mutants. Specifically, soluble library 5.2 mutants were generated by reducing the disulfide bond between Aga1p and Aga2p on the surface of yeast displaying library 5.2, using Immobilized TCEP Disulfide Reducing Gel (Thermo Scientific) for 15 min at room temperature, and separating soluble mutants from cells and resin by centrifugation. The libraries to be sorted were labeled to saturation with 3.8 nM soluble CD25, followed by addition of soluble library 5.2 mutants for 25 min at 37°C. Clones retaining bound CD25 were detected with Alexa Fluor 647-conjugated rabbit anti-6xHis as before.

Affinity maturation progress was monitored by titration of library populations with soluble CD25, as done above for individual clones. The affinity of library 6.2 clones were determined by titration with soluble CD25 at concentrations ranging from 2.5 pM to 50 nM. At low concentrations, the criterion of 10-fold excess soluble CD25 relative to yeast-displayed IL-2 mutant requires labeling at low cell density, which makes subsequent cell collection by centrifugation difficult. To facilitate cell pelleting, non-displaying EBY100 cells were mixed in with cells displaying library 6.2 clones, at a ratio of 50 to 1, for all titration measurements.

[1] Library populations and individual clones are named in the format L.S and L.S-C, respectively. L refers to the number of rounds of mutagenesis by error-prone PCR, S refers to the number of selections by FACS after mutagenesis, and C is the clone number. For example, Library 1.2 refers the population of clones of the first mutagenesis library after two rounds of selection by FACS, and clone 1.2-16 refers to clone #16 within that population.

Fluorescence measurements by flow cytometry and CD25 concentration were fitted to Equation 2.1 as before.

Selective-reversion mutants of library 6.2 clones were created by QuikChange site-directed mutagenesis using oligonucleotides (Integrated DNA Technologies) containing the desired mutations. The CD25 binding affinity of each mutant was determined by CD25 titration as described for library 6.2 clones above.

2.2.3. *Soluble expression and purification of IL-2 and QQ 6.2-10*

DNA encoding IL-2 and QQ 6.2-10 were each subcloned NheI to BamHI into a pRS316-based secretion plasmid containing the galactose-inducible GAL1-10 promoter, the engineered secretion leader αpp8 (78), and a C-terminal FLAG tag. Each secretion plasmid was co-transformed with pRS314 into the yeast strain YVH10 (79).

Transformed cells were grown in SD-SCAA, pH 6 (20 g/L dextrose, 6.7 g/L yeast nitrogen base without amino acids, 3.85 g/L synthetic casamino acids [-trp, -leu, -ura], 5.4 g/L Na_2HPO_4, 8.56 g/L $NaH_2PO_4 \cdot H_2O$), at 30°C, in baffled Tunair flasks. After reaching logarithmic growth phase (OD_{600} ~ 5), cells were pelleted and resuspended in SG-SCAA with 0.05% (w/v) BSA, pH 6 (20 g/L galactose, 2 g/L dextrose, 6.7 g/L yeast nitrogen base without amino acids, 3.85 g/L synthetic casamino acids [-trp, -leu, -ura], 5.4 g/L Na_2HPO_4, 8.56 g/L $NaH_2PO_4 \cdot H_2O$, 0.5 g/L BSA) to induce protein secretion. Three days after induction, cell culture supernatants were harvested and concentrated by ultrafiltration using Ultracel YM-10 membranes (Millipore). IL-2 and QQ 6.2-10 were purified by immunoaffinity chromatography using anti-FLAG M2 Affinity Gel (Sigma-Aldrich) and size exclusion chromatography using a Superdex 200 column (Amersham Biosciences). Protein purity was verified by silver staining of SDS-PAGE gels using SilverXpress Silver Staining Kit (Invitrogen) and western blotting using anti-FLAG M2 peroxidase conjugate (Sigma-Aldrich). Protein concentrations were determined by quantitative western blotting, using Amino-terminal FLAG-BAP Fusion Protein (Sigma-Aldrich) as standard.

2.2.4. *CTLL-2 cell culture and assays*

CTLL-2 cells were cultured in RPMI-1640 supplemented with sodium bicarbonate, fetal bovine serum (FBS), L-glutamine, sodium pyruvate, and penicillin-streptomycin (Invitrogen). For maintenance, cells were passaged every other day to 200,000 cells/ml in media supplemented with 150 pM wild-type mouse IL-2 (R&D Systems).

For surface persistence and viability assays, cells were passaged to 400,000 cells/ml and cultured in cytokine-free medium for 12 hours prior to pulse with yeast-secreted IL-2 or QQ 6.2-10. Thirty minutes after IL-2 or QQ 6.2-10 addition, cells were pelleted and resuspended in cytokine-free medium. Cell-surface cytokine levels were determined by labeling with mouse anti-FLAG M2 antibody (Sigma-Aldrich) followed by Alexa Fluor 488-conjugated goat anti-mouse IgG (Invitrogen). Cell culture viability was determined using the CellTiter-Glo Luminescent Cell Viability Assay (Promega), according to manufacturer's instructions. Luminescence was measured using an Infinite M1000 microplate reader (Tecan).

2.2.5. *2C cell culture and proliferation assay*[2]

Single-cell suspensions were prepared from spleens of $RAG1^{-/-}$ 2C transgenic TCR (2C/RAG) mice (80) by rubbing spleens between frosted microscope slides. Splenocytes were cultured in RPMI-1640 supplemented with sodium bicarbonate, FBS, L-glutamine, sodium pyruvate, non-essential amino acids, HEPES, β-mercaptoethanol, and penicillin-streptomycin (Invitrogen). Cells were stimulated with 1 μg/ml SIYRYYGL (SIY) peptide and 200 pM wild-type mouse IL-2 (R&D Systems). Two days after seeding, cells were passaged to 500,000 cells/ml and restimulated with IL-2. Two days after passaging, cells were transferred to cytokine-free medium for 12 hours, then labeled with CellTrace CFSE (Invitrogen), resuspended to 500,000 cells/ml, and pulsed for 30 min with yeast-secreted IL-2 or QQ 6.2-10. Aliquots were removed at indicated time points to determine cellular CFSE content by flow cytometry.

---

[2] The experiment described in this section was performed in collaboration with Eileen M. Higham of the Chen Lab at MIT. We both contributed to the design of the experiment. EMH performed procedures in mice, while I produced protein and handled cell treatments *in vitro*.

2.2.6. *Adoptive transfer of IL-2 treated 2C cells and intraprostatic IL-2 injection*[3]

Overall, *in vivo* activated 2C cells were generated as described (81). Briefly, naïve 2C cells were isolated from the lymph nodes and spleen of 2C/RAG mice and adoptively transferred into C57BL/6 mice by retro-orbital injection. Immediately following adoptive transfer, mice were infected with a WSN strain of recombinant influenza A engineered to express the SIY epitope (WSN-SIY). Five days after cell transfer and flu infection, mediastinal lymph nodes (MLN) were harvested and single-cell suspensions prepared. Cells were labeled with CellTrace CFSE (Invitrogen), resuspended to 500,000 cells/ml, and stimulated for 30 min at 37°C with 100 pM yeast-secreted IL-2 or QQ 6.2-10. Cells were strained over mesh, pelleted and resuspended in 100 µl PBS, and injected retro-orbitally into C57BL/6 mice. Two days after transfer, spleen and lymph nodes were harvested for analysis by flow cytometry as described (81).

In vitro activated 2C T cells were generated as described in Section 2.2.5, using SIY peptide and commercial murine IL-2. Four days after seeding and without cytokine withdrawal, 2C splenocytes were stimulated for 30 min at 37°C with 250 pM yeast-secreted IL-2 or QQ 6.2-10. Cells were strained over mesh, pelleted and resuspended in 100 µl PBS, and injected retro-orbitally into C57BL/6 mice. Two days after transfer, spleen was harvested for analysis by flow cytometry as described (81).

Intraprostatic injection of IL-2 or QQ 6.2-10 into transgenic adenocarcinoma of the mouse prostate (TRAMP) mice and TRAMP mice expressing SIY (TRAMP-SIY) was performed generally as described (82). Briefly, naïve 2C cells were isolated from the lymph nodes and spleen of 2C/RAG mice and adoptively transferred into TRAMP or TRAMP-SIY mice by retro-orbital injection. Immediately following adoptive transfer, mice were infected with WSN-SIY. Seven days after cell transfer and flu infection, 133 pmol (2.8 µg) yeast-secreted IL-2 or QQ 6.2-10 was injected into the prostate. Four days after intraprostatic injection, lungs and prostates were harvested for analysis by flow cytometry as described (81, 82). Intracellular IFN-γ staining was performed using the Mouse IFN-γ Secretion Assay Detection Kit from Miltenyi Biotec (81).

---

[3] The experiments described in this section were performed in collaboration with Eileen M. Higham of the Chen Lab at MIT. We both contributed to experimental design and data analysis. EMH performed procedures in mice, while I produced protein and handled cell treatments *ex vivo*.

2.2.7. *Expression and purification of Fc/IL-2 fusion proteins*

A vector encoding the heavy chain of mouse IgG2a from C57BL/6 mice was a gift of Jeffrey V. Ravetch (The Rockefeller University). The aspartic acid at position 265 (83) was replaced by alanine (D265A) through QuikChange site-directed mutagenesis using oligonucleotides (Integrated DNA Technologies) containing the desired mutation. DNA encoding the non-lytic D265A Fc (hinge, C_H2, and C_H3 domains), henceforth referred to simply as Fc, was cloned into gWIZ (Genlantis) behind a human IgG light chain secretion leader through site-directed mutagenesis, following a variation of the QuikChange protocol (84). IL-2 and QQ 6.2-10 with C-terminal 6xHis tags were subsequently cloned into the vector C-terminal to the Fc, separated by a short G_3S linker, yielding gWIZ-Fc-IL2 and gWIZ-Fc-QQ6210, respectively. To enable expression of monovalent Fc/IL-2 fusions, a vector encoding the Fc with a C-terminal FLAG tag, gWIZ-Fc-FLAG, was also constructed. Plasmid DNA was transformed into XL1- Blue for amplification. DNA was purified from cells using PureLink HiPure Maxiprep Kit (Invitrogen) and sterile filtered.

Fc/IL-2 fusion proteins were expressed in HEK293 cells (Invitrogen) according to manufacturer's instructions. For expression of bivalent Fc/IL-2 fusions, HEK293 cells were transfected with gWIZ-Fc-IL2 or gWIZ-Fc-QQ6210 using polyethylenimine in FreeStyle 293 media supplemented with OptiPro (Invitrogen). For expression of monovalent Fc/IL-2 fusions, HEK293 cells were co-transfected with gWIZ-Fc-IL2 or gWIZ-Fc-QQ6210 with gWIZ-Fc-FLAG. Seven days post transfection, culture supernatants were harvested by centrifugation at 15,000 x *g* for 30 min at 4°C and sterilized by filtration through 0.22 μm filters (Nalgene).

Bivalent Fc/IL-2 fusions were purified from HEK293 culture supernatants using Protein A Agarose (Millipore). Monovalent Fc/IL2 fusions were purified by sequential TALON His-tag metal affinity chromatography (Clontech) and anti-FLAG affinity chromatography (Sigma-Aldrich). Elution fractions of all proteins were concentrated using 15-ml 30-kDa Amicon Ultra Centrifugal Devices (Millipore) and buffered exchanged into PBS. Protein purity was verified by Coomassie Brilliant Blue staining of SDS-PAGE gels using SimplyBlue SafeStain (Invitrogen) and western blotting using peroxidase-conjugated Fc fragment-specific goat anti-mouse IgG

(Thermo Scientific). Protein concentrations were determined by quantitative western blotting, using mouse anti-FLAG M2 antibody (Sigma-Aldrich) as standard.

2.2.8. *Adoptive transfer of Fc/IL-2 treated OT-1 cells*[4]

Single-cell suspensions were prepared from spleen and lymph nodes of age-matched $RAG1^{-/-}$ OT-1 transgenic TCR (OT-1) mice on C57BL/6 or congenic B6.Thy1.1 background. Red blood cells of the spleen were lysed with ammonium chloride, and final cell suspensions were passed through mesh filters to remove hair and debris. $Thy1.2^{+}$ and $Thy1.1^{+}$ cells were cultured separately in RPMI-1640 supplemented with sodium bicarbonate, FBS, L-glutamine, sodium pyruvate, non-essential amino acids, HEPES, β-mercaptoethanol, and penicillin-streptomycin (Invitrogen) and were stimulated with 1 μg/ml SIINFEKL peptide and 200 pM wild-type mouse IL-2 (R&D Systems). Two days after seeding, cells were passaged to 500,000 cells/ml and restimulated with IL-2. One day after passaging, cells were stimulated for 1 hour at 37°C with 250 pM Fc/IL-2 or Fc/QQ6210. The two populations were combined to yield 50-50 mixtures, as determined by flow cytometry using APC-conjugated anti-Thy1.2 IgG, clone 53-2.1 (eBiosciences) and FITC-conjugated anti-Thy1.1 IgG, clone OX-7 (BD Biosciences). Cell mixes were strained over mesh, pelleted and resuspended in 100 μl PBS, and injected retro-orbitally into $RAG^{-/-}$ mice (Jackson Laboratory).

Two or nine days after cell transfer, single-cell suspensions were prepared from spleen and lymph nodes. Red blood cells of the spleen were lysed with ammonium chloride, and final cell suspensions were passed through mesh filters to remove hair and debris. Cells were labeled with APC-conjugated anti-Thy1.2, FITC-conjugated anti-Thy1.1, and PE-conjugated anti-Vα2 TCR, clone B20.1 (BD Pharmingen) and analyzed using an Accuri C6 flow cytometer.

---

[4] The experiments described in this section were performed in collaboration with S. Peter G. Bak of the Chen Lab at MIT. We both contributed to the design of the experiments. SPGB performed all procedures with mice, while I produced protein and handled cell treatments *ex vivo*.

2.2.9. *Cell-surface IL-2 tethering*

To enable site-specific biotinylation of IL-2, IL-2 was expressed with the sortase A recognition motif LPETG and a c-myc epitope tag at the C-terminus, using YVH10 for secretion and anti-FLAG affinity chromatography and size exclusion for purification, as described in section 2.2.3. A plasmid encoding His-tagged *Staphylococcus aureus* sortase A was a gift of Hidde L. Ploegh (MIT). Sortase A was expressed in BL21(DE3) by IPTG induction and purified using TALON His-tag metal affinity resin (Clontech). $(G_3S)_3$-biotin peptide was synthesized by the Biopolymers and Proteomics Core Facility at MIT. Sortase-catalyzed biotinylation was performed essentially as described (85). Specifically, 10 μM purified IL-2 was incubated for 6 hours at 37°C with 120 μM sortase A and 300 μM $(G_3S)_3$-biotin peptide in sortase buffer (50 nM Tris, pH 7.5, 150 mM NaCl, 10 mM $CaCl_2$). Excess $(G_3S)_3$-biotin was removed by concentrating the reaction mixture and buffer exchanging into PBS using 15-ml 10-kDa Amicon Ultra Centrifugal Devices (Millipore). Reaction completion was confirmed by western blotting using streptavidin-horseradish peroxidase conjugate (GE Healthcare) and 9E10 mouse anti-c-myc antibody (Covance) followed by peroxidase-conjugated Fc fragment-specific goat anti-mouse IgG (Thermo Scientific). Biotinylated IL-2 was pre-loaded onto streptavidin (New England Biolabs) by mixing at a ratio of 3 to 1 and incubating for 1 hour at room temperature.

CTLL-2 cells were biotinylated through cell-surface primary amines using sulfo-NHS-LC-LC-biotin (Thermo Scientific). Specifically, cells were resuspended to 10^6 cells per 100 μl in PBS with 100 μM sulfo-NHS-LC-LC biotin and incubated at room temperature for 15 min. The reaction was quenched with 100 mM glycine in PBS, pH 7, and cells were washed twice with cell culture media. Cells were seeded at 100,000 cells/ml and incubated with complexed streptavidin/IL-2 for 2 hours before transfer to cytokine-free medium. Cell-surface IL-2 levels and cell culture viability were determined by flow cytometry and the CellTiter-Glo luminescence assay, respectively, as described in section 2.2.4.

2.2.10. *Adoptive transfer of biotinylated OT-1 T cells*[5]

Tumor inoculation, adoptive cell transfer, and bioluminescence imaging were performed essentially as described (86). Cell-surface biotinylation was performed as described above for CTLL-2 cells. Briefly, E.G7-OVA cells (87) were cultured in RPMI-1640 with GlutaMAX, supplemented with FBS, sodium pyruvate, non-essential amino acids, HEPES, β-mercaptoethanol, penicillin-streptomycin, and geneticin (Invitrogen). Cells were passaged every other day to 100,000 cells/ml. On the day of tumor inoculation, B6-albino mice (Jackson Laboratories) were anesthetized with isoflurane and fur was shaved from the right flanks to expose skin. $4x10^6$ cells in 50 µl PBS were injected subcutaneously into each mouse using 27G½ syringe needles. Seven days after tumor inoculation, and on the day of adoptive OT-1 T cell transfer, mice were sub-lethally irradiated with 500 cGy from a ^{137}Cs source.

For biotinylation and adoptive transfer, single-cell suspensions were prepared from spleens of firefly luciferase transgenic OT-1 mice and passed through mesh filters to remove hair and debris. Cells were cultured in RPMI-1640 with GlutaMAX, supplemented with FBS, sodium pyruvate, non-essential amino acids, HEPES, β-mercaptoethanol, penicillin-streptomycin (Invitrogen), 2 µg/ml concanavalin A (Sigma-Aldrich), and 1 ng/ml IL-7 (PeproTech). Two days after seeding, cells were biotinylated using 10, 100, or 100 µM sulfo-NHS-LC-LC-biotin as described for CTLL-2 cells in Section 2.2.9 above. After quenching with 100 mM glycine in PBS, pH 7, cells were resuspended to 10^6 cells per 100 µl PBS with 0.1% (w/v) BSA and labeled with Alexa Fluor 647-conjugated streptavidin (Invitrogen) by incubation with 20 µg/ml at 4°C for 15 min. $20x10^6$ cells in 100 µl PBS were injected retro-orbitally into each irradiated tumor-bearing B6-albino mouse.

Immediately and two days after adoptive transfer, mice were injected intra-peritoneally (i.p.) with 6 mg XenoLight D-Luciferin Potassium Salt (Caliper Life Sciences) in 400 µl PBS and imaged for bioluminescence using an IVIS Spectrum imaging system (Caliper Life Sciences). Data was acquired and analyzed using Living Image software (Caliper Life Sciences).

---

[5] The experiment described in this section was performed in collaboration with Matthias T. Stephan of the Irvine Lab at MIT. We both contributed to the design of the experiment. MTS performed all procedures with mice and analyzed data, while I performed cell-surface biotinylation *ex vivo*.

2.3. Results

2.3.1. *Yeast surface display of murine IL-2*

Wild-type murine IL-2, henceforth referred to as IL-2, was displayed on the surface of yeast using the yeast display vector pCTCON2 and yeast display strain EBY100. Display of full-length Aga2p/IL-2 fusion was confirmed by flow cytometry, using anti-HA and anti-c-myc antibodies (Figure 2-1a). Titration with soluble murine CD25 confirmed yeast-displayed IL-2 to be properly folded, with an equilibrium dissociation constant, K_d, of 45 nM. CD25 titrations with concurrent anti-HA or anti-c-myc labeling indicated that c-myc detection interferes with CD25 binding, while HA detection does not (Figure 2-1b). Anti-HA staining was therefore used to detect protein expression for all subsequent yeast display experiments.

2.3.2. *Affinity maturation of IL-2 by yeast surface display*

To guide our mutagenesis approach and assess our affinity maturation progress, we built a model of the mouse IL-2 / IL-2 receptor complex, shown in Figure 2-2, based on the crystal structure of the human IL-2 / IL-2 receptor complex (76). The model indicates that residues in potential contact with CD25 locate to several discontinuous stretches of the protein amino acid sequence. Therefore, we chose to randomize the entire IL-2 coding sequence.

Given IL-2's already appreciable affinity for CD25, we chose to be conservative in our mutagenesis, aiming for one to two amino acid changes per protein. Since changing many amino acids simultaneously would likely change the overall protein fold, this conservative approach reduces the likelihood of generating loss-of-binding mutants. Moreover, this conservative approach restricts the potential protein sequence space, enabling more adequate sampling by yeast surface display libraries.

Toward this goal, we performed error-prone PCR at conditions predicted to yield the desired mutagenesis rate and generated a yeast-displayed IL-2 library consisting of 3.1×10^7 transformants. Eleven of 16 sequenced clones contained one or two amino acid changes. Of the remaining five clones, two contained no amino acid changes and three contained three amino

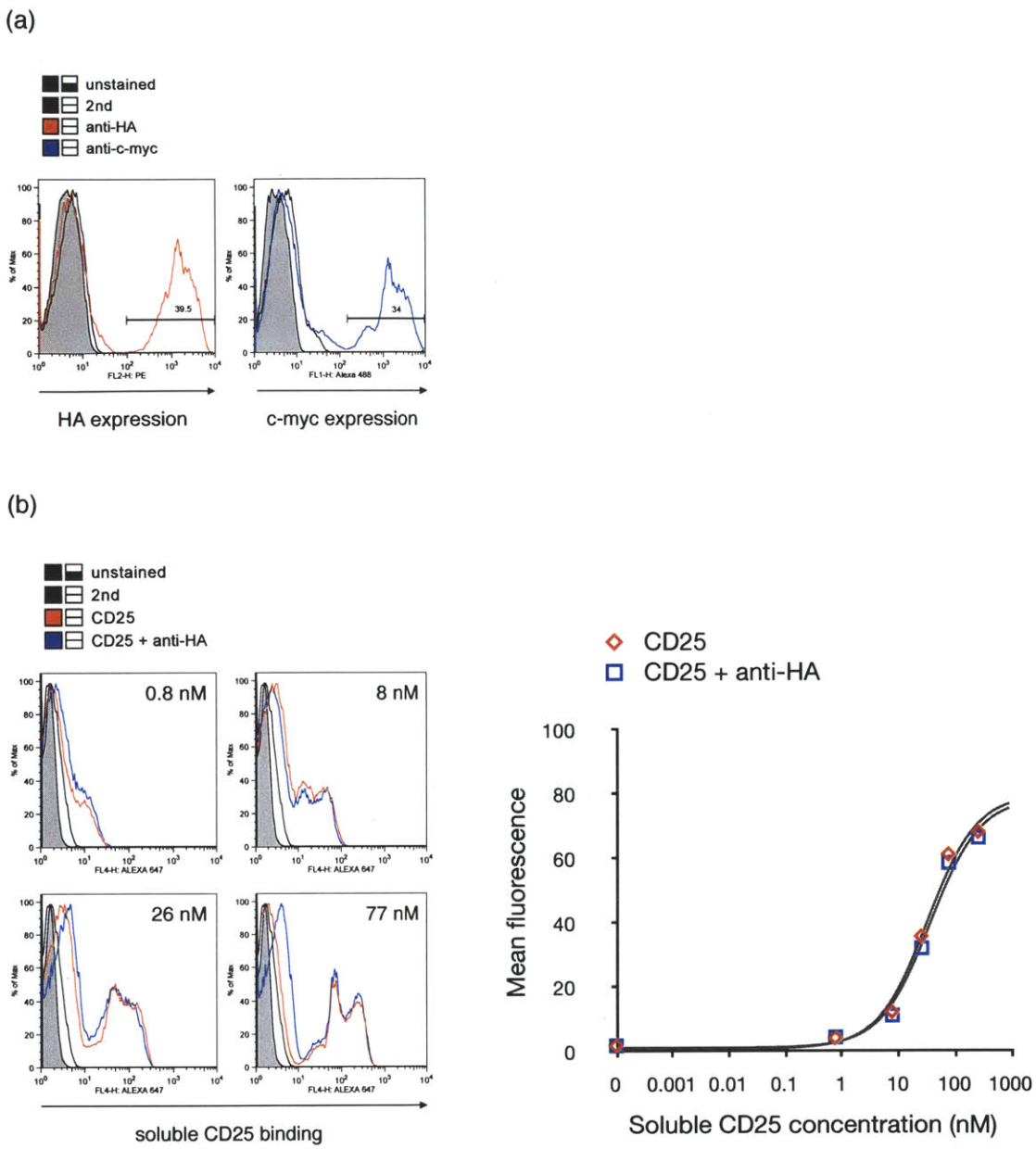

Figure 2-1: Yeast surface display of murine IL-2. (a) Detection of full-length Aga2p/IL-2 fusion protein displayed on the surface of yeast by anti-HA (left) and anti-c-myc (right) antibodies. (b) Detection of soluble CD25 binding to yeast-displayed IL-2, alone or with concurrent detection of Aga2p/IL-2 expression by anti-HA antibody. Flow cytometry histograms (left) at indicated concentrations of soluble CD25. Titration curves (right) with mean fluorescence measurements (symbols) fitted to monovalent binding isotherm (lines).

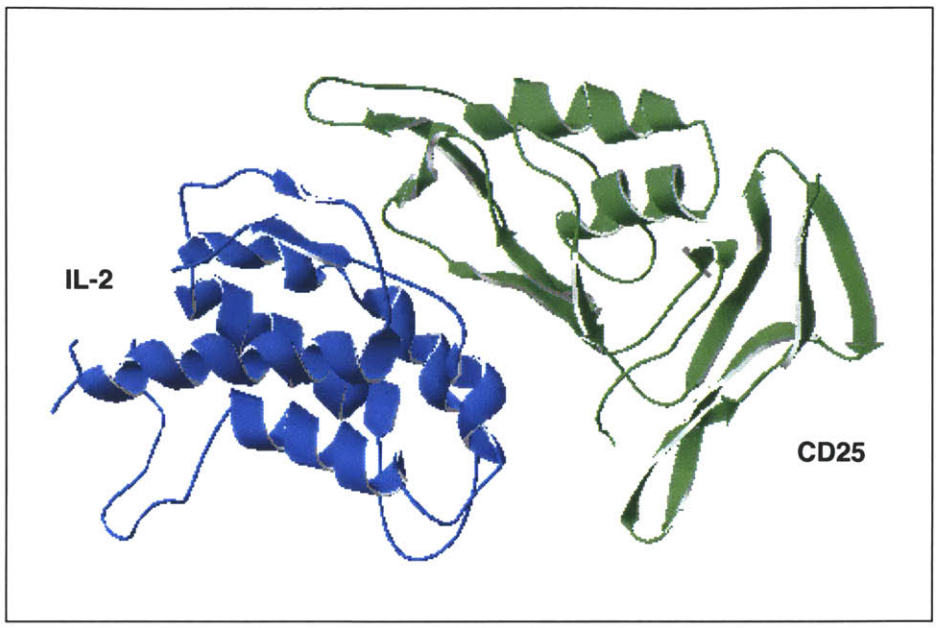

Figure 2-2: Homology model of murine IL-2 in complex with CD25. Model was generated using SWISS-MODEL (75), based on the structure of the human IL-2 / IL-2 receptor complex (76). IL-2 is shown in blue; CD25 is shown in green.

acid changes. The amino acid changes were distributed throughout the whole protein, as shown in Figure 2-3.

The library was screened six times by FACS, with near-equilibrium labeling of soluble CD25 at concentrations successively decreasing from 7.7 nM to 1 nM. DNA sequencing of a selection of clones after every two rounds of FACS indicated an accumulation of mutants with proline or threonine in place of serine at position 126, as shown in Figure 2-4. As determined by yeast-surface titration with soluble CD25, single amino acid changes to proline (S126P) or threonine (S126T) improved CD25 binding affinity approximately three-fold, with K_d = 16.1 nM and K_d = 12.4 nM, respectively. Encouragingly, this position locates to the CD25-binding face of IL-2 (Figure 2-5) and is occupied by proline or threonine in several other animal species (Figure 2-6).

Figure 2-3: Low-rate mutagenesis of whole IL-2 coding sequence by error-prone PCR. Amino acid sequences of 16 clones from library 1.0. Amino acid differences from wild-type IL-2 are indicated by letters.

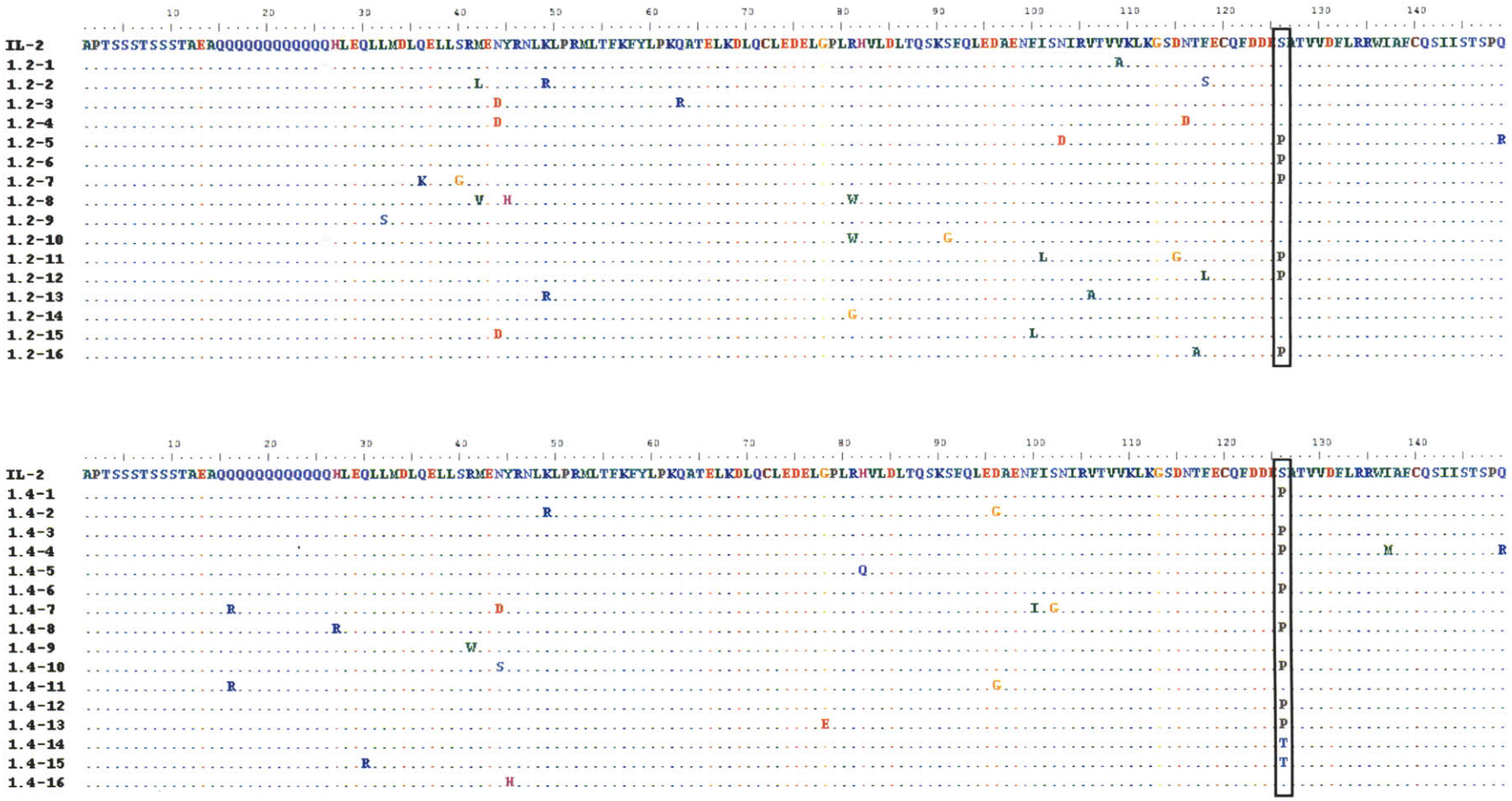

Figure 2-4: Proline and threonine are preferred at position 126 of IL-2. Amino acid sequences of 16 clones from library 1.2 (top) and library 1.4 (bottom). Position 126 is boxed.

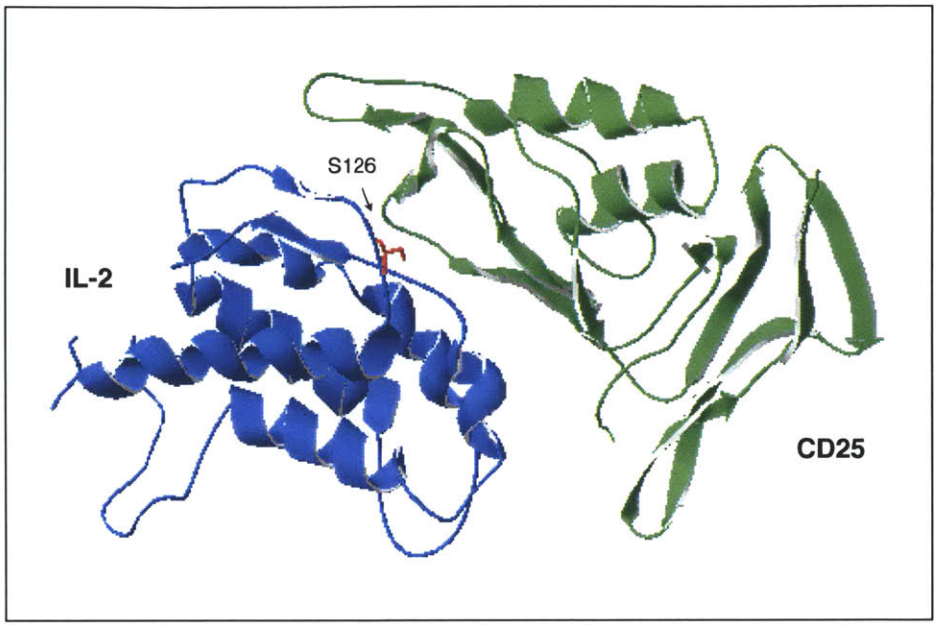

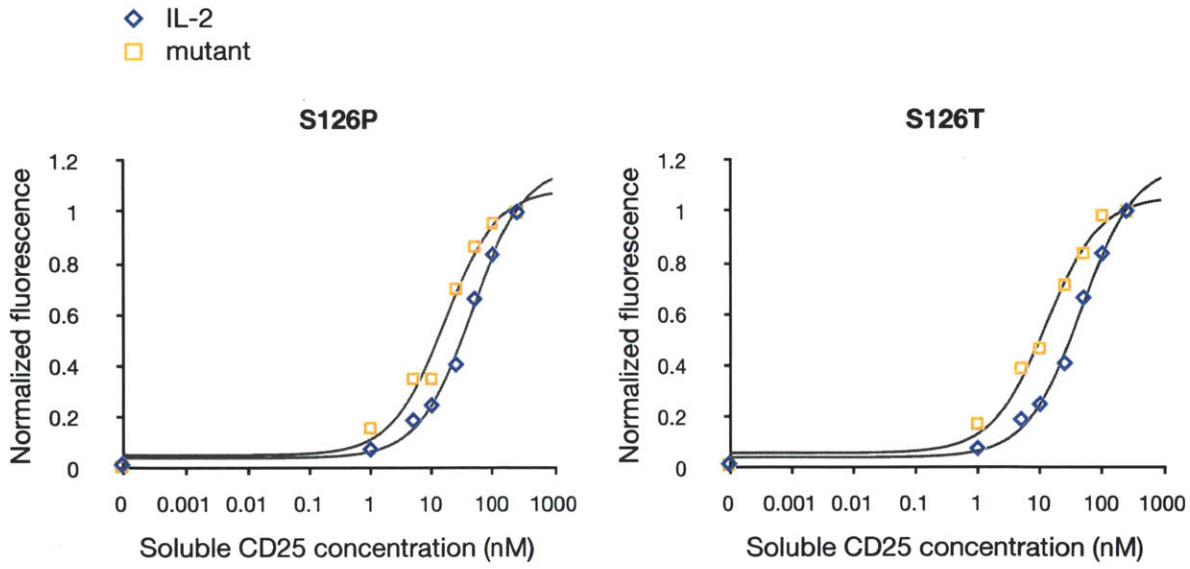

Figure 2-5: Single amino acid changes S126P and S126T improve CD25 binding affinity. Serine 126, shown in red, locates to the IL-2/CD25 binding interface (top). S126P (bottom, left) and S126T (bottom, right) IL-2 displayed on the surface of yeast were assayed for binding to soluble CD25 at 37°C. Symbols indicate measurements; lines indicate theoretical curve fits. Fluorescence measurements were normalized to the maximum signal of each IL-2 clone.

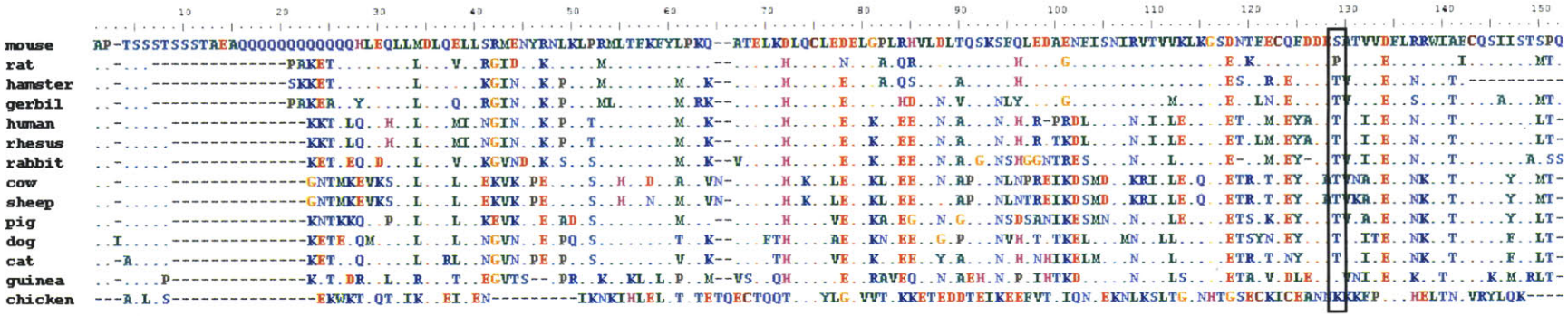

Figure 2-6: Position 126 of IL-2 is occupied by proline or threonine in other animal species. Sequence alignment was performed using ClustalW. Position 126 is boxed.

Five additional rounds of diversification and screening was performed to isolate mutants with further improved CD25 binding affinity. For each round, diversification by error-prone PCR was followed by two FACS selections, to enrich higher-affinity clones for further mutagenesis. DNA sequencing of 16 clones from library 6.2 indicated a consensus at position 126 for proline (Figure 2-7). All mutations of these clones locate to either the CD25-interacting or the IL-2Rβ-interacting faces of IL-2, as shown in Figure 2-8. Yeast-surface titrations of six of these clones indicated achievement of approximately 500-fold improvement in CD25-binding affinity, with $K_d \sim 100$ pM.

To avoid disrupting IL-2Rβ signaling, the putative IL-2Rβ-binding mutations were reverted to wild-type by site-directed mutagenesis. Reversion mutants[6] retained high CD25-binding affinity, shown in Table 2-1 and Figure 2-9, suggesting that the putative IL-2Rβ-binding mutations likely accumulated due to benefits for yeast expression.

Table 2-1: Equilibrium dissociation constants, K_d, of IL-2 and its mutants for CD25.

	K_d (nM)		K_d (pM)		K_d (pM)
IL-2	45.1	**6.2-3**	123		
S126P	16.1	**6.2-4**	193	**QQ 6.2-4**	143
S126T	12.4	**6.2-8**	187	**QQ 6.2-8**	240
		6.2-10	63	**QQ 6.2-10**	88
		6.2-11	86	**QQ 6.2-11**	184
		6.2-13	95	**QQ 6.2-13**	202

[6] Reversion mutants of library 6.2 are named by their original clone name preceded by "QQ", referring to the two rounds of site-directed mutagenesis (QuikChange) required to remove the putative IL-2Rβ-binding mutations.

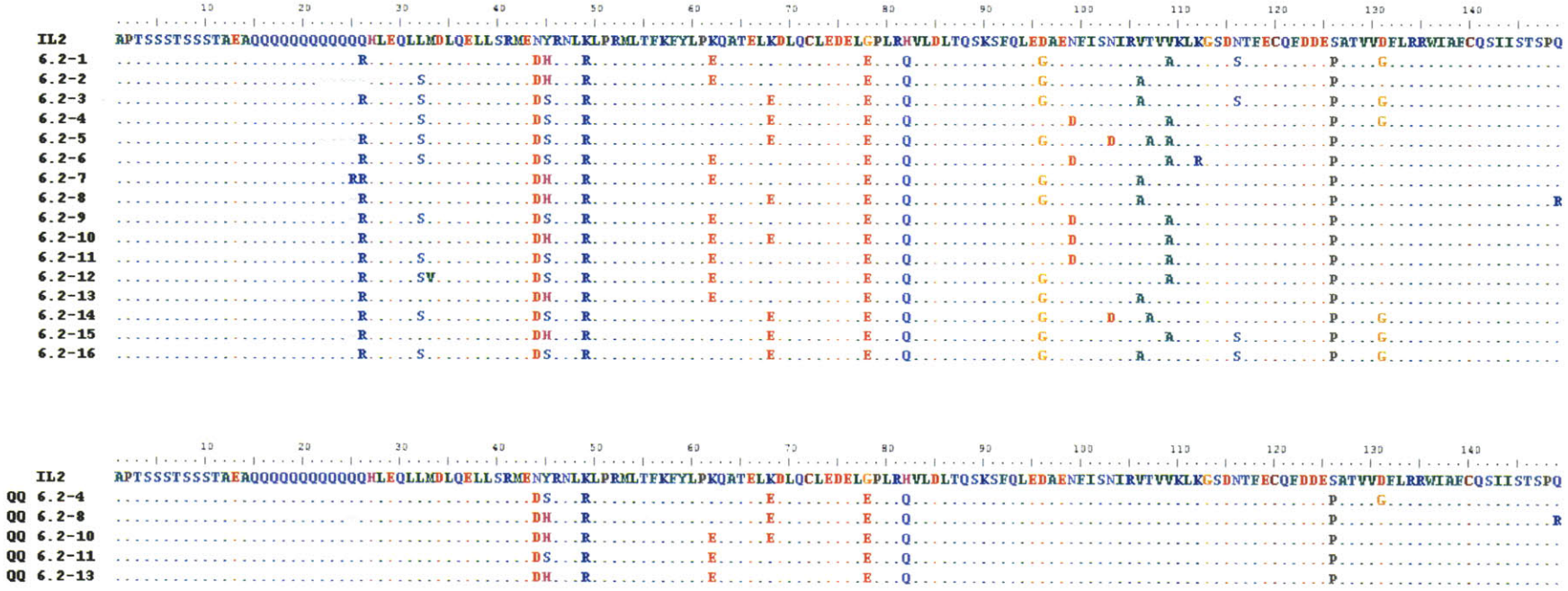

Figure 2-7: Sequence refinement of high-affinity CD25-binding IL-2 mutants. Amino acid sequences of 16 clones from library 6.2 (top). Amino acid sequences of IL-2 mutants after reverting putative IL-2Rβ-binding mutations of library 6.2 clones back to wild-type (bottom).

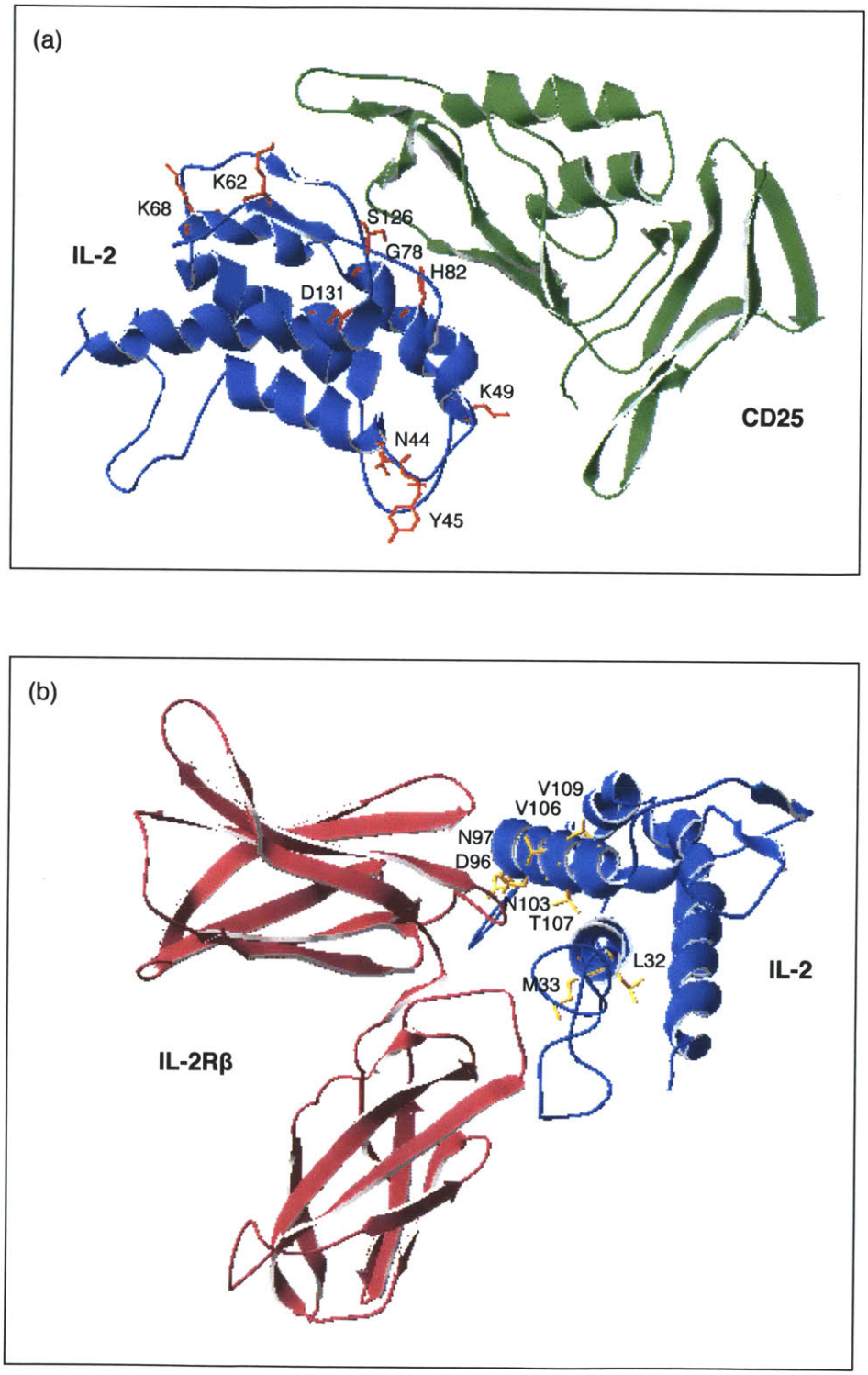

Figure 2-8: Amino acid mutations in high-affinity CD25-binding IL-2 mutants locate to CD25- or IL-2Rβ-binding faces of IL-2. Residues mutated in clones of library 6.2 locate to the IL-2/CD25 binding interface (a) or the IL-2/IL-2Rβ binding interface (b), highlighted in red and orange, respectively. IL-2 is shown in blue; CD25 is shown in green; IL-2Rβ is shown in magenta. Homology model was generated using SWISS-MODEL (75), based on the structure of the human IL-2 / IL-2 receptor complex (76).

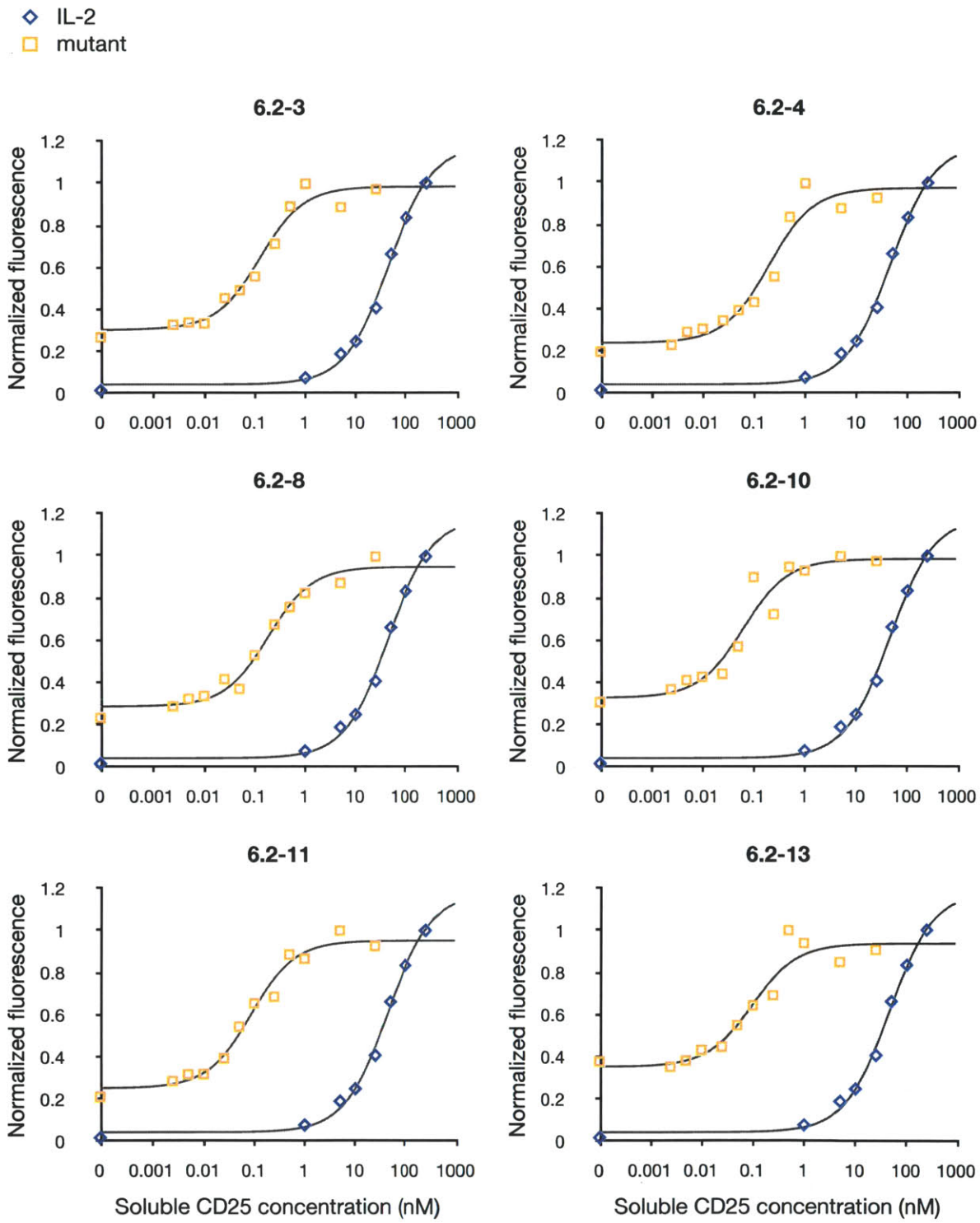

Figure 2-9: High-affinity CD25-binding IL-2 mutants. Clones of library 6.2 were individually displayed on the surface of yeast, mixed with non-displaying EBY100, and assayed for binding to soluble CD25 at 37°C. Symbols indicate measurements; lines indicate theoretical curve fits. Fluorescence measurements were normalized to the maximum signal of each IL-2 clone.

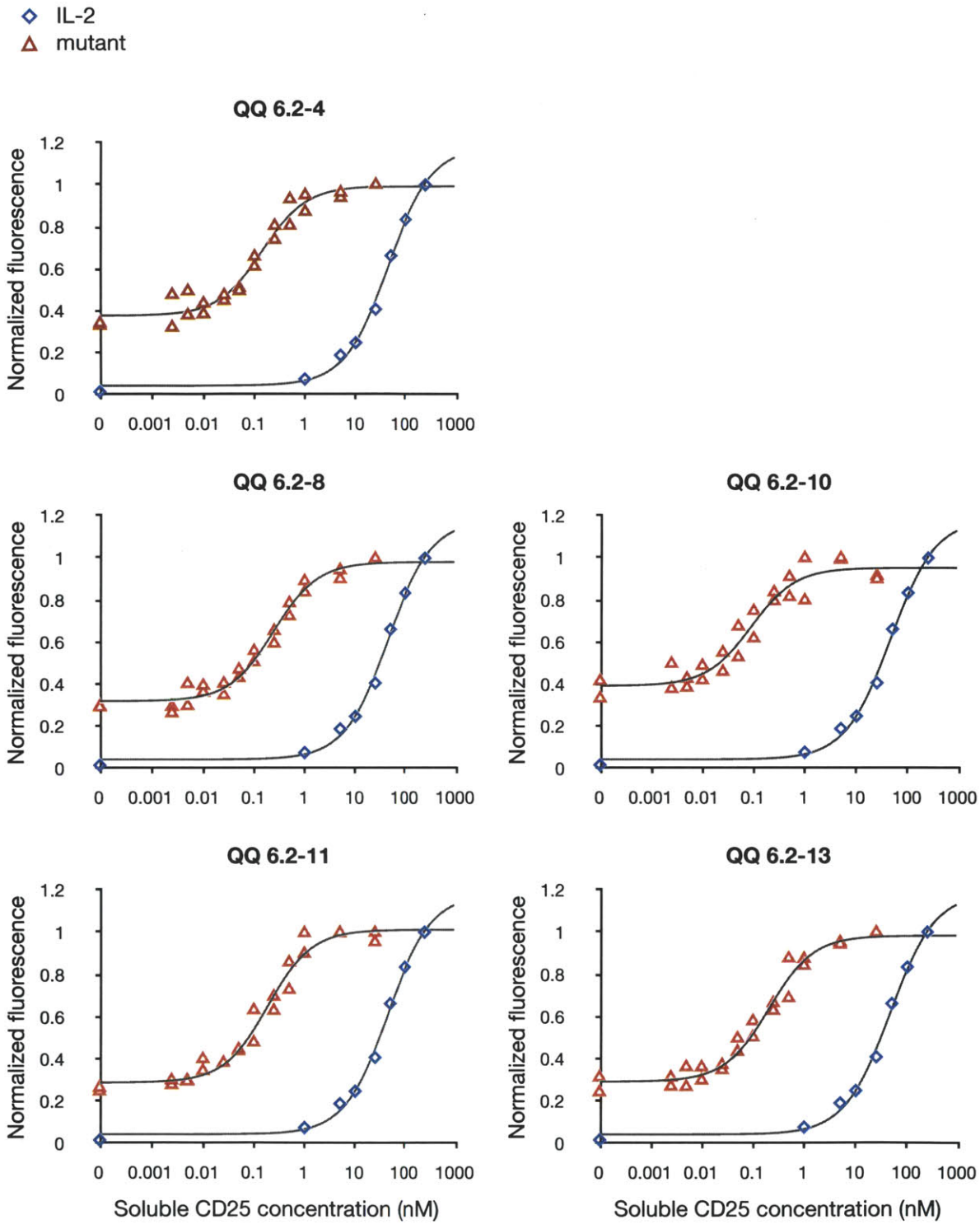

Figure 2-10: Selective-reversion mutants of library 6.2 retain high-affinity binding to CD25. IL-2 mutants were displayed on the surface of yeast, mixed with non-displaying EBY100, and assayed for binding to soluble CD25 at 37°C. Symbols indicate measurements; lines indicate theoretical curve fits. Fluorescence measurements were normalized to the maximum signal of each IL-2 clone.

2.3.3. *High-affinity IL-2 persists on T-cell surface and potently stimulates growth* in vitro

To verify that the high-affinity CD25-binding mutant selected by yeast surface display exhibits high-affinity binding to CD25 expressed on the surface of immune cells, IL-2 and QQ 6.2-10 were secreted and purified from yeast culture supernatants for functional characterization *in vitro*. Following a 30-minute cytokine pulse, designed to approximate systemic clearance *in vivo*, IL-2 dependent murine CTLL-2 cells pulsed with QQ 6.2-10 retained more cytokine on their surfaced and remained viable longer than IL-2 pulsed cells (Figure 2-11). Comparably, primary 2C T cells pulsed for 30 minutes with QQ 6.2-10 proliferated more extensively *in vitro* than IL-2 treated cells (Figure 2-12).

2.3.4. *IL-2 mutant QQ 6.2-10 does not potently stimulate T-cell growth* in vivo

To evaluate the capacity of high-affinity mutant QQ 6.2-10 to stimulate T-cell proliferation *in vivo*, QQ 6.2-10 was used to stimulate *in vivo*- or *in vitro*-activated primary 2C cells before their adoptive transfer into C57BL/6 mice. In these approximations of clinical adoptive cell therapy, QQ 6.2-10 treatment did not significantly increase the extent of cell division of *in vivo*-activated 2C cells, generated from the mediastinal lymph nodes of 2C mice infected with WSN-SIY influenza, compared to IL-2 (Figure 2-13a), and only modestly increased the extent of cell division of *in vitro*-activated 2C cells, generated by stimulating naïve 2C lymph node and spleen cells with SIY peptide and commercial murine IL-2 *in vitro* (Figure 2-13b). Direct injection of QQ 6.2-10 into the prostate of TRAMP mice did not significantly increase the number of T cells in the prostate and only modestly increased their level of IFN-γ secretion (Figure 2-13c).

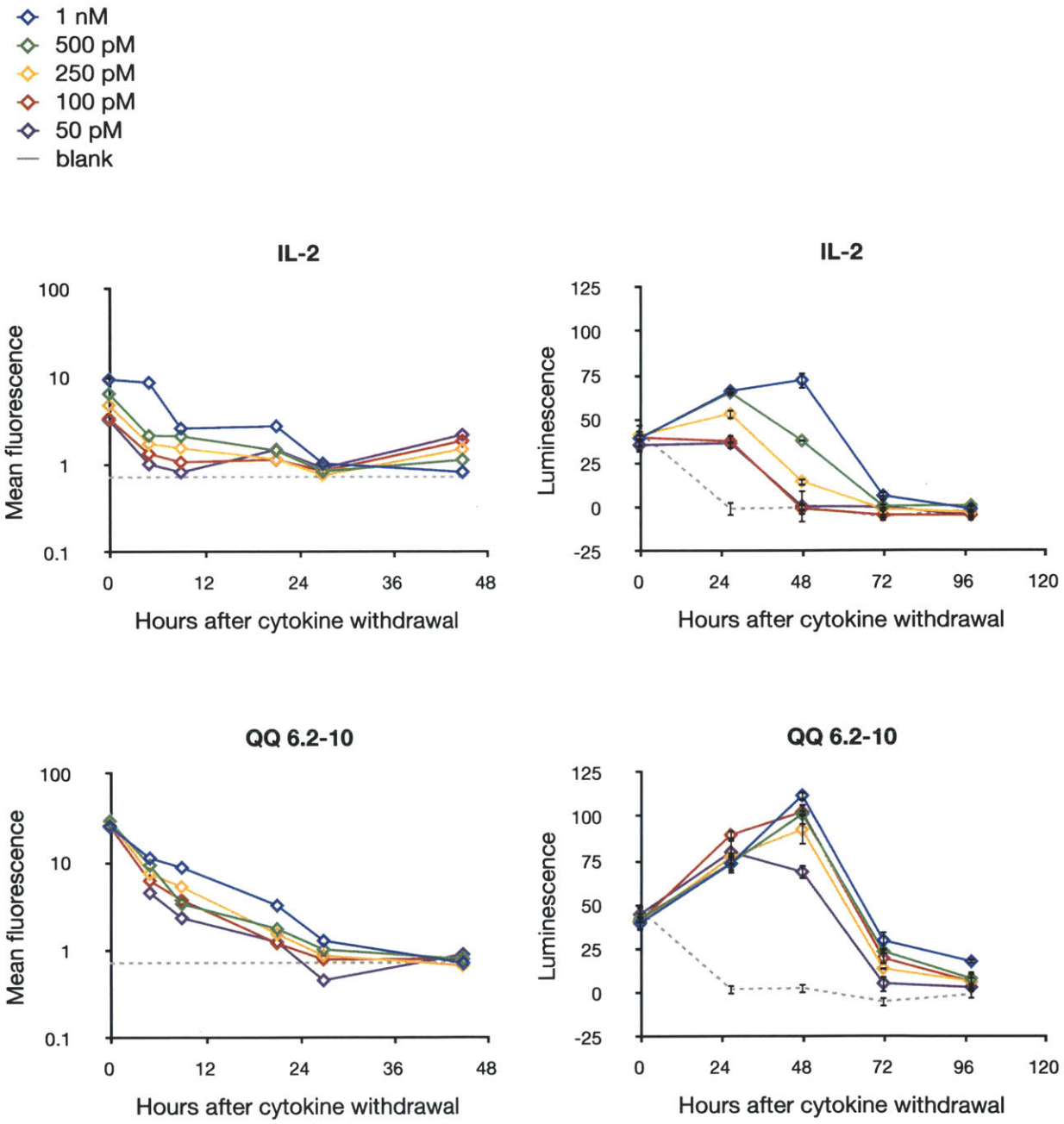

Figure 2-11: High-affinity CD25-binding mutant QQ 6.2-10 persists on T-cell surface and potently stimulates T-cell growth *in vitro*. CTLL-2 cells were stimulated with IL-2 (top) or QQ 6.2-10 (bottom) for 30 min and then transferred to cytokine-free media. After cytokine withdrawal, cytokine retained on the cell surface was detected using anti-FLAG antibody (left); cell culture viability was deduced from cellular ATP content, assayed by ATP-dependent luciferase activity (right).

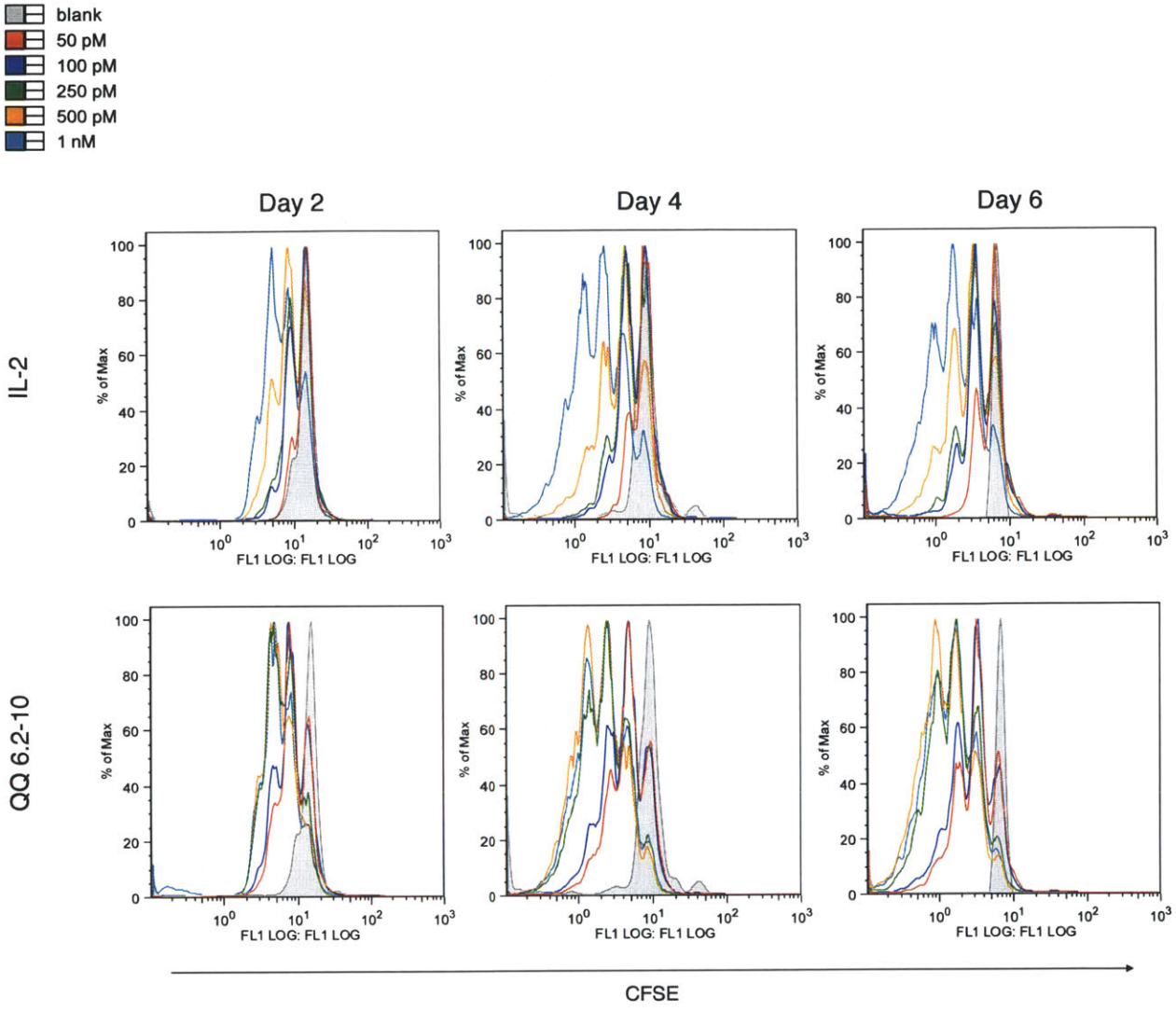

Figure 2-12: High-affinity CD25-binding mutant QQ 6.2-10 potently stimulates primary T-cell proliferation *in vitro*. 2C splenocytes were labeled with CFSE and pulsed for 30 min with IL-2 (top) or QQ 6.2-10 (bottom). Cell culture samples were analyzed for cellular CFSE content at indicated time points after cytokine withdrawal.

On pages 50-51:

Figure 2-13: High-affinity CD25-binding mutant QQ 6.2-10 fails to potently stimulate T cells *in vivo*. CFSE-labeled *in vivo*- (a) and *in vitro*-activated (b) 2C cells were treated with IL-2 or QQ 6.2-10 and adoptively transferred into C57BL/6 mice. (a) Two days after adoptive transfer, spleen and lymph node cells were stained with anti-2C TCR antibody 1B2 and anti-Thy1.2. CFSE profiles of gated cells are shown. (b) Three days after adoptive transfer, splenocytes were stained with anti-2C TCR antibody 1B2 and anti-CD8α. CFSE profiles of gated cells are shown. (c) IL-2 or QQ 6.2-10 were injected into prostates of TRAMP mice. Four days after injection, prostate tissues were harvested, digested, and stimulated with SIY peptide *in vitro* for intracellular IFN-γ staining.

(a)

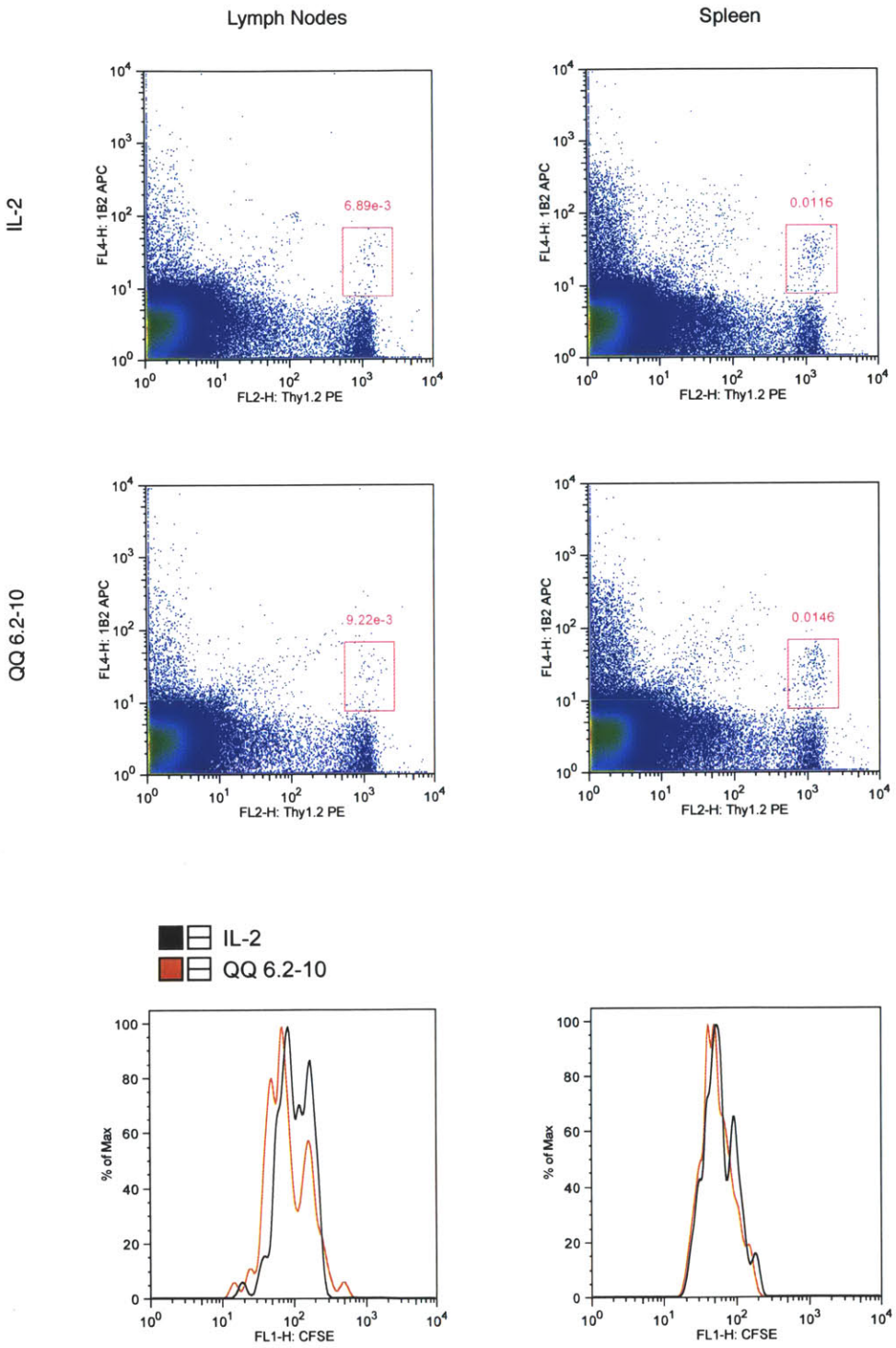
Lymph Nodes
Spleen
IL-2
QQ 6.2-10
6.89e-3
0.0116
9.22e-3
0.0146
FL4-H: 1B2 APC
FL2-H: Thy1.2 PE
IL-2
QQ 6.2-10
% of Max
FL1-H: CFSE

(b)

(c)

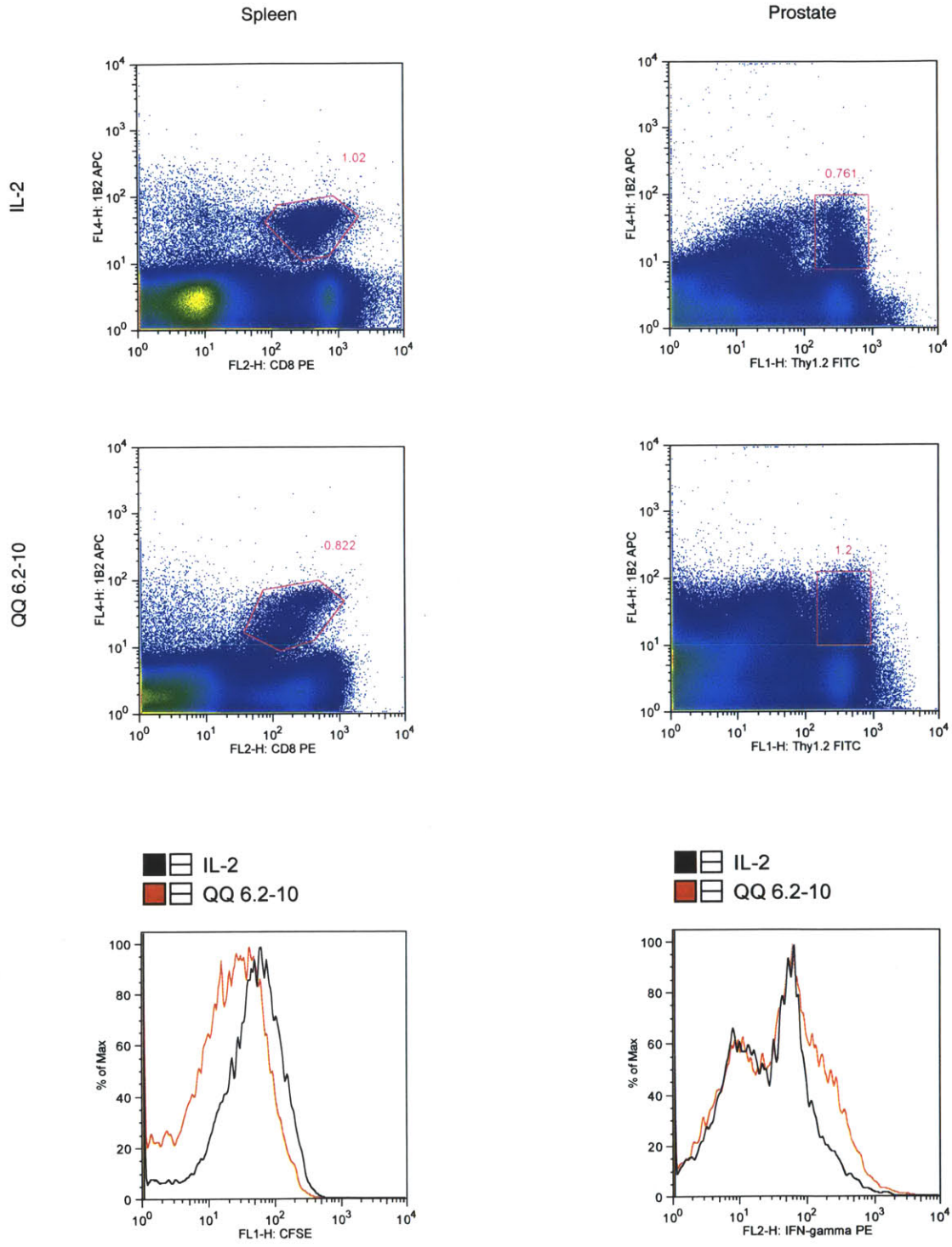
Spleen
Prostate
IL-2
QQ 6.2-10
FL4-H: 1B2 APC
FL2-H: CD8 PE
FL1-H: Thy1.2 FITC
1.02
0.761
0.822
1.2
IL-2
QQ 6.2-10
% of Max
FL1-H: CFSE
FL2-H: IFN-gamma PE

2.3.5. *IL-2 mutant QQ 6.2-10 dissociates and rebinds in* in vitro *assay*

We hypothesized that the discrepancy between the potent stimulation of T-cell growth by QQ 6.2-10 *in vitro* and its modest effects *in vivo* were due to an artifact of the *in vitro* assay. Specifically, in the *in vitro* assay, after cytokine withdrawal, cytokines that dissociate from CD25 have the opportunity to rebind and further signal, whereas *in vivo*, the rebinding probability is greatly reduced due to both the larger accessible volume as well as systemic clearance. Indeed, the addition of excess soluble CD25 to CTLL-2 cultures, to scavenge dissociated QQ6.2-10 after cytokine withdrawal, significantly reduced the amount of QQ 6.2-10 detectable on the cell surface and the ability of QQ 6.2-10 to prolong CTLL-2 survival (Figure 2-14). These results highlight the critical importance of proper *in vitro* assay design and data interpretation.

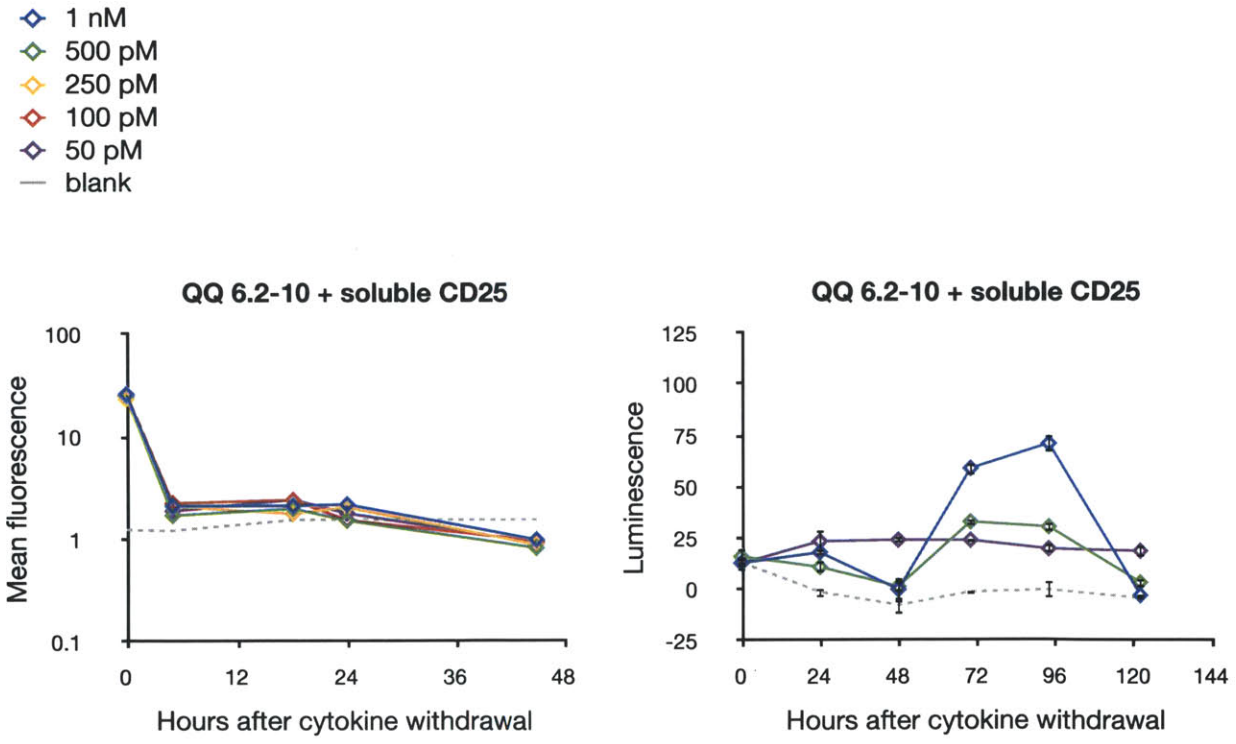

Figure 2-14: QQ 6.2-10 dissociates and rebinds following cytokine withdrawal in *in vitro* assays. CTLL-2 cells were pulsed for 30 min with QQ6 6.2-10 and resuspended in cytokine-free media with 10-fold excess soluble CD25. QQ 6.2-10 retained on the cell surface was detected using anti-FLAG antibody (left) and cell culture viability was measured by ATP-dependent luminescence assay (right).

2.3.6. *Extending IL-2 circulation lifetime via Fc fusion*

The IgG class of antibodies naturally exhibits long serum half-lives of 6 to 8 days due to selective salvaging by the neonatal Fc receptor (FcRn). FcRn binds IgG at the CH2-CH3 hinge region of the Fc fragment. (88) Therefore, in an effort to increase the persistence of IL-2 *in vivo*, we fused IL-2 and QQ 6.2-10 each to the Fc fragment of mouse IgG2a. Besides FcRn, the Fc fragment of IgG also interacts with Fcγ receptors (FcγR) and complement, leading to antibody-dependent cell-mediated cytotoxicity (ADCC) and complement-dependent cytotoxicity (CDC), respectively. As these effector functions are undesirable for this application, we mutated the aspartic acid at position 265 of the mouse IgG2a Fc to alanine (D265A), which has been shown to significantly reduce FcγR binding and complement activation (89).

Bivalent and monovalent IL-2 and QQ 6.2-10 fused to D265A mouse IgG2a Fc, designated bivalent and monovalent Fc/IL-2 and Fc/QQ6210, were purified from HEK293 cell culture supernatants and used to treat in vitro activated OT-I cells prior to adoptive transfer into RAG-deficient mice. In particular, congenically marked Thy1.2$^+$ and Thy1.1$^+$ OT-I cells, each treated with Fc/IL-2 or Fc/QQ6210, were transferred as a 50-50 mixture into a common host, to eliminate potential confounding effects of variability between hosts. The lack of endogenous T cells in RAG-deficient mice also significantly simplifies analysis of T-cell composition and may resemble conditions following lymphodepleting chemotherapy, in preparation for adoptive cell therapy. As shown in Figure 2-15, analysis of lymph node and spleen cells 2 and 9 days after transfer did not reveal any proliferative advantage to Fc/QQ6210 treatment over Fc/IL-2 treatment, for either the bivalent (Figure 2-15a) or monovalent (Figure 2-15b) fusion format.

(a)

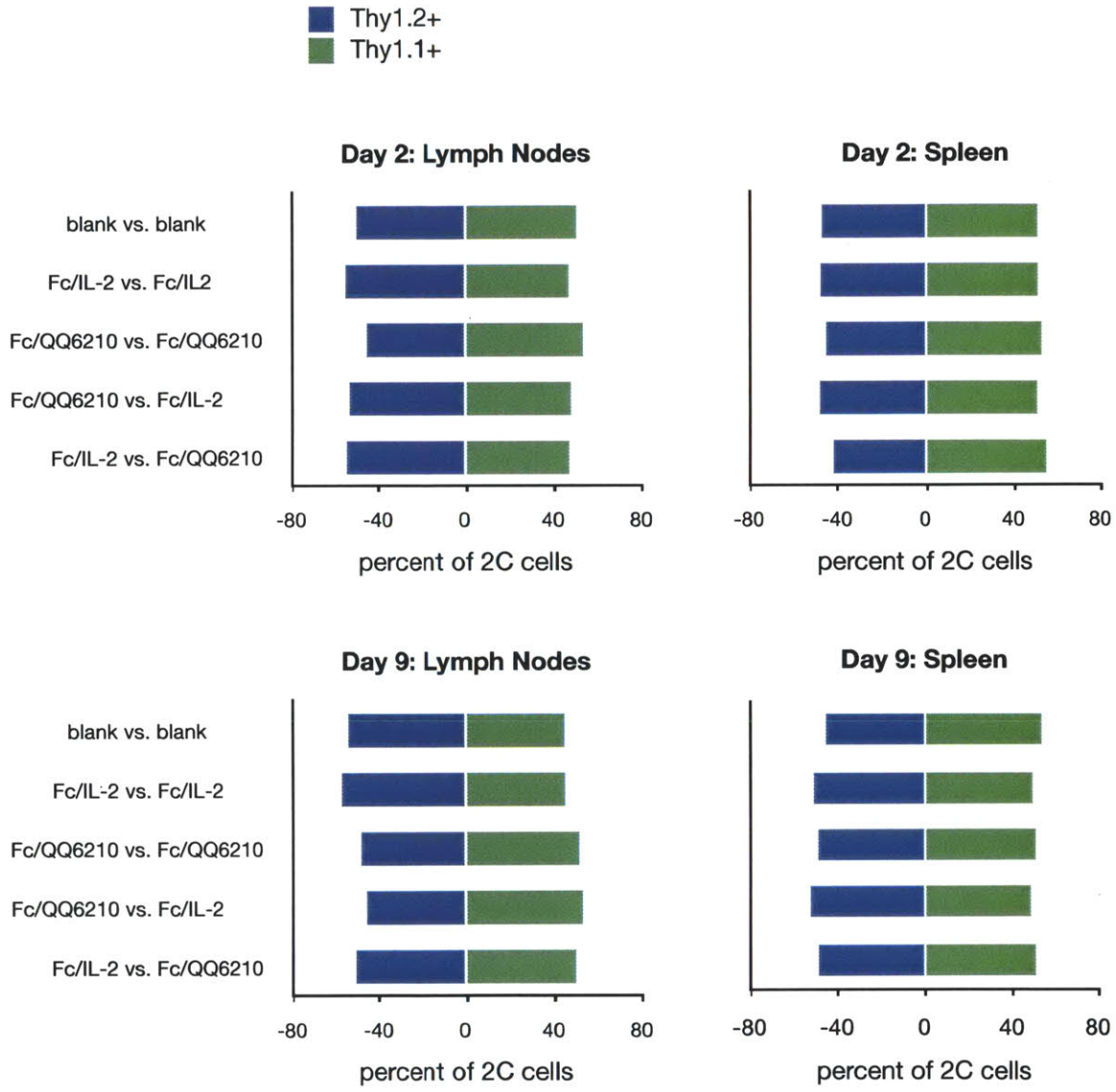

Figure 2-15: Comparable proliferation of Fc/IL-2- and Fc/QQ6210-treated OT-I cells in RAG-deficient mice. Thy1.2+ and Thy1.1+ OT-I cells pulsed with bivalent (a) or monovalent (b) Fc/IL-2 or Fc/QQ6210 were transferred into RAG-deficient mice as 50-50 mixtures. Two or nine days after adoptive transfer, composition of Thy1.2+ and Thy1.1+ cells in the lymph nodes and spleens were determined by flow cytometry. Cells were gated on TCR Vα2 expression; bars indicate the percentage of TCR Vα2-expressing cells that are also Thy1.2+ (negative values) or Thy1.1+ (positive values).

(b)

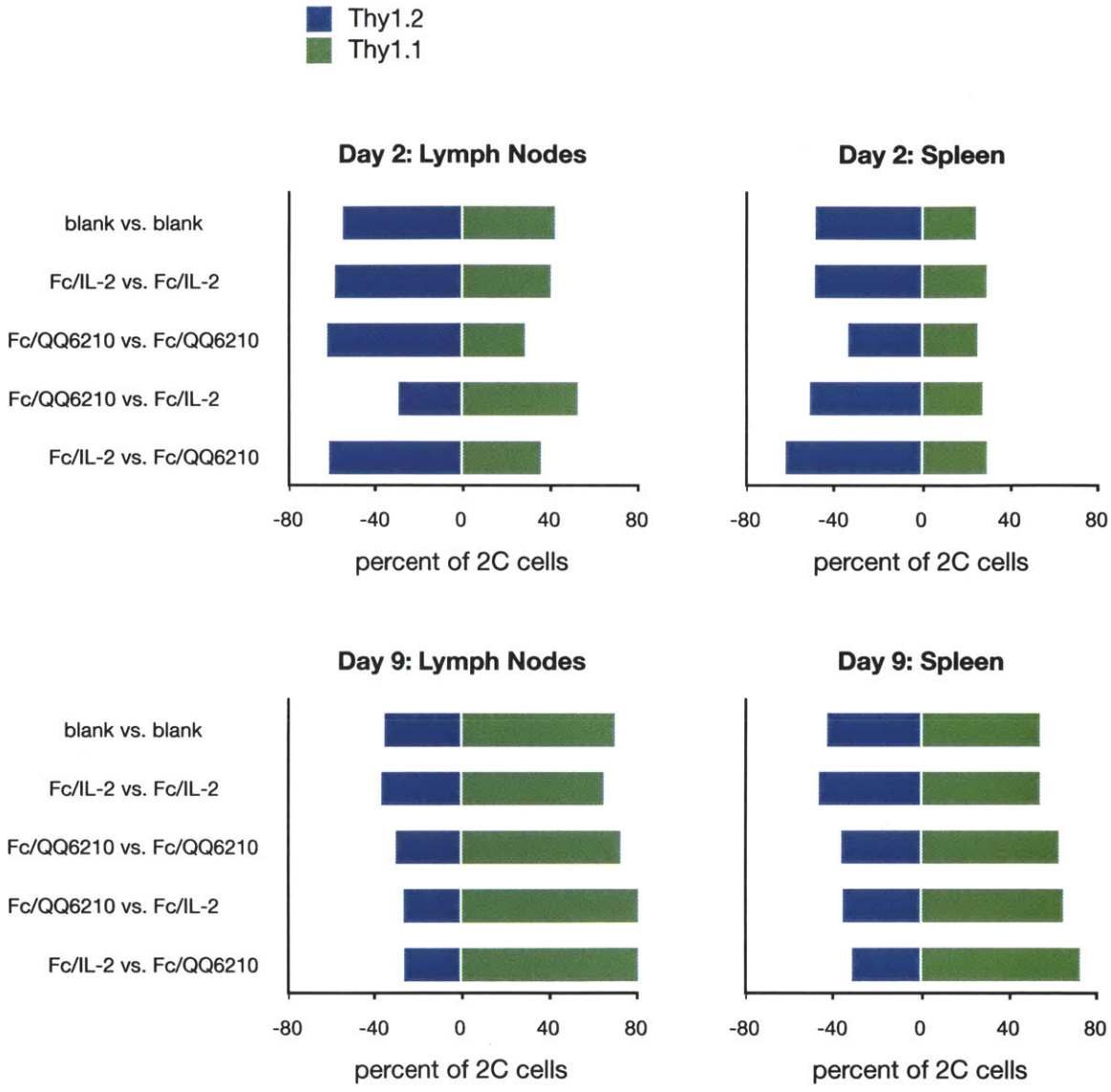
Thy1.2
Thy1.1
Day 2: Lymph Nodes
Day 2: Spleen
blank vs. blank
Fc/IL-2 vs. Fc/IL-2
Fc/QQ6210 vs. Fc/QQ6210
Fc/QQ6210 vs. Fc/IL-2
Fc/IL-2 vs. Fc/QQ6210
-80
-40
0
40
80
percent of 2C cells
Day 9: Lymph Nodes
Day 9: Spleen

2.3.7. *Cell-surface tethering of IL-2 potently stimulates T cell growth* in vitro

In another attempt at increasing the persistence of IL-2 at the T-cell surface, we tethered IL-2 directly to the cell using streptavidin sandwiches. Specifically, IL-2 was biotinylated site-specifically using sortase A and CTLL-2 cells were biotinylated at surface primary amines. Biotinylated IL-2 was then complexed with streptavidin, for tethering onto biotinylated CTLL-2 cells. As shown in Figure 2-16, compared to control conditions without streptavidin, CTLL-2 cells with tethered IL-2 retained more IL-2 on their surface and remained viable longer.

2.3.8. *Cell-surface biotinylation does not interfere with T cell trafficking* in vivo

To determine whether cell-surface biotinylation interferes with T-cell trafficking and localization to antigenic sites, OT-I T cells were biotinylated at , loaded with Alexa Fluor 647-conjugated streptavidin, and adoptively transferred into B6-albino mice bearing E.G7-OVA tumors. As shown in Figure 2-16a, biotinylated OT-I cells trafficked to tumor sites comparably to untreated OT-I cells, suggesting that cell-surface biotinylation does not significantly hinder T-cell trafficking. Moreover, biotinylated T cells bring their cargo with them, as indicated by the dose-dependent fluorescence detected in excised tumors, shown in Figure 2-16b.

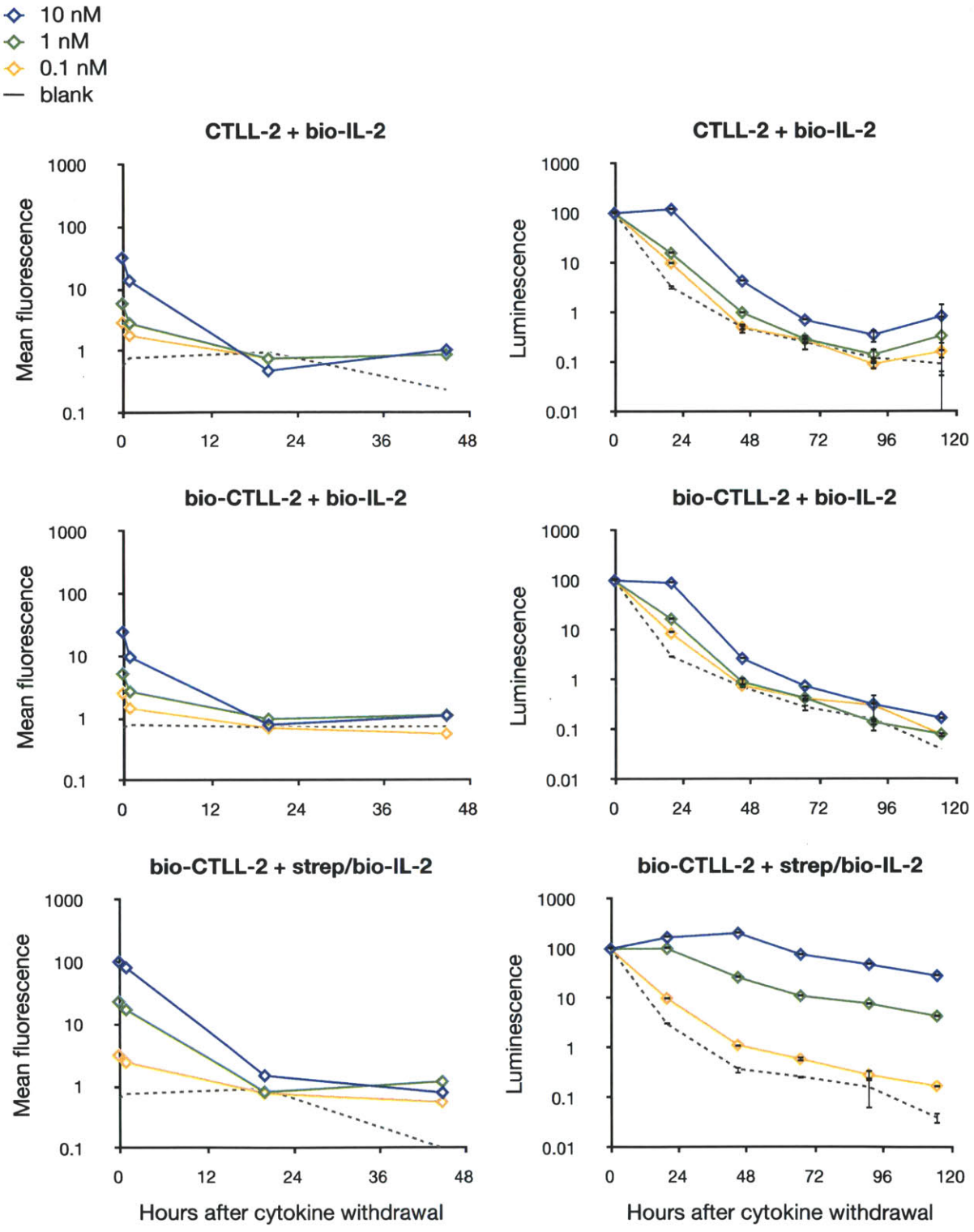

Figure 2-16: Cell surface tethered IL-2 potently stimulates T-cel growth *in vitro*. Untreated (top) or biotinylated (middle and bottom) CTLL-2 cells were treated with biotinylated IL-2 alone (top and middle) or complexed with streptavidin (bottom). IL-2 remaining on the cell surface was detected using anti-FLAG antibody (left) and cell culture viability was measured through ATP-dependent luminescence (right).

(a)

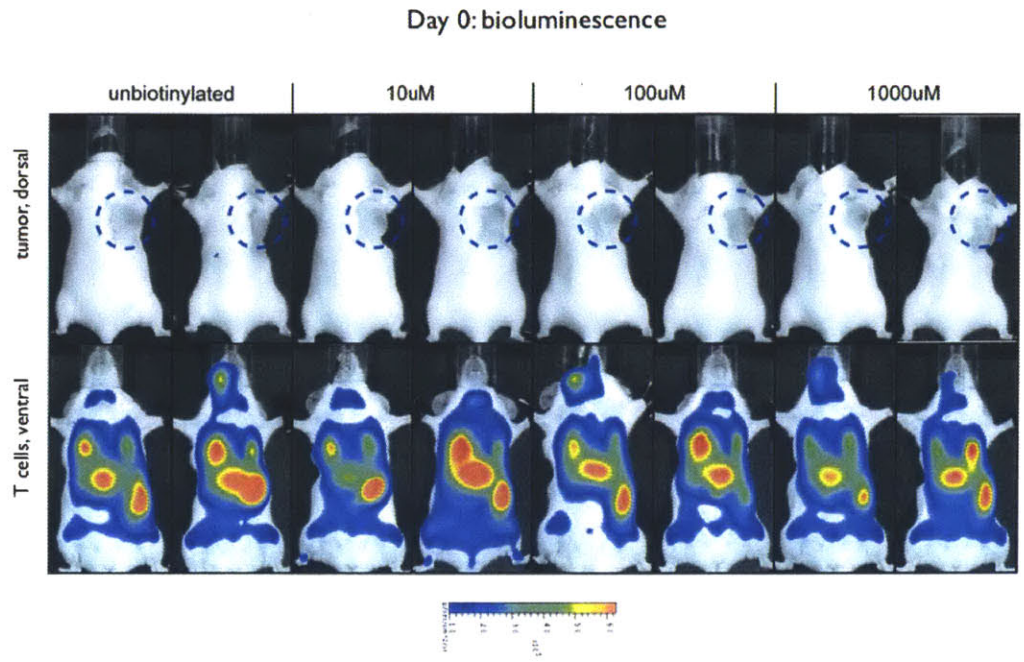
Day 0: bioluminescence
unbiotinylated
10uM
100uM
1000uM
tumor, dorsal
T cells, ventral

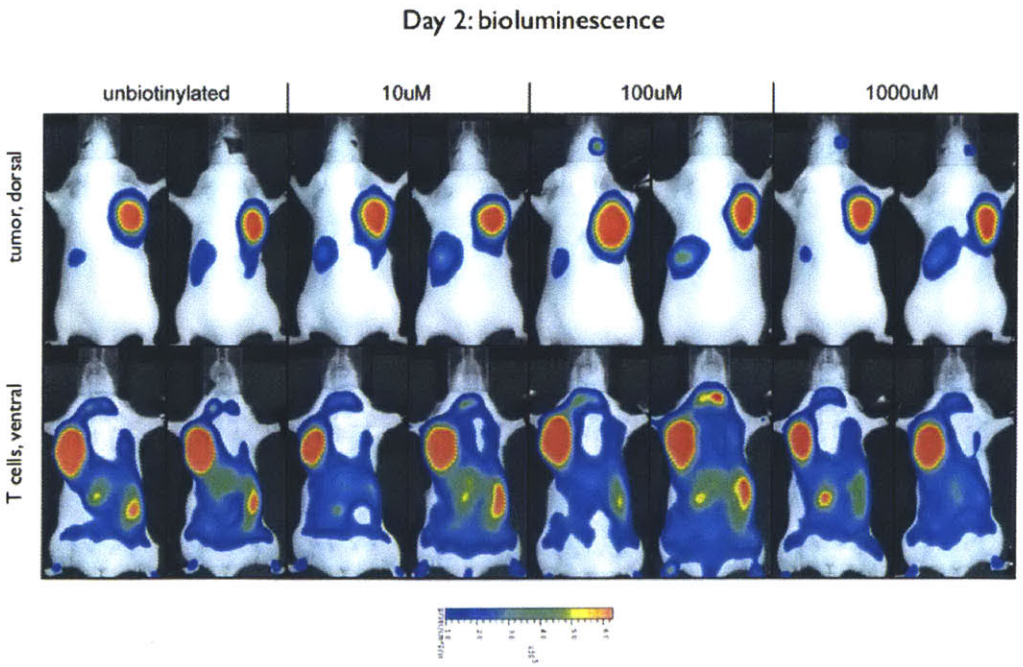
Day 2: bioluminescence
unbiotinylated
10uM
100uM
1000uM
tumor, dorsal
T cells, ventral

(b)

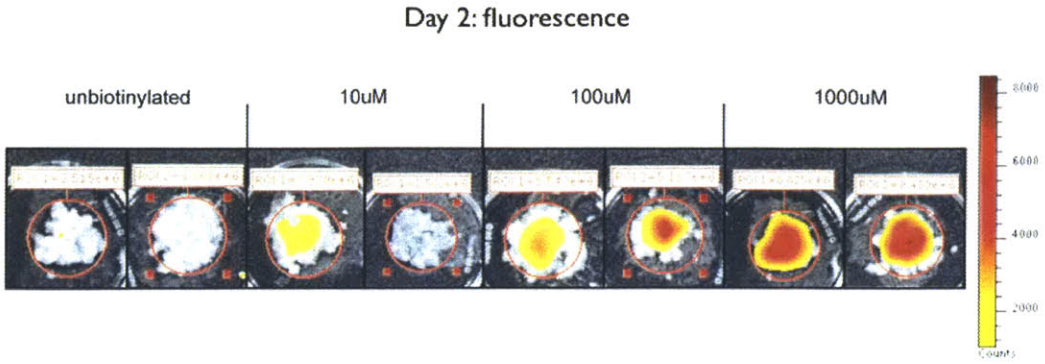

Figure 2-17: Biotinylated OT-I T cells traffick to OVA-expressing tumors. Splenocytes from firefly luciferase transgenic OT-I mice were biotinylated at 10, 100, or 100 μM sulfo-NHS-LC-LC-biotin, loaded with Alexa Fluor 647-conjugated streptavidin, and adoptively transferred into B6-albino mice bearing 7-day old subcutaneous E.G7-OVA tumors (n = 2 mice per group). (a) *In vivo* bioluminescence imaging of firefly luciferase expressing OT-I T cells immediately (top) and 2 days after (bottom) adoptive transfer. (b) *Ex vivo* fluorescence imaging of Alexa Fluor 647-conjugated streptavidin in excised tumors.

2.4. Discussion

Despite initial promising results from *in vitro* T-cell growth assays, we did not detect significant proliferative or functional advantage to treatment with high-affinity CD25-binding mutant QQ 6.2-10 *in vivo*. In particular, we evaluated the use of QQ 6.2-10 for stimulating both *in vivo*- and *in vitro*-activated T cells for adoptive transfer, as well as direct injection into animal tissue. The modest differences between wild-type IL-2 and high-affinity QQ 6.2-10 suggest that increasing the CD25 binding affinity by 500-fold is insufficient for improving IL-2 function *in vivo*. Furthermore, the extent of QQ 6.2-10 dissociation and rebinding after cytokine withdrawal clearly underscores the importance of proper *in vitro* assay design.

Extending the serum persistence of QQ 6.2-10 by fusion to antibody Fc did not reveal any significant advantage to high CD25-binding affinity either. However, it is important to note that cells treated with Fc/IL-2 and Fc/QQ6210 were transferred into RAG-deficient mice. While the lack of endogenous T cells in these animals enables facile analysis of transferred T-cell

populations, RAG-deficient mice have been reported to support the proliferation and differentiation of even naïve T cells, and without any exogenous IL-2 to boot (90). Our inability to detect any difference between Fc/IL-2 and Fc/QQ6210 treatment in this model is therefore not surprising; a standard lab mouse strain would have been better suited for our studies.

Tethering IL-2 directly onto the cell surface remains a promising approach to increase the persistence of IL-2 for potent stimulation of T-cell growth. Our *in vitro* viability assays indicate significant advantage to tethering IL-2 and our *in vivo* T-cell trafficking study suggests that T-cell trafficking is tolerant of extensive cell-surface modification. IL-2 tethering using streptavidin sandwiches, however, can serve only as a proof-of-concept, as streptavidin is severely immunogenic. Chemical conjugation via free thiols and amines on IL-2 or the cell surface is an potentially viable method for cell-surface tethering.

3. Effects of CD25 binding on IL-2 immune stimulation and toxicity

3.1. Introduction

Krieg and colleagues recently reported the expression of functional trimeric IL-2 receptors on the surface of lung endothelial cells and proposed that vascular leak syndrome resulting from IL-2 treatment is due to IL-2 stimulation of this cell type. The interaction of IL-2 with CD25 in particular was implicated in toxicity, as pulmonary edema was less severe in mice treated with anti-CD25 antibody, in CD25-deficient host mice, or in mice treated with IL-2 pre-complexed with an anti-IL-2 antibody proposed to preferentially direct IL-2 to cells expressing high levels of IL-2$\beta\gamma_c$ instead of CD25. Furthermore, relative to wild-type IL-2 and CD25-directed IL-2/anti-IL-2 antibody complexes, IL-2$\beta\gamma_c$-directed IL-2/anti-IL-2 antibody complexes were found to more potently expand memory phenotype $CD8^+$ T cells and NK cells as well as to more efficiently control tumor growth in mice. (65)

Because of the complexity of the IL-2/anti-IL-2 antibody complexes employed by Krieg *et al.*, it remains possible that mechanisms other than CD25 binding underly the observed differences in immune stimulation and toxicity between the different IL-2 treatments. To examine the effect of CD25 binding on IL-2 immunostimulatory activity and toxicity directly, we generated a panel of IL-2 with varying CD25 binding affinities, including wild-type IL-2, high-affinity CD25-binding QQ 6.2-10 (described in Chapter 2), and a rationally designed non-CD25 binding IL-2 mutant named E76G. In our evaluation of these cytokines, using murine CTLL-2 cells *in vitro* and C57BL/6 mice *in vivo*, we employed only proteins of mouse origin, in contrast to Krieg *et al.* who used IL-2 and antibodies of human origin.

3.2. Materials and Methods

3.2.1. *Design and characterization of non-CD25 binding IL-2 mutants*

Mutations at amino acid positions 76, 82, and 121 of IL-2 were introduced into pCT-mIL2 by PCR using oligonucleotides (Integrated DNA Technologies) containing the desired mutation. EBY100 yeast transformed with these clones were grown and induced as described in Chapter 2. Assessment of IL-2 expression and binding to soluble CD25 by flow cytometry were performed using anti-HA and anti-c-myc antibodies and soluble CD25, respectively, as before. Yeast-displayed proteins were denatured by incubating induced yeast at 80-90°C for 30 min. Anti-mouse IL-2 antibody S4B6 was a generous gift of Vinay Mahajan of the Chen Lab at MIT. Anti-mouse IL-2 antibodies JES6-1A12 and JES6-5H4 were purchased from eBioscience. Anti-IL-2 antibodies were detected using Alexa Fluor 488-conjugated goat anti-mouse IgG (Invitrogen).

3.2.2. *Expression and purification of monovalent Fc/IL-2 fusion proteins*[7]

Mutations E76A and E76G were introduced into gWIZ-Fc-IL-2 through QuikChange site-directed mutagenesis using oligonucleotides (Integrated DNA Technologies) containing the desired mutation. Monovalent Fc/IL-2 fusions were expressed in HEK293 cells and purified by sequential TALON His-tag metal affinity chromatography and anti-FLAG affinity chromatography as described in Chapter 2. Elution fractions were concentrated using 15-ml 30-kDa Amicon Ultra Centrifugal Devices (Millipore) and buffered exchanged into PBS.

Protein concentration was determined using the Beer-Lambert Law:

$$A = \varepsilon l c, \tag{3.1}$$

where A is the absorbance at 280 nm, ε is the extinction coefficient, l is the path length, and c is the sample concentration. Absorbance at 280 nm was measured using a NanoDrop 2000c (Thermo Scientific). The extinction coefficients and molecular weights of Fc/IL-2 fusion proteins were estimated from their amino acid sequences, shown in Table 3-1. Dynamic light scattering

[7] Dynamic light scattering of Fc/IL-2 proteins was performed by Tiffany F. Chen of the Wittrup Lab at MIT.

of purified Fc/IL-2 fusion proteins was performed using a DynaPro NanoStar Light Scatterer (Wyatt Technology); data was analyzed using Dynamics Software (Wyatt Technology).

Table 3-1: Extinction coefficients and molecular weights of monovalent Fc/IL-2 fusion proteins.

	Molecular weight (g/mol)	Extinction coefficient, ε (M^{-1} cm^{-1})
Fc/IL-2	72514.5	69870
Fc/QQ6210	72592.4	68380
Fc/E76G	72442.4	69870

3.2.3. *Cell culture*

CTLL-2 cells were cultured in RPMI-1640 with GlutaMAX, supplemented with FBS, sodium pyruvate, non-essential amino acids, HEPES, β-mercaptoethanol, and penicillin-streptomycin (Invitrogen). For maintenance, cells were passaged every other day to 100,000 cells/ml in media supplemented with 10 ng/ml wild-type mouse IL-2 (PeproTech). For viability assay, cells were passaged to 150,000 cells/ml in cytokine-free media, to which Fc/IL-2 fusion proteins were added to indicated concentrations. Cell culture viability was determined from culture samples using the CellTiter-Glo Luminescent Cell Viability Assay (Promega), following manufacturer's instructions. Luminescence was measured using an Infinite M1000 microplate reader (Tecan).

Cell surface expression of CD25 and IL-2Rβ (CD122) were detected using FITC-conjugated rat anti-CD25 IgG, clone 3C7 (BD Pharmingen), and rat anti-CD122 IgG, clone TM-β1 (BD Pharmingen) followed by Alexa Fluor 488-conjugated goat anti-mouse IgG (Invitrogen), respectively. Receptor expression levels were quantified using Quantum Simply Cellular anti-Rat IgG beads (Bangs Laboratories) as standard.

3.2.4. *Mice*

C57BL/6 mice (The Jackson Laboratory) were housed in the animal facility of the Koch Institute at MIT and used at 8 to 10 weeks of age. Experiments were performed in the context of an

animal protocol approved by the MIT Division of Comparative Medicine, in accordance of federal, state, and local guidelines.

3.2.5. *Pharmacokinetics*

Fc/IL-2 fusions were labeled with IRDye 800CW (LI-COR Biosciences) according to manufacturer's instructions. Unreacted dye was removed using Zeba desalting columns (Thermo Scientific). Labeled proteins, 50 μg in 100 μl PBS per dose, were administered i.v. by retro-orbital injection. At time = 0, 0.5, 1, 3, 5, 8, 24, 48, and 96 hours after injection, blood samples were collected from the tip of the tail into heparin-coated capillary tubes (VWR International). Samples were stored at 4°C, protected from light, until analysis.

On the day of analysis, blood samples were centrifuged (5 min at 1500 x g at 4°C) to remove cellular components. The plasma was transferred to fresh capillary tubes and scanned using an Odyssey Infrared Imaging System (LI-COR Biosciences). Signal was acquired in the 800 nm channel. Using the image processing program ImageJ (US National Institutes of Health), each sample was approximated as a line of width 2 and the mean intensity along was line was determined. The mean fluorescence intensities were then fit to a biexponential decay:

$$MFI(t) = Ae^{-\alpha t} + Be^{-\beta t} \tag{3.2}$$

where MFI is the mean fluorescence intensity, t is time, and A, α, B, and β are constant free parameters to be fitted.

3.2.6. *Flow cytometry*

6 μg IL-2 or 25 μg Fc/IL-2, Fc/QQ6210, or Fc/E76G, each in 100 μl PBS, were injected retro-orbitally into C57BL/6 mice. Four days after injection, mice were euthanized by CO_2 asphyxiation.

Single-cell suspensions of spleen were prepared by rubbing spleen between two frosted microscope slides. Red blood cells were lysed with ammonium chloride and passed through mesh filters to remove hair and debris. Cells were labeled with CellTrace Calcein Violet

(Invitrogen) and PE-conjugated anti-CD3, clone 145-2C11 (eBioscience), APC-conjugated anti-CD4, clone RM4-5 (BD Biosciences), Alexa Fluor 647-conjugated anti-CD8α, clone 53-6.7 (Biolegend), and/or APC-conjugated anti-NK1.1, clone PK136 (eBioscience) in PBS with 0.1% (w/v) BSA. For intracellular Foxp3 staining, cells were labeled with Pacific Blue-conjugated anti-CD4, clone GK.5 (Biolegend) and PE-conjugated anti-CD25, clone PC61 (Biolegend) antibodies, fixed and permeabilized using the Foxp3 Fix/Perm Buffer Set (Biolegend) according to manufacturer's instructions, and then stained with Alexa Fluor 647-conjugated anti-Foxp3, clone MF-14 (Biolegend).

Samples were analyzed using a LSR II flow cytometer using FACS Diva software (BD Biosciences). Flow cytometry data was analyzed using FlowJo software (Tree Star). Total cell number per spleen was calculated based on number of cells processed by the cytometer and the fraction of splenocyte suspension analyzed.

3.2.7. *Pulmonary wet weight*

Four days after injection of Fc/IL-2 fusion proteins, lungs were extracted and placed into scintillation vials. Samples were weighed, frozen in liquid nitrogen, and lyophilized for 48 hours at room temperature under vacuum. Pulmonary wet weight was calculated by subtracting the sample weight after lyophilization from the initial sample weight.

3.3. Results

3.3.1. *Rational design of non-CD25 binding IL-2*

Inspection of the mouse IL-2 / IL-2 receptor complex homology model, described in Chapter 2, revealed three amino acid residues in intimate contact with CD25: glutamic acid at position 76 (E76), histidine at position 82 (H82), and glutamine at position 121 (Q121), shown in Figure 3-1. To disrupt CD25 binding, each of these residues was mutated to one of four alternative amino acids that differ from the wild-type residue in size, polarity, or charge: R/F/A/G in place of E76; E/S/A/G in place of H81; or R/S/A/G in place of Q121.

These 12 mutants were displayed on the surface of yeast and tested for CD25 binding by labeling with soluble CD25 at 5 or 50 nM. While all H82 and Q121 mutants retained CD25 binding capacity, no CD25 binding was detected for E76 mutants, shown in Figure 3-2c. Labeling of E76 mutants with anti-mouse IL-2 antibodies, with or without thermal denaturation, suggested that mutants E76A and E76G are well-folded proteins with no detectable binding even at 50 nM soluble CD25. Specifically, anti-IL-2 antibody JES6-1A12 binds yeast-displayed IL-2 both before and after thermal denaturation, indicating that it is not conformation-specific. Anti-IL-2 antibodies S4B6 and JES6-5H4 bind native IL-2, but not denatured IL-2, suggesting that they are both conformation-specific antibodies. In their native form, IL-2 mutants E76R and E76F are not recognized by either S4B6 or JES6-5H4, while E76A and E76G are both recognized by S4B6, but not JES6-5H4. Both S4B6 and JES6-5H4 have been reported to complex with IL-2 to selectively promote the expansion of IL-2R$\beta\gamma_c^+$ cells and are thought direct preferential IL-2R$\beta\gamma_c$-binding by IL-2 through themselves binding IL-2 near the CD25 binding site. Loss of recognition by these antibodies could therefore indicate disruption of overall protein folding or of only the CD25 binding site. The partial retention of S4B6 folding by E76A and E76G suggests that they are likely to be properly folded. E76A and E76G were therefore chosen for further characterization *in vitro*.

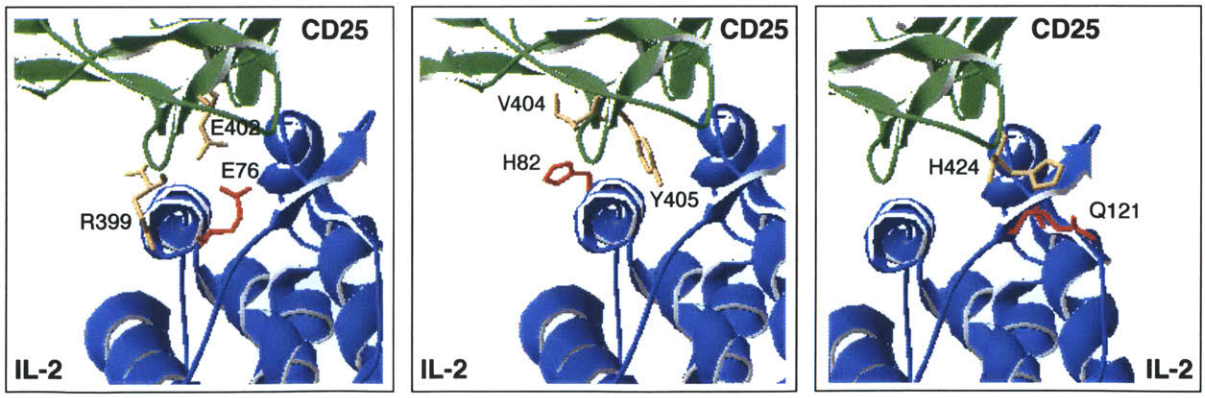

Figure 3-1: Rational design of non-CD25 binding IL-2. IL-2 residues glutamic acid 76 (left), histidine 82 (middle), and glutamine 121 (right), shown in red, are in intimate contact with CD25. IL-2 is shown in blue; CD25 is shown in green. Model was generated using SWISS-MODEL (75).

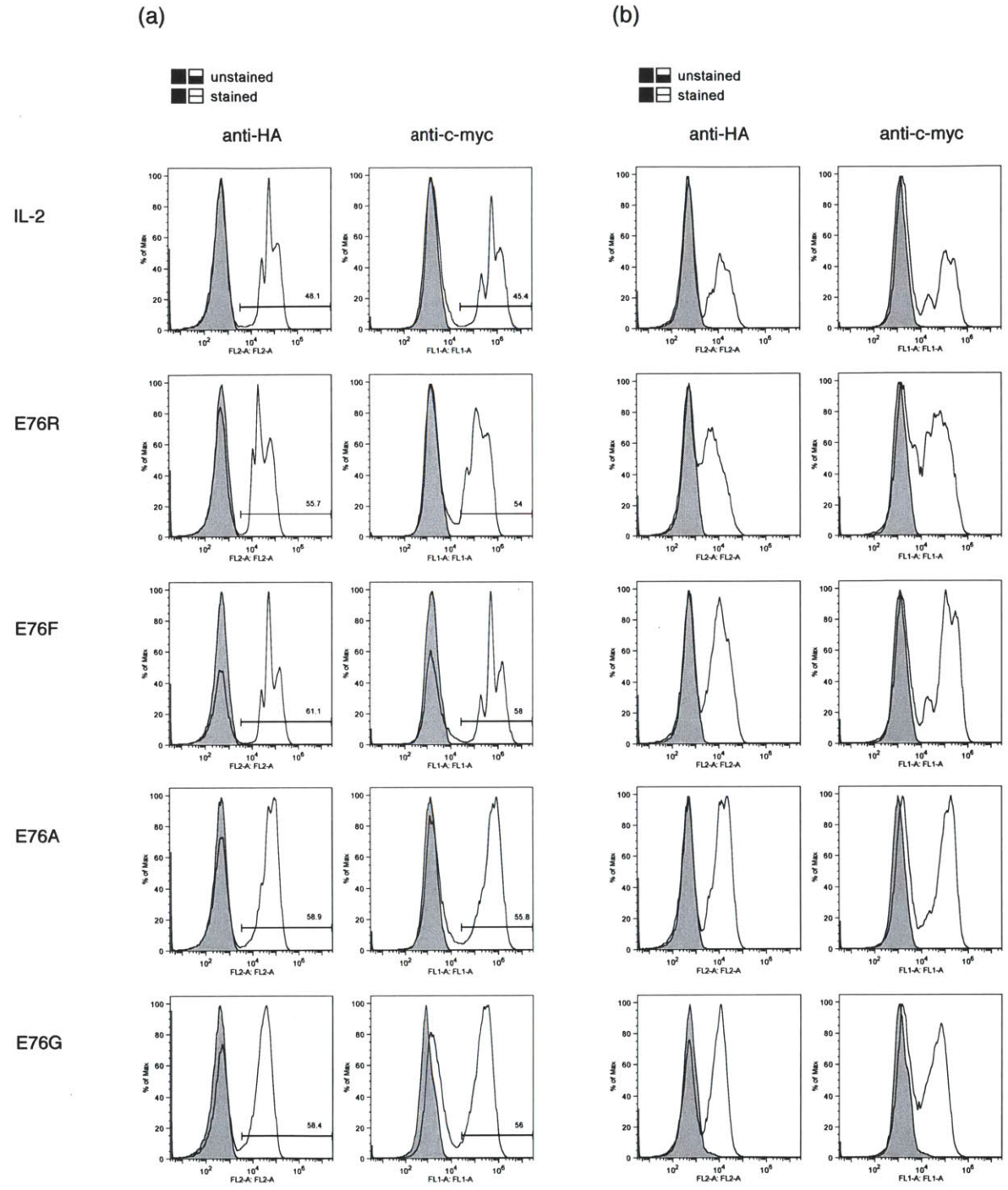

Figure 3-2: Single amino acid substitutions E76A and E76G in IL-2 ablate CD25 binding without disrupting protein fold. Detection of yeast surface displayed IL-2 and IL-2 mutants using anti-HA and anti-c-myc antibodies, before (a) and after (b) thermal denaturation of yeast-displayed proteins. Binding of 50 nM soluble CD25 and anti-IL-2 antibodies S4B6, JES6-1A12, JES6-5H4 to yeast-displayed IL-2 and IL-2 mutants before (c) and after (d) thermal denaturation.

(c)

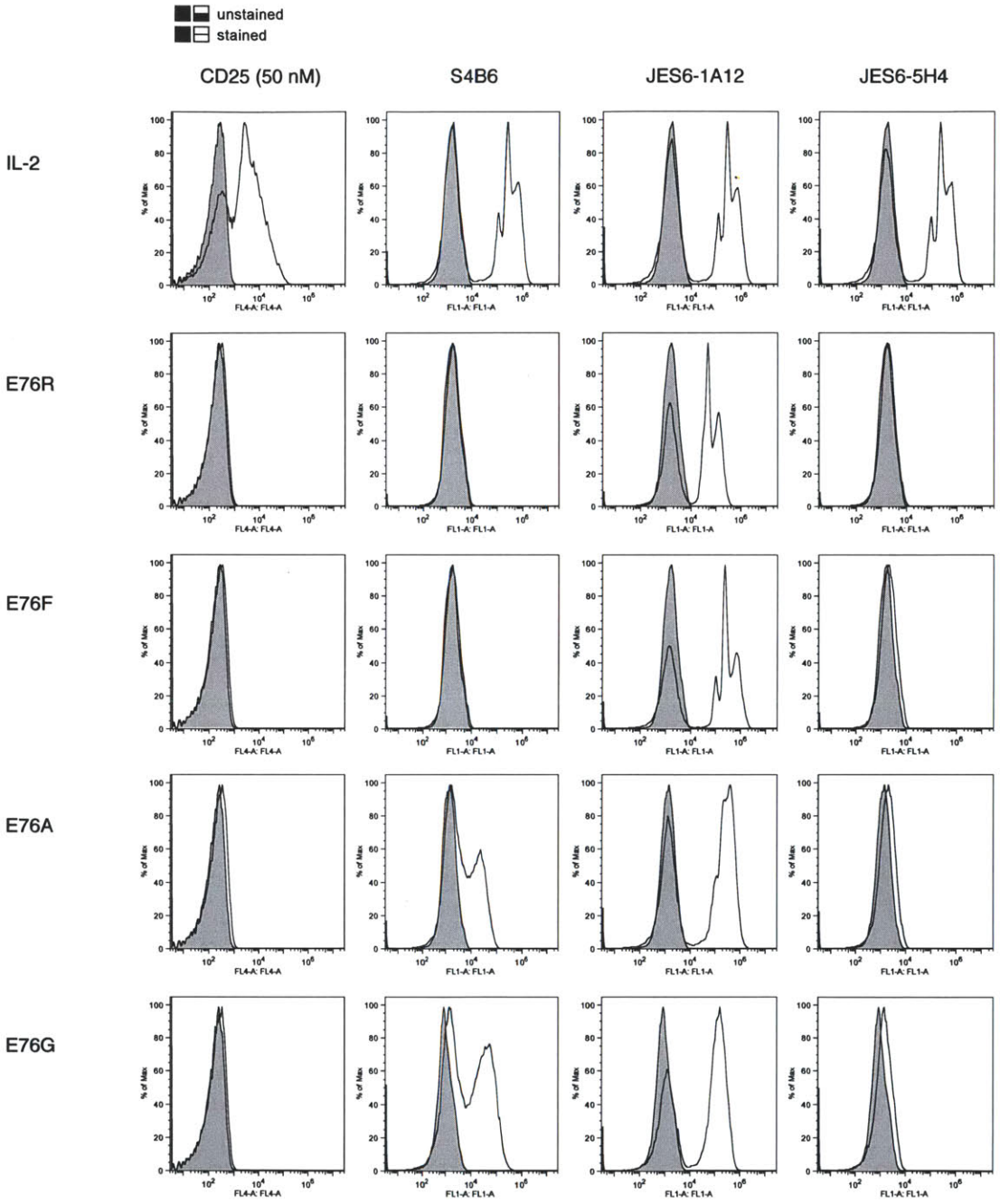
unstained
stained
CD25 (50 nM)
S4B6
JES6-1A12
JES6-5H4
IL-2
E76R
E76F
E76A
E76G
% of Max
FL4-A: FL4-A
FL1-A: FL1-A

(d)

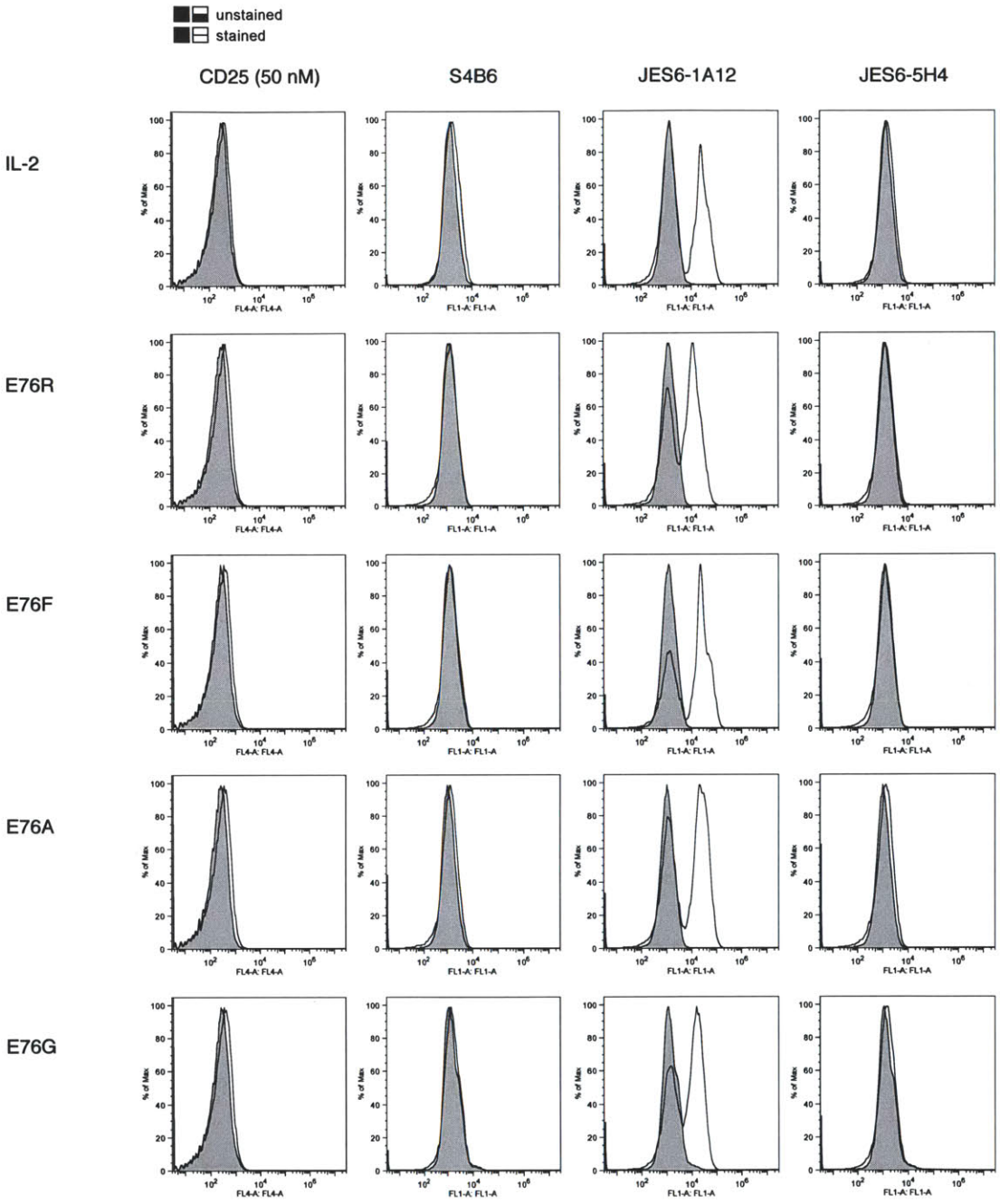
unstained
stained
CD25 (50 nM)
S4B6
JES6-1A12
JES6-5H4
IL-2
E76R
E76F
E76A
E76G
% of Max
FL4-A: FL4-A
FL1-A: FL1-A

3.3.2. *Production of monovalent Fc/IL-2 fusion proteins*

To evaluate the effect of CD25 binding on IL-2 bioactivity, IL-2 and the IL-2 mutants QQ 6.2-10, E76A, and E76G were expressed as fusions to antibody Fc containing the D265A mutation to reduce Fc activation of ADCC and CDC (89). Monovalent forms of these fusion proteins were purified and are henceforth referred to as Fc/IL-2, Fc/QQ6210, Fc/E76A, and Fc/E76G, or as Fc/IL-2 fusion proteins collectively. Monodispersity of the purified proteins was confirmed by dynamic light scattering (DLS), shown in Figure 3-3.

Fc/IL-2

Peak	R (nm)	%Pd	MW-R (kDa)	%Int	%Mass
1	5.3	19	167	34.8	97.9
2	18.7	54.7	3202	63.8	2.1
3	3733.9	0	767932000	1.4	0

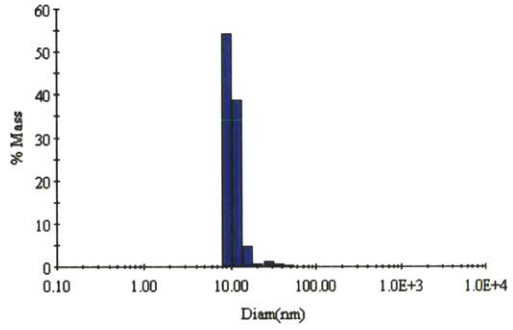

Fc/E76A

Peak	R (nm)	%Pd	MW-R (kDa)	%Int	%Mass
1	6.2	66.2	238	96.2	99.9
2	3733.9	0	767932000	3.8	0.1

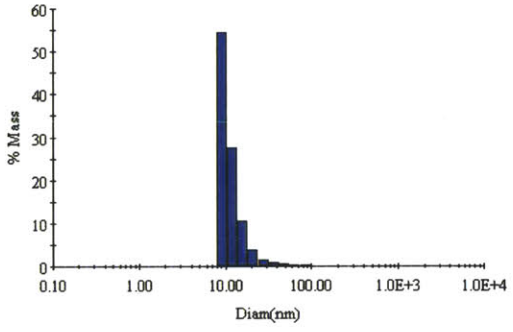

Fc/QQ6210

Peak	R (nm)	%Pd	MW-R (kDa)	%Int	%Mass
1	6	73.3	223	100	100

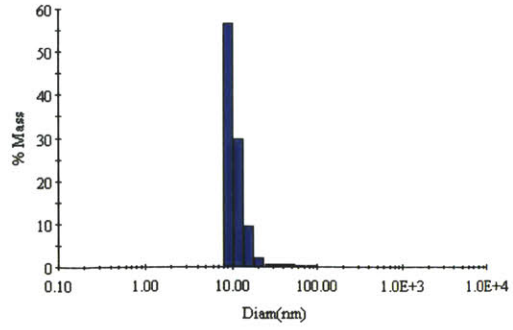

Fc/E76G

Peak	R (nm)	%Pd	MW-R (kDa)	%Int	%Mass
1	6.4	67.6	256	100	100

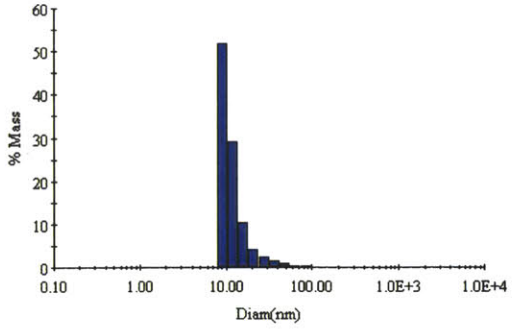

Figure 3-3: Purified monovalent Fc/IL-2 fusion proteins are monodisperse by DLS analysis.

3.3.3. *Monovalent Fc/IL-2 fusion proteins stimulate CTLL-2 cell growth*

To verify that IL-2 and IL-2 mutants remain functional in Fc fusion format, IL-2 dependent CTLL-2 cells were cultured with Fc/IL-2, Fc/QQ6210, Fc/E76A, or Fc/E76G at 100 pM, 1 nM, and 10 nM. As shown in Figure 3-4, under static conditions, all Fc/IL-2 fusion proteins support CTLL-2 growth, suggesting that IL-2 and the IL-2 mutants are functional as Fc fusions. In particular, the ability of Fc/E76A and Fc/E76G to support CTLL-2 is further indication that they are well-folded proteins with functional IL-2R$\beta\gamma_c$ signaling capacity. The different growth kinetics resulting from Fc/E76A and Fc/E76G stimulation is likely due to their inability to bind CD25, since IL-2R$\beta\gamma_c$ binds IL-2 with 100-fold lower than trimeric IL-2R$\alpha\beta\gamma_c$ and CD25 is present at much higher levels, approximately 10^6 copies per cell compared to IL-2Rβ's $5x10^4$ copies per cell. Fc/E76G was selected for further characterization *in vivo*.

3.3.4. *Fc/IL-2 fusion proteins exhibit prolonged circulation half-life*

Fc/IL-2 fusion proteins labeled with IRDye 800 were injected intravenously into mice as a 50-μg bolus. Analysis of blood samples collected over four days after injection, shown in Figure 3-5 and Table 3-2, indicates that all Fc/IL-2 fusions exhibit significantly prolonged circulation half-life compared to IL-2.

Table 3-2: Pharmacokinetic properties of monovalent Fc/IL-2 fusion proteins

	A	B	α (hr^{-1})	β (hr^{-1})	$t_{½,\alpha}$ (hr)	$t_{½,\beta}$ (hr)
Fc/IL-2	0.50 ± 0.15	0.70 ± 0.53	0.12 ± 0.08	0.05 ± 0.01	1.9 ± 0.9	16.4 ± 3.6
Fc/QQ6210	0.44 ± 0.11	0.07 ± 0.02	0.19 ± 0.01	0.02 ± 0.00	3.6 ± 0.2	34.3 ± 3.2
Fc/E76G	0.71 ± 0.05	0.16 ± 0.02	0.25 ± 0.06	0.03 ± 0.00	3.0 ± 0.7	25.4 ± 1.8

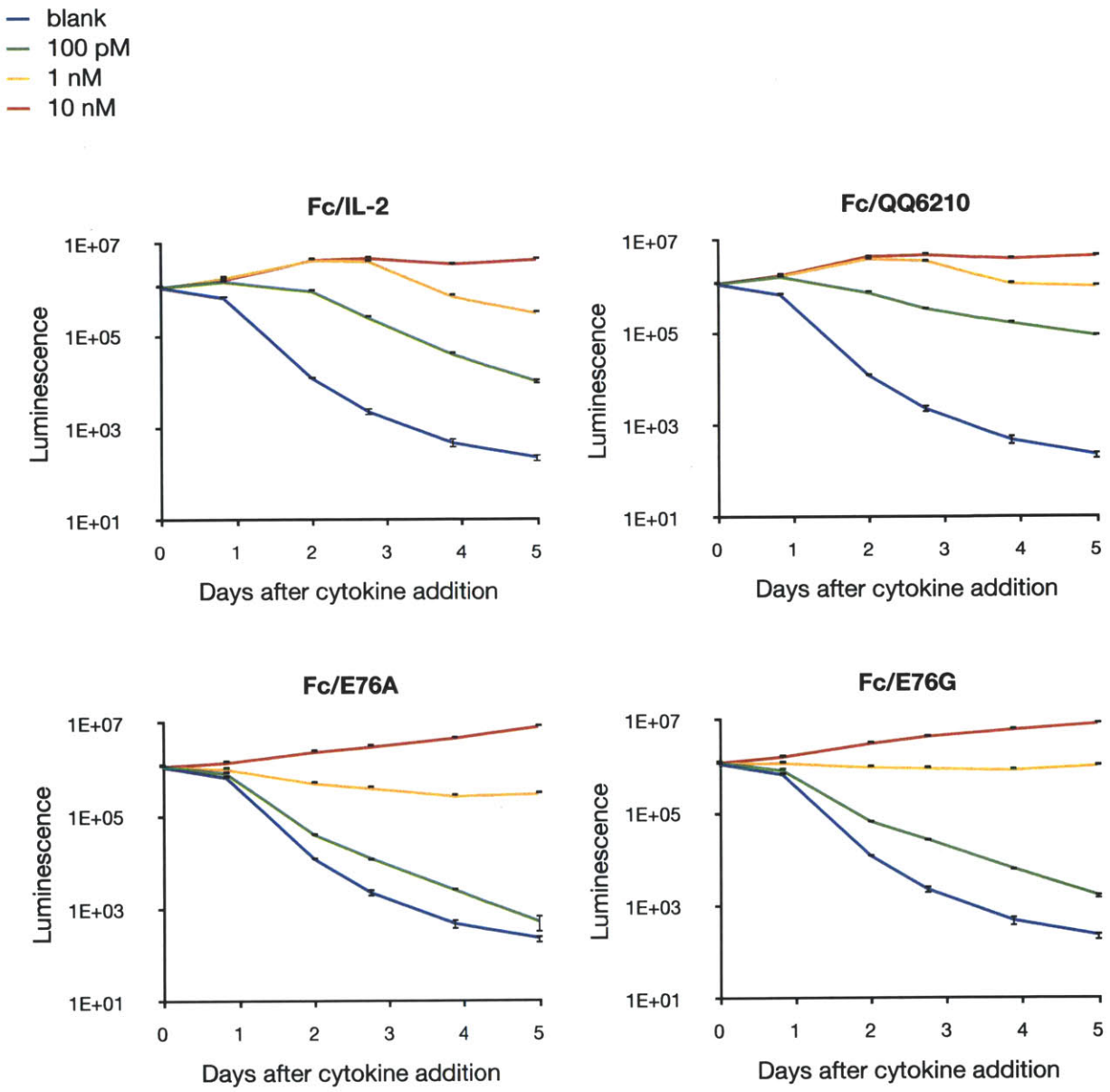

Figure 3-4: Fc/IL-2 fusion proteins functionally signal through IL-2 receptor. Fc/IL-2, Fc/QQ6210, Fc/E76A, or Fc/E76G were added to cytokine-free CTLL-2 cultures at time $t = 0$. Samples were removed from cultures over five days to measure viability through stimulation of ATP-dependent luciferase activity. Error bars represent standard deviation for measurements of three samples.

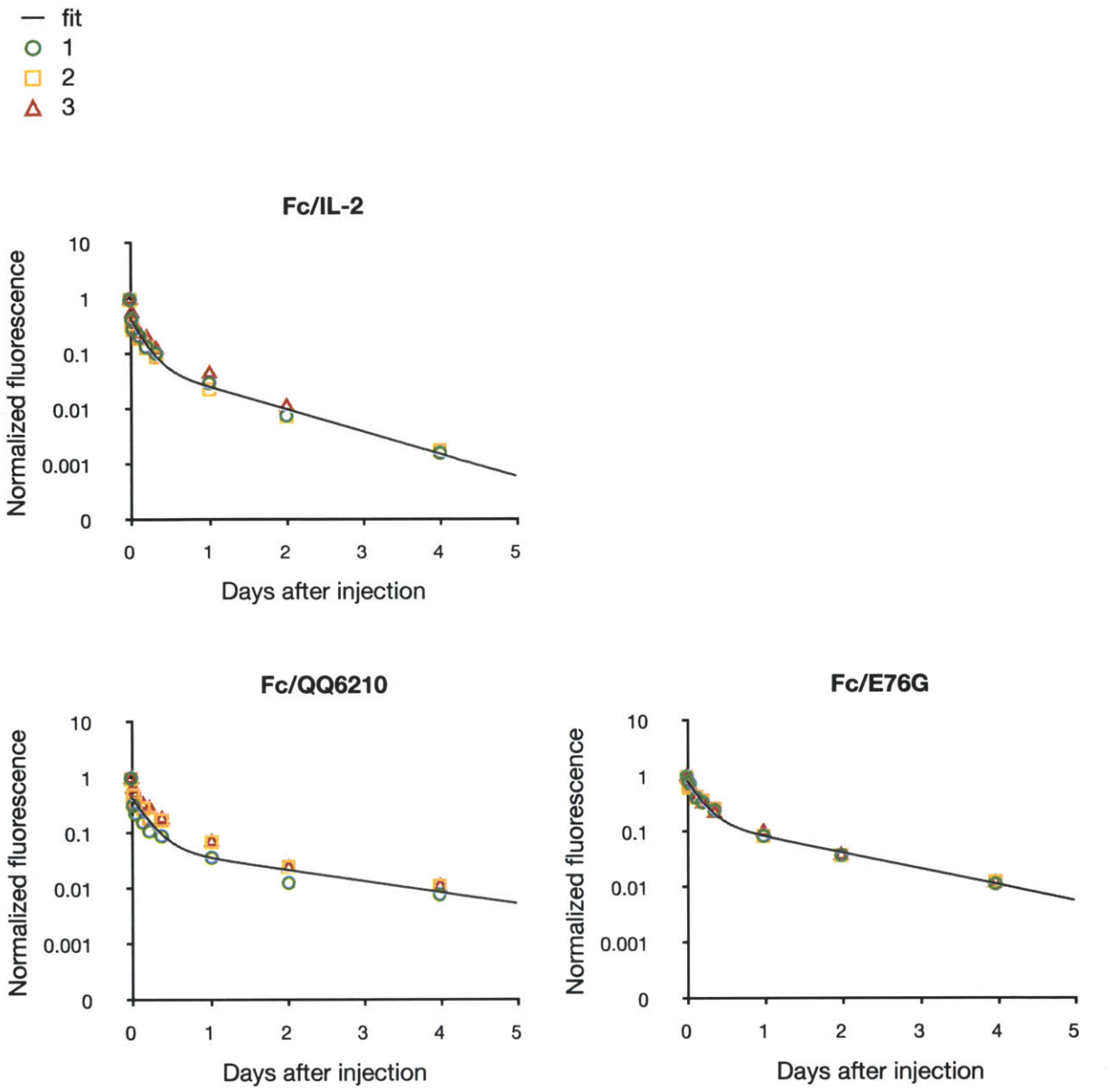

Figure 3-5: Fc/IL-2 fusion proteins exhibit prolonged plasma persistence. Fc/IL-2 fusion proteins labeled with IRDye 800 were injected intravenously into mice (n = 3 mice per group) as a 50-µg bolus. Blood samples were collected over 4 days after injection and plasma fluorescence levels were measured. Symbols indicate measurements; lines indicate theoretical curve fits. Fluorescence measurements were normalized to the maximum signal from each Fc/IL-2 clone.

3.3.5. *Non-CD25 binding Fc/E76G stimulates NK cell expansion*

To evaluate effect of CD25 binding affinity on the immunostimulatory activity and toxicity of IL-2, C57BL/6 mice were injected intravenously with 25 μg each of Fc/IL-2, Fc/QQ6210, or Fc/E76G, or 6 μg IL-2 or PBS as controls. Four days after injection, all mice treated with Fc/IL-2 fusion proteins exhibited significantly enlarged spleens, shown in Figure 3-6. Analysis of splenocytes by flow cytometry showed that Fc/IL-2 and Fc/QQ6210 expanded $CD8^+$ T cell and NK cells approximately 2-fold compared to PBS and IL-2 treatment, while Fc/E76G expanded these populations up to 5-fold. The notable expansion of $CD8^+$ T and NK cells further validates functional IL-2R$\beta\gamma_c$ binding by E76G.

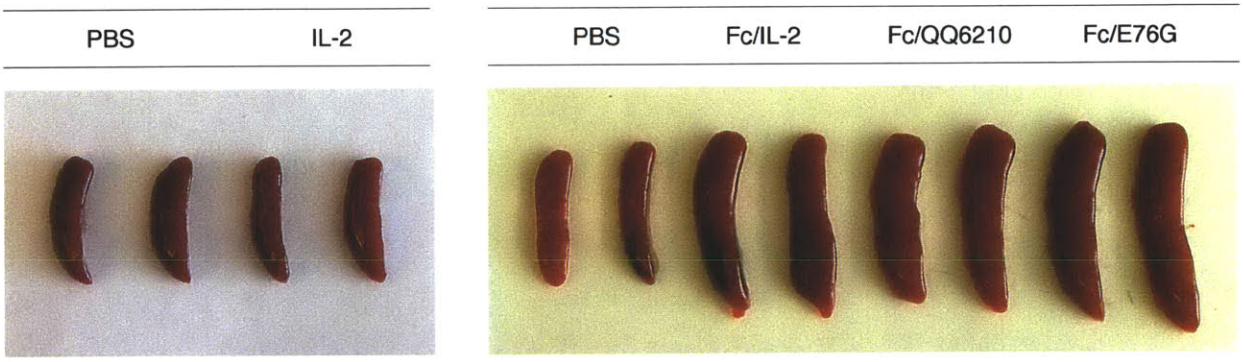

Figure 3-6: Fc/IL-2 and mutants induce splenomegaly. C57BL/6 mice (n = 3 mice per group) were injected intravenously with PBS, 6 μg IL-2, or 25 μg of Fc/IL-2, Fc/QQ6210, or Fc/E76G. Four days after treatment, spleens were analyzed for T and NK cell composition. Two representative spleens per group are shown.

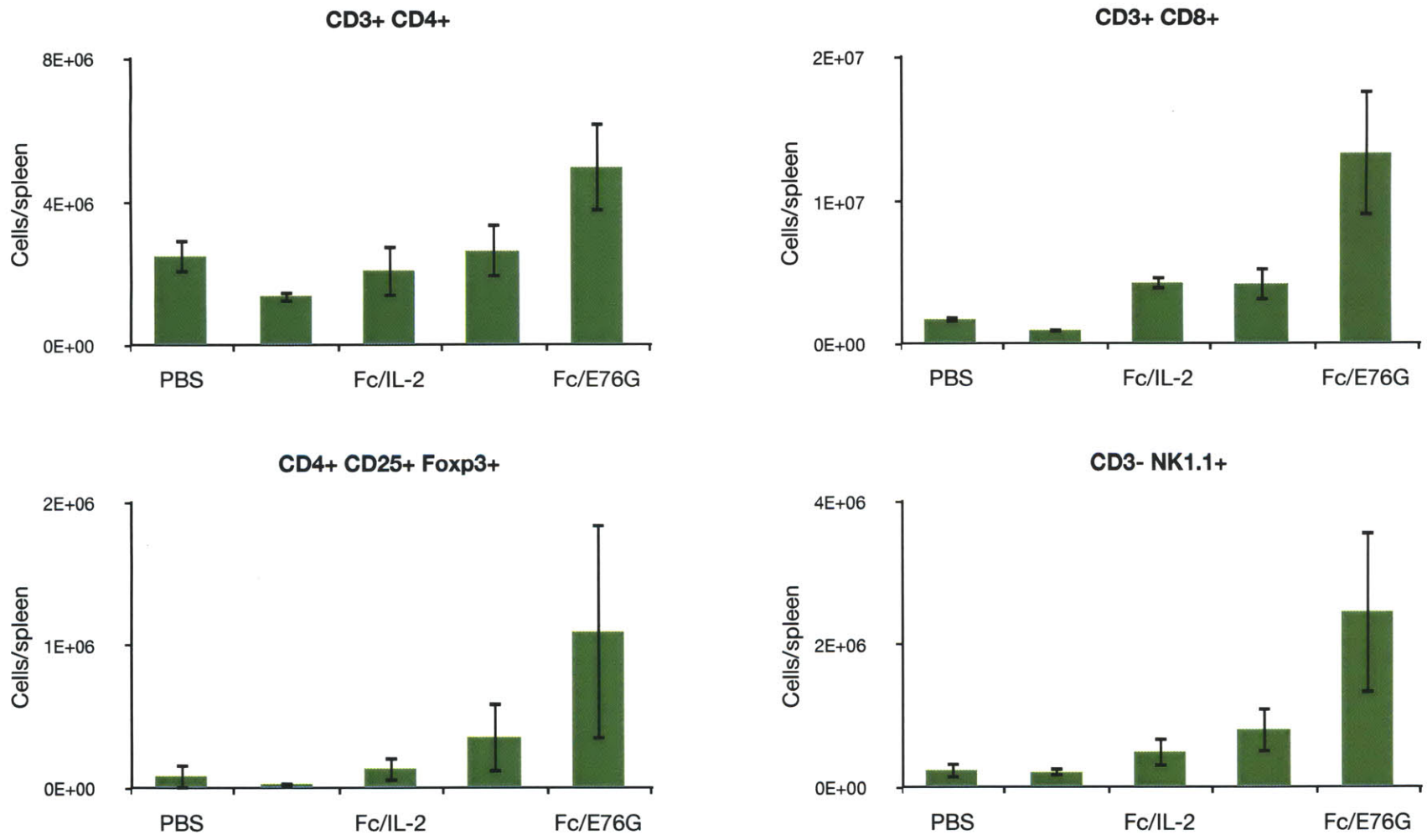

Figure 3-7: Fc/IL-2 fusion proteins stimulate CD8⁺ T-cell and NK-cell expansion. C57BL/6 mice (n = 3 mice per group) were injected intravenously with PBS, 6 μg IL-2, or 25 μg of Fc/IL-2, Fc/QQ6210, or Fc/E76G. Four days after treatment, spleens were analyzed for T and NK cell composition by flow cytometry.

3.3.6. *Ablation of CD25 binding affinity increases IL-2 toxicity*

As shown in Figure 3-8, four days after treatment with 6 μg IL-2 or 25 μg Fc/IL-2, Fc/QQ6210, or Fc/E76G, mice treated with Fc/E76G showed the most significant weight loss relative to PBS-treated controls. Lung wet weight, an indicator for pulmonary edema, was comparable between all treatment groups.

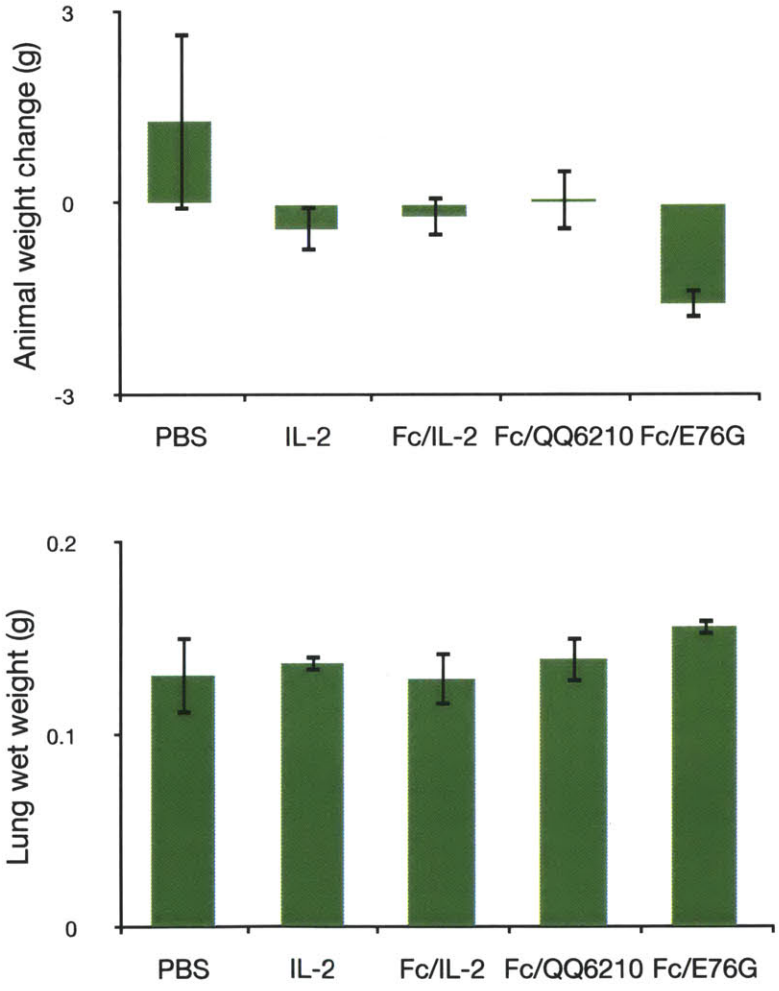

Figure 3-8: Ablation of CD25 binding affinity increases IL-2 toxicitiy. Whole animal weight (top) and lung wet weight (bottom) of C57BL/6 mice (n = 3 mice per group) 4 days after intravenous administration of PBS, 6 μg IL-2 or 25 μg Fc/IL-2, Fc/QQ6210, or Fc/E76G.

3.4. Discussion

Using a set of IL-2 variants with a range of CD25 binding affinities, we found ablation of CD25 binding to significantly expand the $CD8^+$ T and NK cell populations. However, in contrast to the conclusions of Krieg *et al.*, we find disruption of CD25 binding to significantly increase toxicity, as indicated by whole animal body weight. Our data shows a correlation between NK cell expansion and IL-2 treatment toxicity, consistent with many previous reports (39, 91).

4. Synergistic Tumor Control by Fc/IL-2 and Antibody TA99

4.1. Introduction

The potent expansion of $CD8^+$ T cells and NK cells by Fc/E76G led us to evaluate the potential of Fc/IL-2 fusion proteins as agents for cancer immunotherapy. We chose the B16 murine melanoma as our model of study, as it has been extensively characterized and is well-established to be highly aggressive in C57BL/6 mice. Derived from a spontaneous tumor in a C57BL/6 mouse at the Jackson Laboratory in 1954 (92), B16 melanoma is poorly immunogenic, with no MHC class II expression and very low expression levels of MHC class I. Moreover, the sub-line B16-F10 has been specifically selected for high metastatic potential (93, 94).

Considerable efforts have been made to treat B16 melanomas. These include passive immunization with antibody TA99, which is a murine IgG2a antibody that recognizes the melanosome antigen tyrosinase-related protein-1 (Tyrp-1) and is of identical specificity as an antibody originally isolated from the serum of a melanoma patient (95, 96), PEGylated IL-2 (97), complexes of IL-2 with anti-IL-2 antibodies (65), and high-affinity IL2Rβ-binding IL-2 (98). While delays in tumor growth were observed, durable cures were not achieved.

More effective approaches have recently been reported by Restifo and colleagues using tripartite therapy, consisting of (1) adoptive transfer of pmel-1 TCR transgenic T cells, which recognize pmel-17, an enzyme involved in pigment synthesis, expressed by the majority of melanoma cells as well as normal melanocytes; (2) viral vaccination against tumor antigen; and (3) administration of exogenous IL-2 (48, 99). Comparable efficacy have been reported for tripartite combination therapy using adoptive transfer of pmel-1 T cells, viral vaccination against tumor antigen, and administration of antibody TA99 (100). Importantly, cells, vaccination, or cytokine or antibody given alone or any two in combination were insufficient to induce tumor destruction (99, 100).

4.2. Materials and Methods

4.2.1. *Protein production*

Monovalent Fc/IL-2 fusion proteins were produced using HEK293 cells and purified by sequential his-tag immobilized metal affinity chromatography and anti-FLAG immunoaffinity chromatography as described in Chapter 3.

XL1-Blue cells harboring gWIZ plasmids encoding the heavy and light chains of antibody TA99, with the mouse IgG2a heavy chain and kappa light chain, were gifts of Cary F. Opel of the Wittrup Lab at MIT. Plasmid DNA was purified from cell cultures using PureLink HiPure Maxiprep Kit (Invitrogen) and sterile filtered. TA99 was expressed in HEK293 cells (Invitrogen) according to manufacturer's instructions. Briefly, HEK293 cells were co-transfected with gWIZ-TA99-HC and gWIZ-TA99-LC using polyethylenimine in FreeStyle 293 media supplemented with OptiPro (Invitrogen). Seven days post transfection, culture supernatants were harvested by centrifugation at 15,000 x g for 30 min at 4°C and sterilized by filtration through 0.22 μm filters (Nalgene). Antibody was purified from HEK293 culture supernatants using Protein A Agarose (Genescript) according to manufacturer's instructions. Elution fractions were concentrated using 15-ml 30-kDa Amicon Ultra Centrifugal Devices (Millipore) and buffered exchanged into PBS. Protein purity was verified by Coomassie Brilliant Blue staining of SDS-PAGE gels using SimplyBlue SafeStain (Invitrogen) and western blotting using peroxidase-conjugated Fc fragment-specific goat anti-mouse IgG (Thermo Scientific). Protein concentration was determined using a NanoDrop 2000c (Thermo Scientific) on the "IgG" setting.

4.2.2. *Cell culture*

The mouse melanoma cell line B16-F10 was a gift of Darrell J. Irvine (MIT). Cells were cultured in DMEM supplemented with FBS, L-glutamine, and pen-strep at 37°C with 5% CO_2. At approximately 70 percent confluency, cells were lifted off of plates using 0.035% trypsin and EDTA. Digestion was quenched with media and the cells pelleted by centrifugation at 1000 rpm. For passaging, cells were resuspended in media to 10^6 cells per 10 ml. For tumor inoculation, cells were resuspended in PBS to 10^6 cells per 50 μl. Cells were verified to be mycoplasma-free

by PCR amplification. Before tumor inoculation, cells were verified to express tyrosinase-related protein 1 (TRP-1) by labeling with antibody TA99 followed by Alexa Fluor 488-conjugated goat anti-mouse IgG (Invitrogen) for analysis by flow cytometry.

4.2.3. *Mice*

C57BL/6 mice (The Jackson Laboratory) were housed in the animal facility of the Koch Institute at MIT and used at 8 to 10 weeks of age. Experiments were performed in the context of an animal protocol approved by the MIT Division of Comparative Medicine, in accordance of federal, state, and local guidelines.

On the day of tumor inoculation, animals were anesthetized with isoflurane. Patches of fur were shaved from the left or right flanks to expose skin. 10^6 cells in 50 μl PBS were injected subcutaneously using 27G1/2 syringe and needle. Every other day following tumor inoculation, the mice were weighed and their tumors measured using digital calipers.

Tumor volumes were calculated using the modified ellipsoid volume formula:

$$tumor\ volume = \tfrac{1}{2}\, l\, w^2\,, \tag{4.1}$$

where l is the longest dimension of tumor and w is the longest dimension perpendicular to l.

Treatment with IL-2 (PeproTech), Fc/IL-2 fusions, and/or TA99 was initiated immediately following tumor inoculation or 6 days later, as indicated in the text. IL-2 (6 μg), Fc/IL-2 fusions (25 μg), and TA99 (100 μg) were each injected retro-orbitally in 100 μl PBS per dose.

4.2.4. *Immune cell depletion*

Rat anti-mouse CD8a (clone 2.43) and mouse anti-mouse NK1.1 (clone PK136) antibodies were purchased from Bio X Cell. Four days after tumor inoculation, and every 4 days thereafter, 400 μg antibody in 100 μl PBS were injected intra-peritoneally.

Cell-type depletion was verified by analysis of splenocytes 4 days after antibody injection by flow cytometry. Single-cell suspensions of spleen were prepared by rubbing spleen between two frosted microscope slides. Red blood cells were lysed with ammonium chloride

and passed through mesh filters to remove hair and debris. Cells were labeled with CellTrace Calcein Violet (Invitrogen) and PE-conjugated anti-CD3, clone 145-2C11 (eBioscience), Alexa Fluor 647-conjugated anti-CD8α, clone 53-6.7 (Biolegend), and/or APC-conjugated anti-NK1.1, clone PK136 (eBioscience) in PBS with 0.1% (w/v) BSA. Samples were analyzed using a LSR II flow cytometer using FACS Diva software (BD Biosciences). Flow cytometry data was analyzed using FlowJo software (Tree Star).

4.2.5. *Histology*

Kidneys, livers, lungs, and spleens were fixed in 10% formalin overnight, embedded in paraffin, sectioned at 6 μm, and stained with hematoxylin and eosin. Tumors were cut in half: one half was fixed and stained as organs above; the other was embedded in O.C.T. media, frozen in isopentane in liquid nitrogen, and sectioned at 6 μm.

4.3. Results

4.3.1. *Scouting for Fc/IL-2 and TA99 treatment conditions*

Given the documented toxicity of IL-2 therapy, and our uncertainty about the efficacy of Fc/IL-2 fusion proteins in controlling B16-F10 tumors, we first scouted for tolerable and effective treatment conditions using one mouse per condition. As shown in Figure 4-1, we initiated therapy at the time of tumor inoculation ("early treatment") or six days after tumor inoculation, when tumor nodules were visible and palpable ("late treatment"). We administered 50 μg of Fc/IL-2, Fc/QQ6210, or Fc/E76G per dose, which had previously well- tolerated in single-dose pharmacokinetics studies, and administered subsequent doses every 3 days. Under this treatment regimen, Fc/IL-2 was lethal upon the fourth or third dose, for early and late treatment, respectively; Fc/QQ6210 was well-tolerated; while Fc/E76G was extremely toxic, being lethal upon the second dose for both therapy initiation times.

To reduce toxicity, we halved each dose to 25 μg while maintaining the dose frequency at once every 3 days, shown in Figure 4-2a. Dose reduction alone did not significantly diminish toxicity, as Fc/E76G remained lethal upon the second dose. We therefore reduced the dose

frequency to once weekly. In all remaining mice, including one treated with Fc/E76G starting six days after tumor inoculation, this regimen did not cause severe visible discomfort.

We likewise scouted for tolerable and effective treatment conditions for Fc/IL-2 fusion proteins in combination with 100 μg antibody TA99, shown in Figure 4-2b. As above, 25 μg Fc/E76G with TA99 once every three days was lethal upon the second dose, while reducing the frequency to once weekly was well-tolerated. Encouragingly, Fc/IL-2 treatment alone and Fc/IL-2 treatment in combination with TA99 delayed tumor growth relative to PBS-treated controls, even when therapy was initiated six days after tumor inoculation.

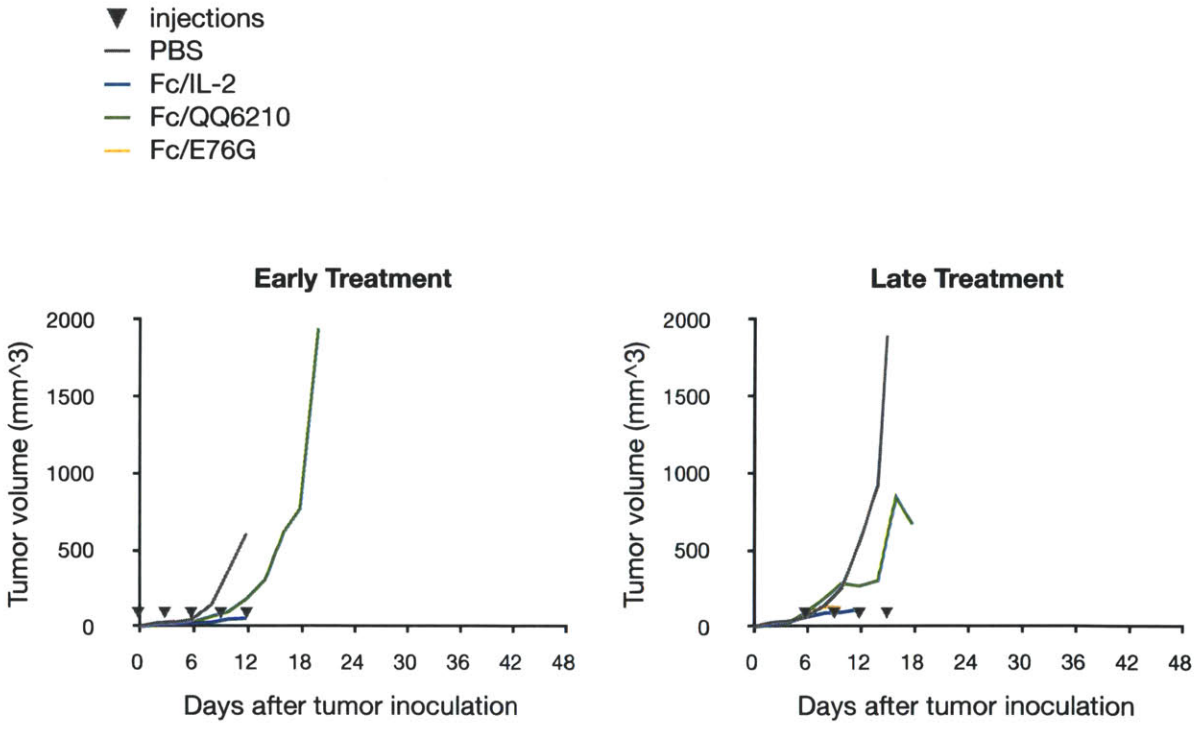

Figure 4-1: Fc/IL-2 and Fc/E76G are lethal at 50 μg once every three days. C57BL/6 mice (n = 1 mouse per group) were injected subcutaneously with 10^6 B16-F10 melanoma cells. Immediately following tumor inoculation (left) or 6 days afterward (right), mice were injected i.v. with PBS or 50 μg Fc/IL-2, Fc/QQ6210 or Fc/E76G. Subsequent doses were administered every 3 days.

(a)

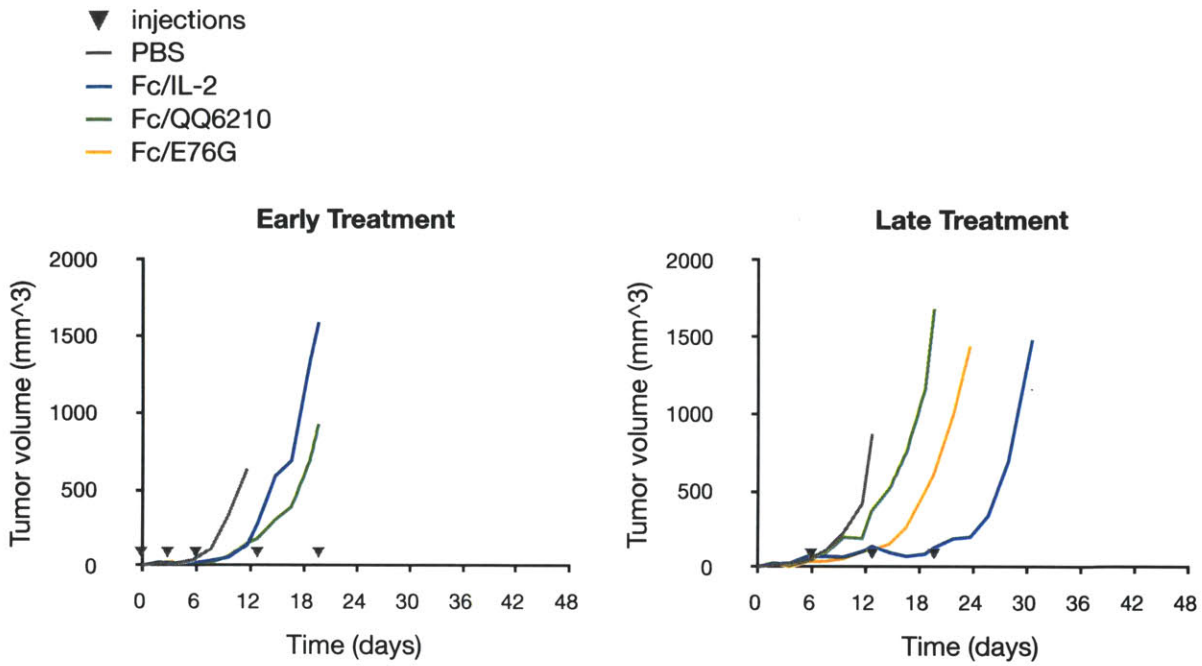

(b)

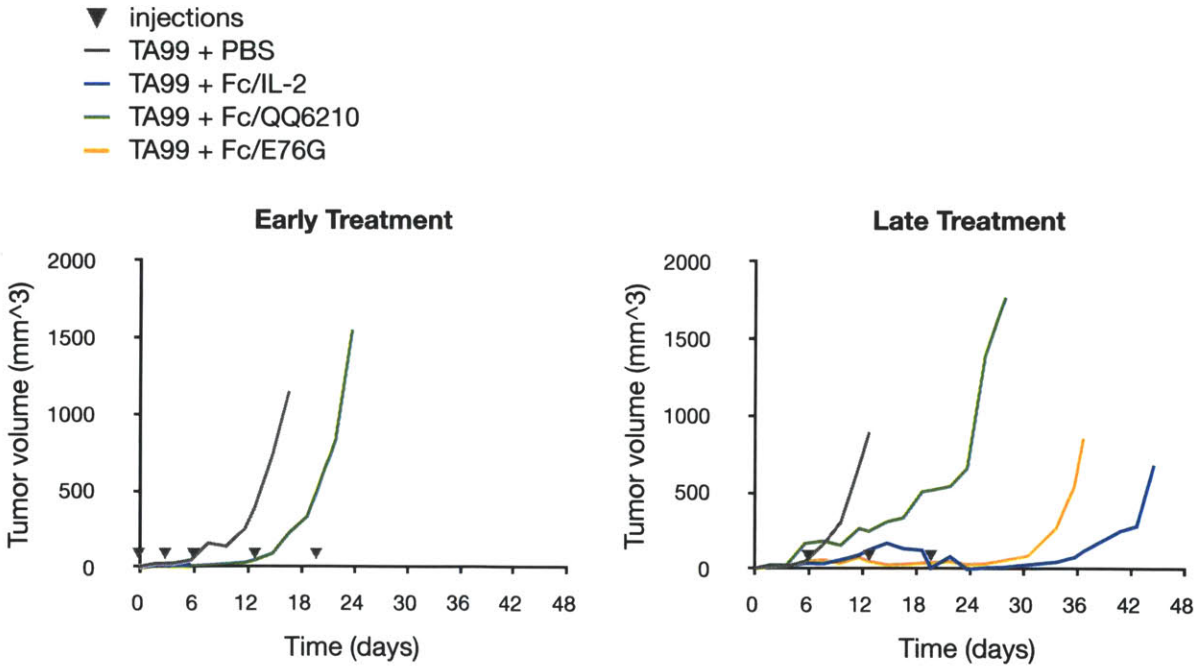

Figure 4-2: Fc/IL-2 fusion proteins are tolerable at 25 µg once weekly. C57BL/6 mice (n = 1 mouse per group) were injected subcutaneously with 10^6 B16-F10 melanoma cells. Immediately following tumor inoculation (left) or 6 days afterward (right), mice were injected i.v. with PBS or 25 µg Fc/IL-2, Fc/QQ6210, or Fc/E76G alone (a) or in combination with 100 µg TA99 (b). Subsequent doses were administered every 3 or 6 days, as indicated.

4.3.2. *B16-F10 tumor treatment with Fc/IL-2 and TA99*

Having established a tolerable dosing regimen for Fc/IL-2, we evaluated its efficacy alone or in combination with TA99 for controlling subcutaneous B16-F10 tumors. Toward this goal, C57BL/6 mice were injected subcutaneously with B16-F10 melanoma cells and tumors were allowed to establish for six days. With tumor nodules visible and palpable, mice were treated with 25 μg Fc/IL-2 or 25 μg Fc/IL-2 in combination with 100 μg TA99, with subsequent doses administered every six days. As controls, B16-F10 tumor-bearing mice were treated with PBS, 6 μg free IL-2, 100 μg TA99, or 6 μg free IL-2 with 100 μg TA99.

As expected for B16-F10 tumors, all PBS-treated mice required euthanasia due to tumor size within two weeks of tumor inoculation, shown in Figure 4-3. Consistent with previous reports, IL-2 or TA99 alone was insufficient to delay B16-F10 growth. IL-2 in combination with TA99 delayed tumor progression in some mice. However, all tumors reached euthanasia criteria within the course of therapy. Fc/IL-2 alone, by contrast, significantly reduced tumor burden, and Fc/IL-2 in combination with TA99 exerted synergistic tumor control. Relative to PBS-treated controls, a single dose of Fc/IL-2 reduced average tumor volume on day 12 by 50%; a single treatment with Fc/IL-2 in combination with TA99 reduced average tumor volume on day 12 by 83%. Continuing therapy with Fc/IL-2 delayed tumors from reaching a volume of 500 mm^3 by 7 days. For Fc/IL-2 and TA99 combination therapy, four of five tumors remained below 85 mm^3 during treatment. Only one of five tumors progressed to reach 500 mm^3, although significantly delayed by 16.7 days relative to PBS-treated controls.

Animal weight is an indicator of overall body condition. The weight of animals treated with all therapies tracked with PBS-treated controls, shown in Figure 4-4, suggesting these therapies were well-tolerated by the mice.

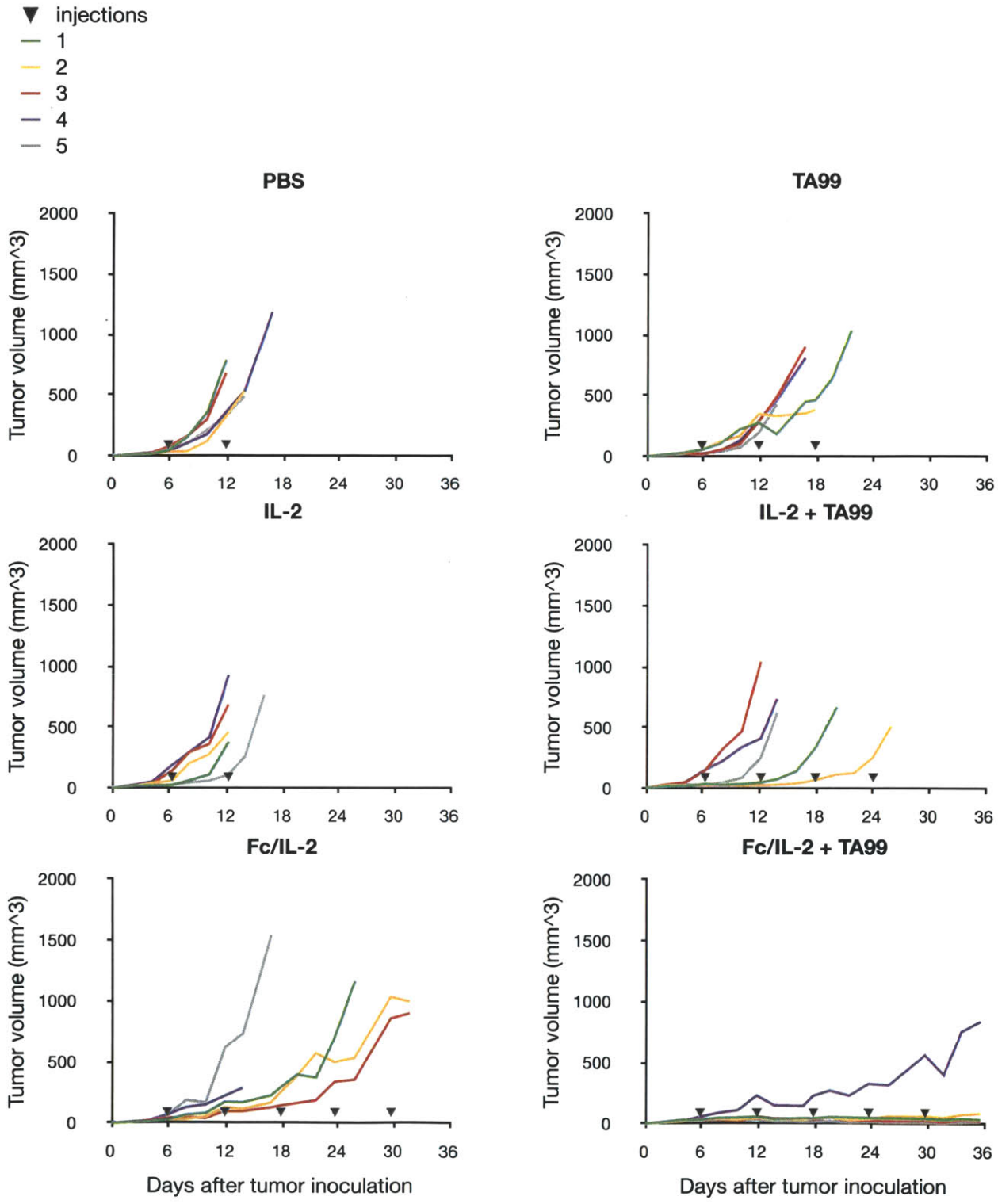

Figure 4-3: Anti-tumor effects of Fc/IL-2 and TA99. C57BL/6 mice (n = 5 mice per group) were injected subcutaneously with 10^6 B16-F10 melanoma cells. Six days after tumor inoculation mice were injected i.v. with PBS, 6 μg IL-2, 25 μg Fc/IL-2, and/or 100 μg TA99. Subsequent doses were administered every 6 days.

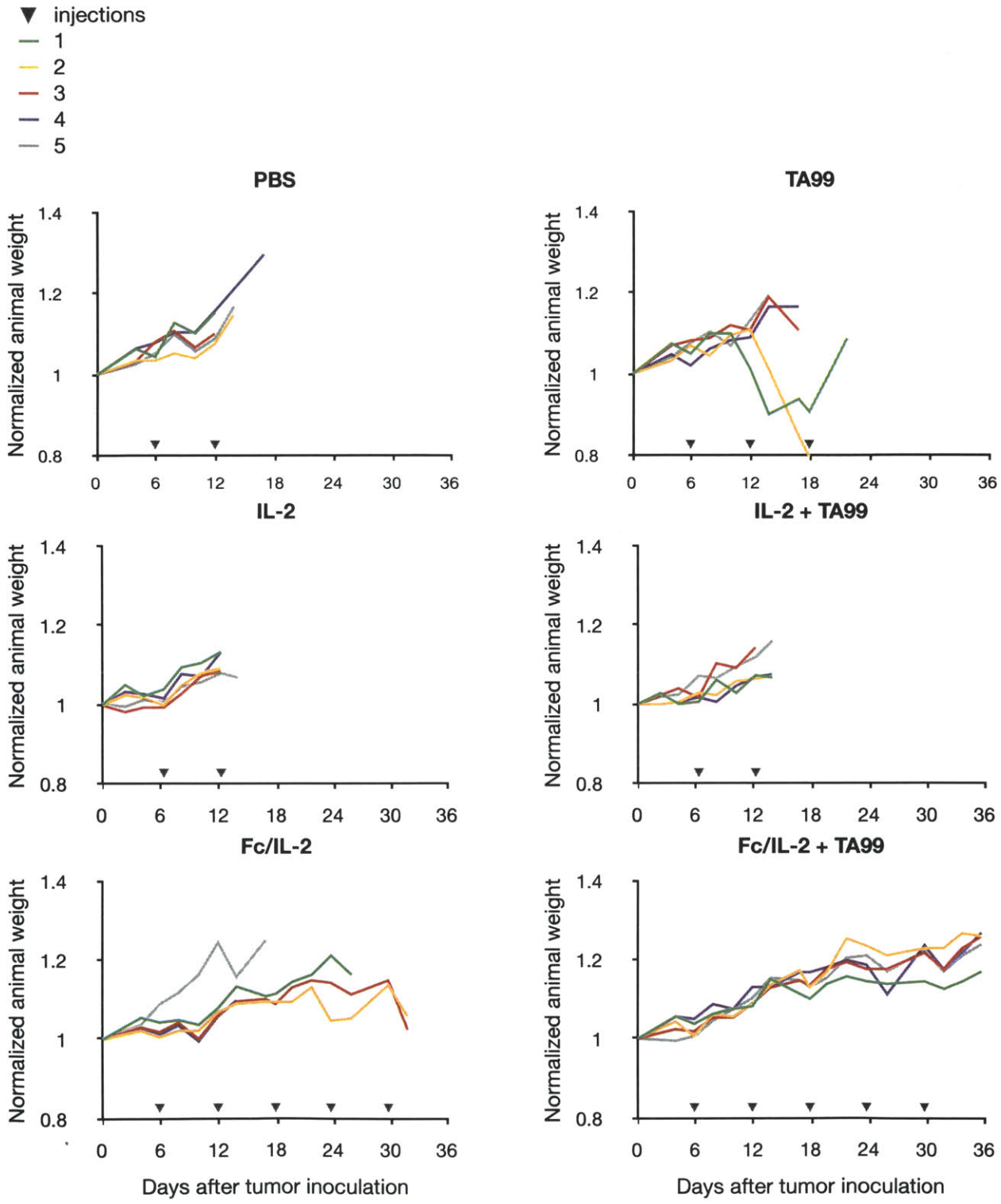

Figure 4-4: Combination Fc/IL-2 and TA99 therapy is well-tolerated. C57BL/6 mice (n = 5 mice per group) were injected subcutaneously with 10^6 B16-F10 melanoma cells. Six days after tumor inoculation mice were injected i.v. with PBS, 6 μg IL-2, 25 μg Fc/IL-2, and/or 100 μg TA99. Subsequent doses were administered every 6 days. Shown is animal weight normalized to initial weight at time of tumor inoculation.

Table 4-2: Unpaired *t*-test P values for Fc/IL-2 and TA99 combination therapy compared with other treatments. Statistically significant differences ($p < 0.05$) are highlighted in bold type.

Days after tumor inoculation	PBS	IL-2	Fc/IL-2	TA99	IL-2 + TA99
4	**0.0038**	**0.0243**	0.1190	**0.0204**	0.1588
6	**0.0047**	**0.0174**	0.1387	**0.0023**	0.1879
8			0.1414		0.0702
11			0.1678		**0.0407**
12			**0.0398**		

H&E stained tumor sections harvested four days after single-dose therapy, shown in Figure 4-5, indicate significant recruitment of lymphocytes to the periphery of tumors treated with Fc/IL-2 and Fc/IL-2 in combination with TA99.

After five doses of Fc/IL-2 and TA99, treatment was stopped to assess the duration of the therapeutic effect and the development of any anti-tumor memory responses. Twelve days after the last treatment, corresponding to 42 days after tumor inoculation, the three remaining mice of this treatment group were re-challenged with 10^5 B16-F10 cells subcutaneously in the opposite flank. Two naïve C57BL/6 mice were similarly inoculated with 10^5 B16-F10 cells as controls. As shown in Figure 4-6, all three primary tumors eventually entered exponential growth and required euthanasia by day 26 after the fifth treatment. However, at the time of euthanasia, 14 days after re-challenge, two of three Fc/IL-2 and TA99 treated mice remained tumor-free at the secondary challenge site.

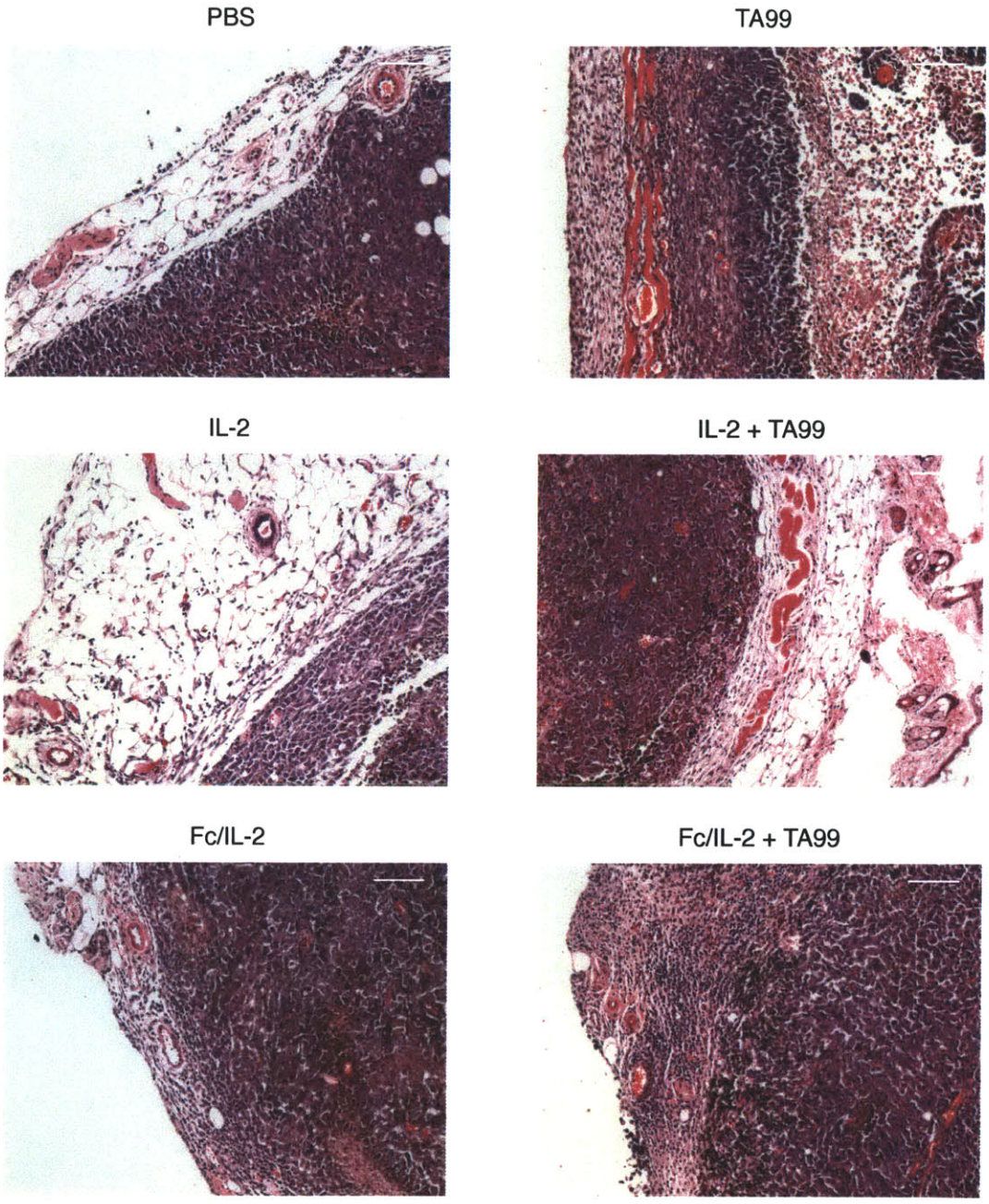

Figure 4-5: Combination Fc/IL-2 and TA99 treatment recruits lymphocytes to tumor periphery. H&E stained sections of subcutaneous B16-F10 tumors 4 days after a single dose of PBS, 6 μg IL-2, 25 μg Fc/IL-2 and/or 100 μg TA99 at 10x magnification. Scale bar represents 100 μm. Images are representative of two experiments.

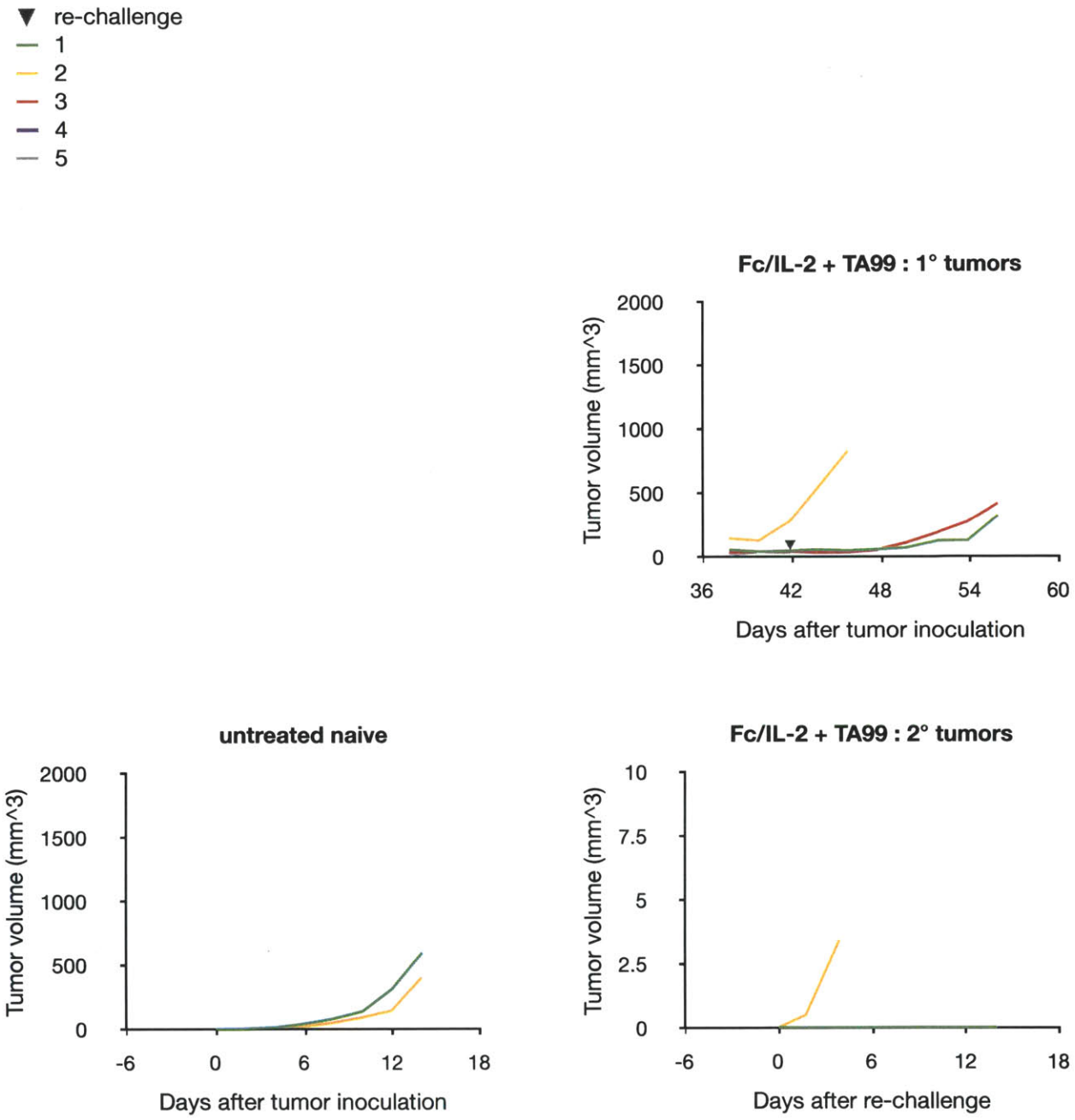

Figure 4-6: Combination Fc/IL-2 and TA99 treatment provides protection against secondary tumor challenge. C57BL/6 mice bearing B16-F10 tumors and treated with five doses of 25 μg Fc/IL-2 and 100 μg TA99 (n = 3) were injected subcutaneously with 10^5 B16-F10 melanoma cells in the opposite flank twelve days after the last treatment. Untreated naïve C57BL/6 mice (n = 2) were also injected subcutaneously with 10^5 B16-F10 melanoma cells.

4.3.3. *Efficacy of combination therapy is sensitive to Fc/IL-2 and TA99 separation*

To determine whether simultaneous administration of Fc/IL-2 and TA99 was required or optimal for therapeutic efficacy, we separated the administration of the two agents by intervals ranging from 0 to 3 days. As before, C57BL/6 mice were injected subcutaneously with 10^6 B16-F10 melanoma cells, and tumors were allowed to establish for six days. With tumor nodules visible and palpable, mice were treated with a single dose each of 25 μg Fc/IL-2 and 100 μg TA99, separated by approximately 0, 6, 12, 18, 24, 48, or 72 hours.

While none of these single-dose treatments cured the mice, all delayed exponential tumor growth. To compare their efficacy quantitatively, we devised the metric $4V_0$, representing the time for tumor volume to double twice. This quantity captures the delayed growth due to treatment as well as the variability in initial tumor volume. Separating administration of the two agents by up to two days did not significantly affect efficacy. However, separating the two agents by three days reduced tumor control effects. For ease of treatment, we selected simultaneous administration for all subsequent experiments.

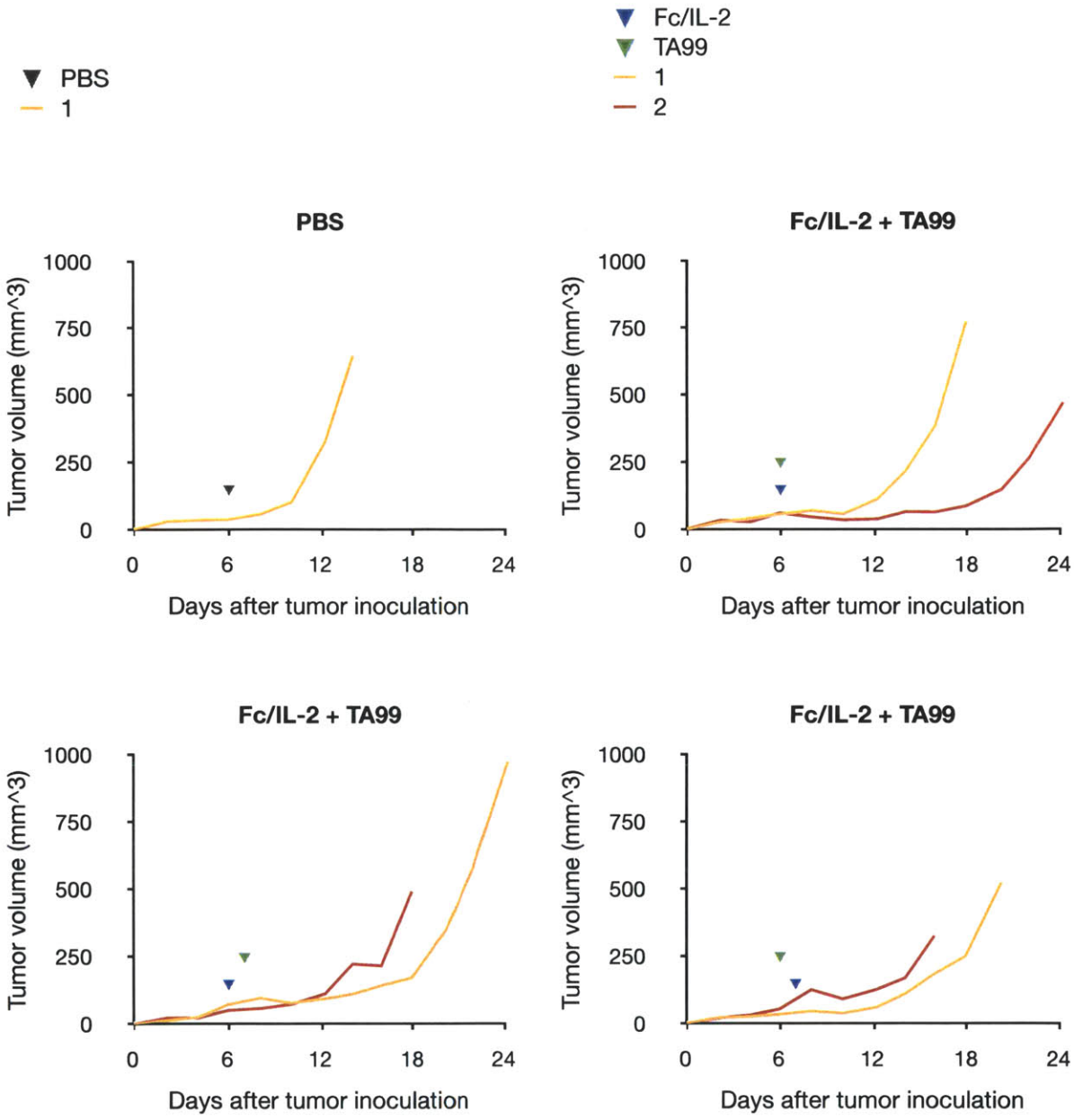

Figure 4-7: Single-dose combination Fc/IL-2 and TA99 therapy delays tumor growth. C57BL/6 mice were injected subcutaneously with 10^6 B16-F10 melanoma cells. Six days after tumor inoculation, mice were injected i.v. with PBS, or a single dose each of 25 μg Fc/IL-2 and 100 μg TA99, simultaneously or separated by 24 hours as indicated.

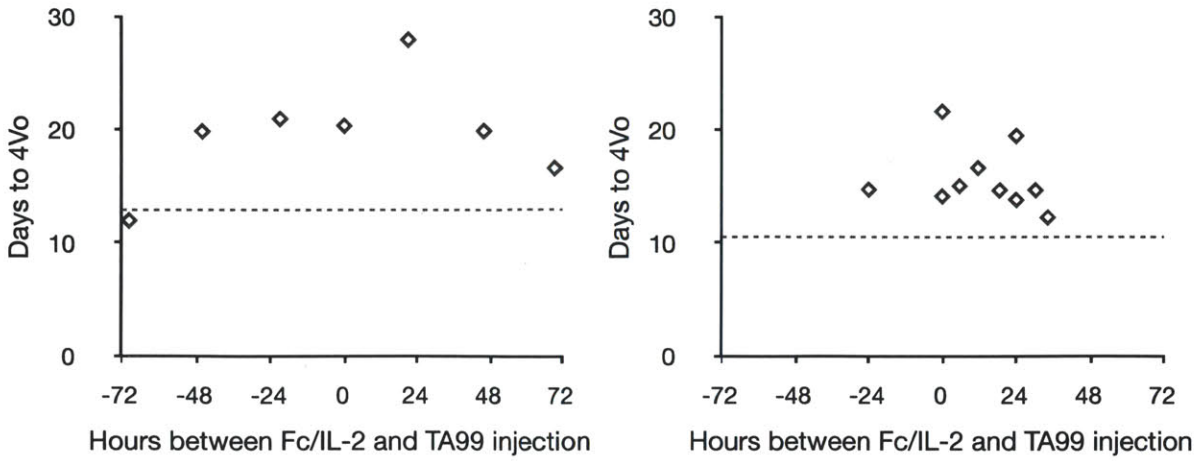

Figure 4-8: Combination Fc/IL-2 and TA99 therapy sensitive to prolonged separation of Fc/IL-2 and TA99 administration. C57BL/6 mice were injected subcutaneously with 10^6 B16-F10 melanoma cells. Six days after tumor inoculation, mice were injected i.v. with PBS (dashed lines), or a single dose each of 25 μg Fc/IL-2 and 100 μg TA99 (diamonds). The y-axis represents the time for tumor volume to double twice from its value at the initiation of treatment, V_0. The x-axis represents the time separation between Fc/IL-2 and TA99 injection, where the time of Fc/IL-2 injection has been set as the reference, $t = 0$. Data shown for two independent experiments.

4.3.4. CD25 binding affinity required for therapeutic effect

We next investigated the effect of CD25 binding affinity on combination Fc/IL-2 and TA99 therapy. Toward this end, as above, C57BL/6 mice were injected subcutaneously with B16-F10 melanoma cells and tumors were allowed to establish for six days. With tumor nodules visible and palpable, mice were treated with 25 μg Fc/QQ610 or Fc/E76G, alone or in combination with 100 μg TA99, with subsequent doses administered every six days. Comparable to treatment with Fc/IL-2, as shown in Figure 4-9, Fc/QQ6210 and Fc/E76G alone delayed tumor progression. In combination with TA99, Fc/QQ6210 suppressed tumor growth during the course of treatment. Tumors treated with Fc/E76G and TA99, however, continued to grow during therapy. As indicated by whole animal weight, shown in Figure 4-10, Fc.QQ6210 was well-tolerated, while Fc/E76G caused several significant instances of weight loss. H&E stained sections of tumors harvested 4 days after a single dose of therapy, Figure 4-11, indicate comparable extent of lymphocyte accumulation at the tumor periphery of Fc/QQ6210 and Fc/E76G treated tumors as Fc/IL-2 treated tumors, alone or in combination with TA99.

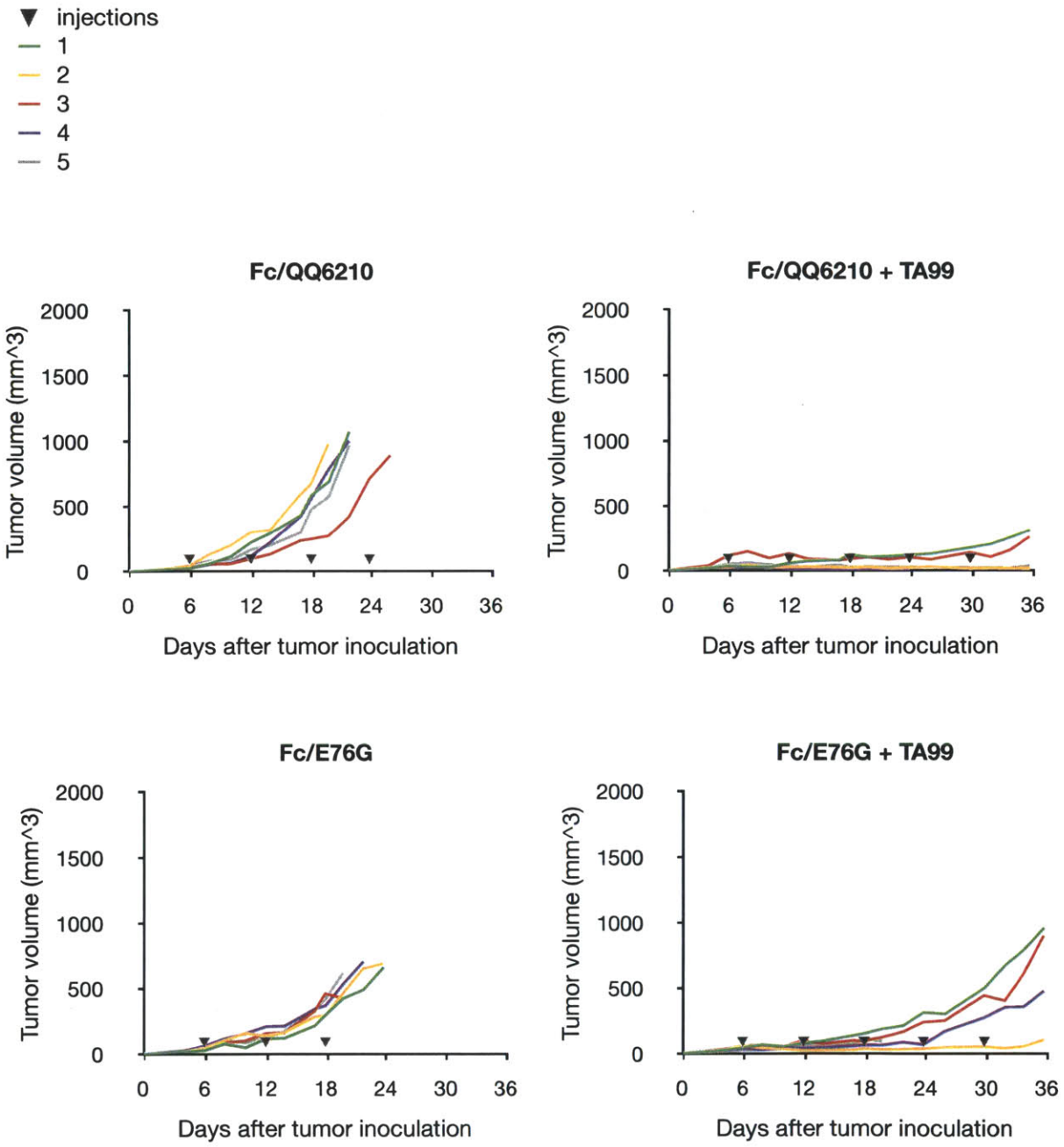

Figure 4-9: CD25 binding affinity is required for combination Fc/IL-2 and TA99 therapy. C57BL/6 mice (n = 5 mice per group) were injected subcutaneously with 10^6 B16-F10 melanoma cells. Six days after tumor inoculation mice were injected i.v. with 25 μg Fc/QQ6210 or Fc/E76G, alone or with 100 μg TA99. Subsequent doses were administered every 6 days.

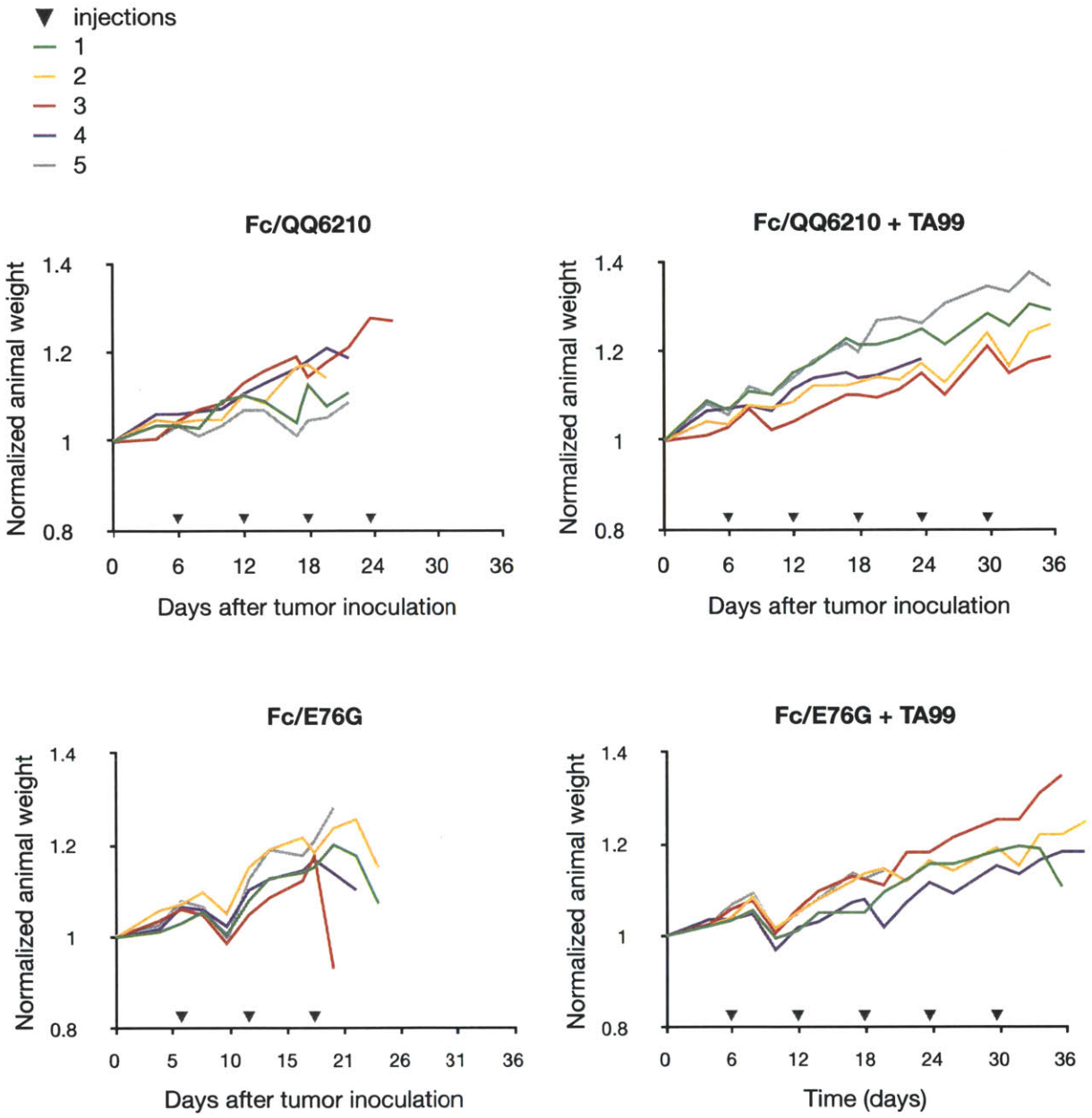

Figure 4-10: Non-CD25 binding Fc/E76G is less well-tolerated. C57BL/6 mice (*n* = 5 mice per group) were injected subcutaneously with 10^6 B16-F10 melanoma cells. Six days after tumor inoculation mice were injected i.v. with PBS or 25 μg Fc/QQ6210 or Fc/E76G, alone (left) or in combination with 100 μg TA99 (right). Subsequent doses were administered every 6 days. Shown is animal weight normalized to initial weight at time of tumor inoculation.

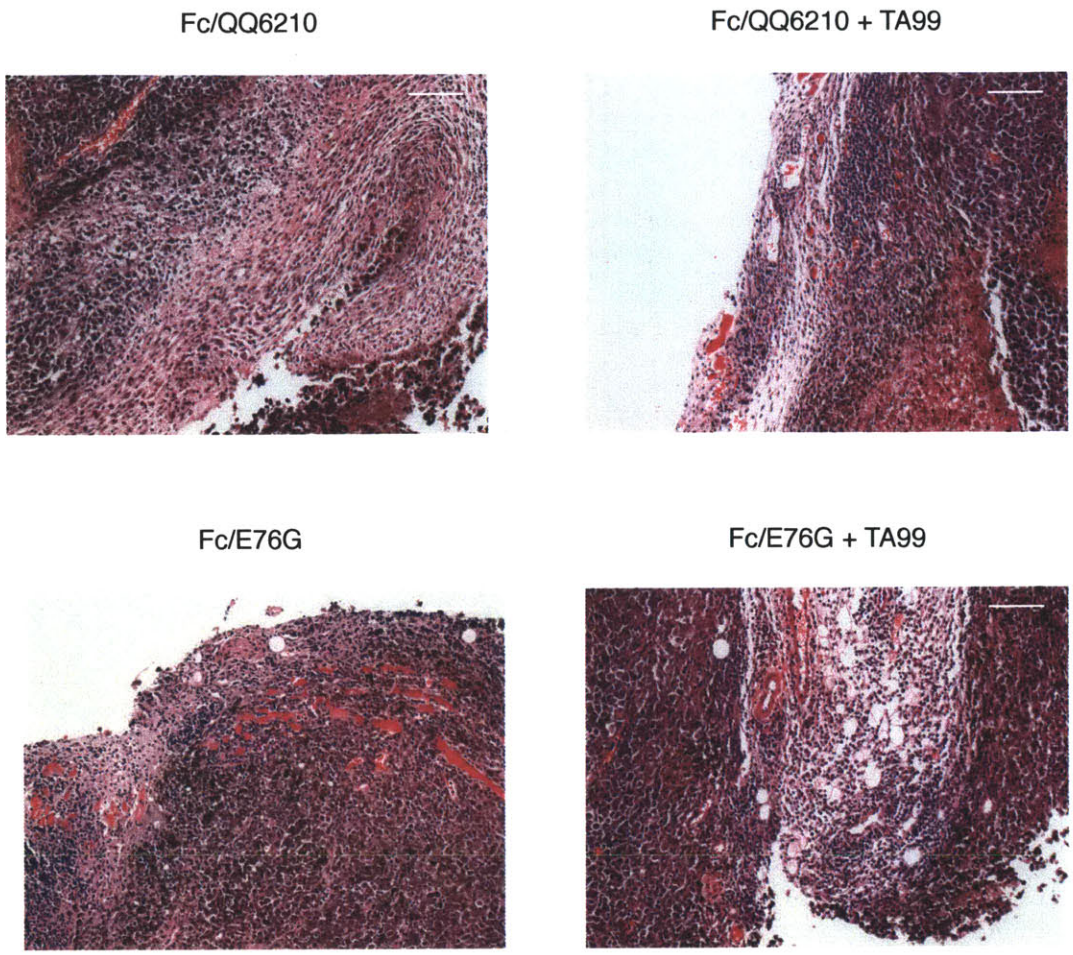

Figure 4-11: Combination therapy using Fc/QQ6210 or Fc/E76G and TA99 recruits lymphocytes to tumor periphery. H&E stained sections of subcutaneous B16-F10 tumors 4 days after a single dose of 25 μg Fc/QQ6210 or Fc/E76G, alone (left) or in combination with 100 μg TA99 (right) at 10x magnification. Scale bar represents 100 μm. Images are representative of two experiments.

After five doses of Fc/QQ6210 or Fc/E76G and TA99, treatment was stopped to assess the duration of the therapeutic effect and the development of any anti-tumor memory responses. Twelve days after the last treatment, corresponding to 42 days after tumor inoculation, the three remaining mice in the Fc/QQ6210 and TA99 group and the one remaining mouse in the Fc/E76G and TA99 group were re-challenged with 10^5 B16-F10 cells subcutaneously in the opposite flank. All four primary tumors eventually entered exponential growth and required euthanasia by day 26 after the last treatment. However, at the time of euthanasia, 14 days after re-challenge, two of three Fc/QQ6210 and TA99 treated mice remained tumor-free at the secondary challenge site.

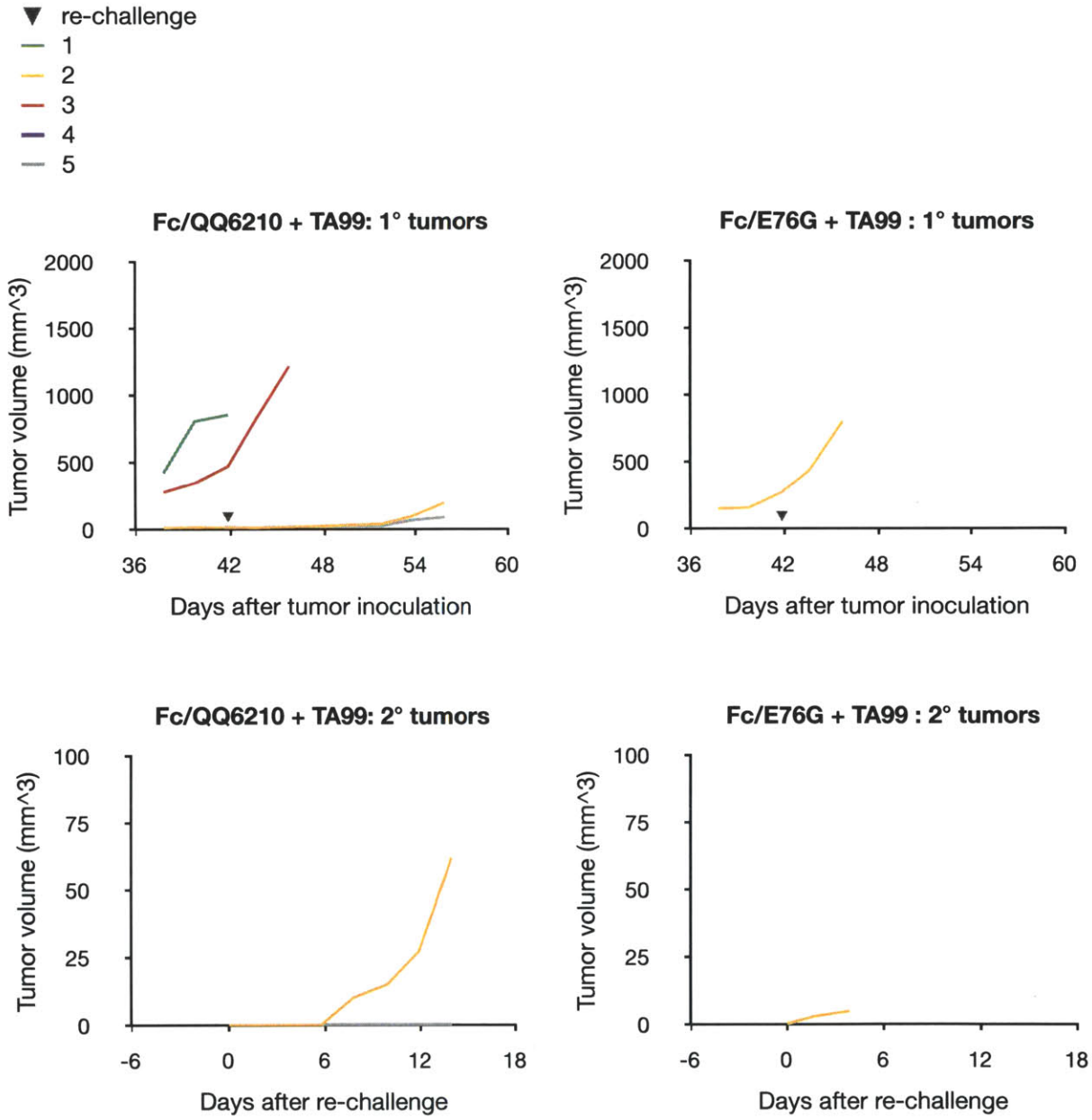

Figure 4-12: Combination Fc/QQ6210 and TA99 treatment provides protection against secondary tumor challenge. C57BL/6 mice bearing B16-F10 tumors and treated with five doses of 25 μg Fc/QQ6210 (n = 3) or Fc/E76G (n = 1) and 100 μg TA99 were injected subcutaneously with 10^5 B16-F10 melanoma cells in the opposite flank twelve days after the last treatment.

4.3.5. *$CD8^+$ T cells and NK cells contribute to therapeutic effect*

To determine whether NK cells or CD8+ T cells contribute to the efficacy of combination Fc/IL-2 and TA99 therapy, these cell types were selectively depleted using anti-NK1.1 and anti-CD8α antibodies during the course of Fc/IL-2 and TA99 combination therapy. As shown in Figure 4-13, NK and $CD8^+$ T cell depletion was verified by flow cytometry. As shown in Figure 4-14, NK cell depletion partially abrogated the anti-tumor efficacy of combination Fc/IL-2 and TA99 therapy, while $CD8^+$ T cell depletion completely abolished efficacy. H&E stains of tumor sections harvested four day after single dose Fc/IL-2 and TA99 treatment, Figure 4-15, show significant lymphocyte infiltration into the tumors of NK cell-depleted mice, but no lymphocyte presence in the tumors of $CD8^+$ T cell-depleted mice.

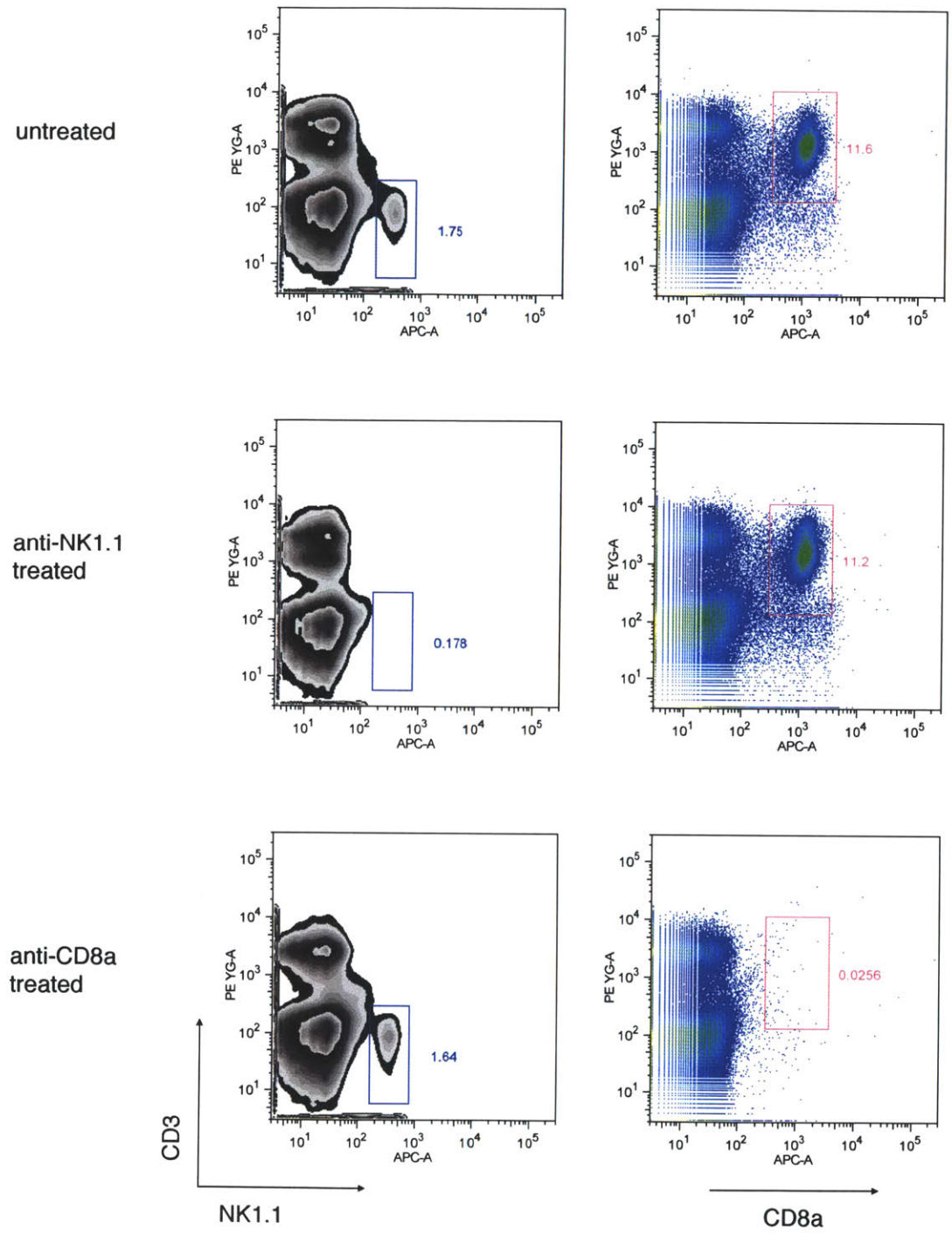

Figure 4-13: Validation of NK or CD8⁺ T cell depletion. C57BL/6 mice (n = 1 mouse per group) were injected subcutaneously with 10^6 B16-F10 melanoma cells. Four days after tumor inoculation, mice were injected i.p. with 400 µg anti-NK1.1 or anti-CD8a antibody. Two days after antibody injection, single-cell suspensions were prepared from spleens and stained with calcein violet AM, PE-conjugated anti-CD3, and APC-conjugated anti-NK1.1 or Alexa Fluor 647-conjugated anti-CD8a. Untreated control did not receive tumor inoculation or antibody injection. Cells gated by forward scatter and calcein violet AM.

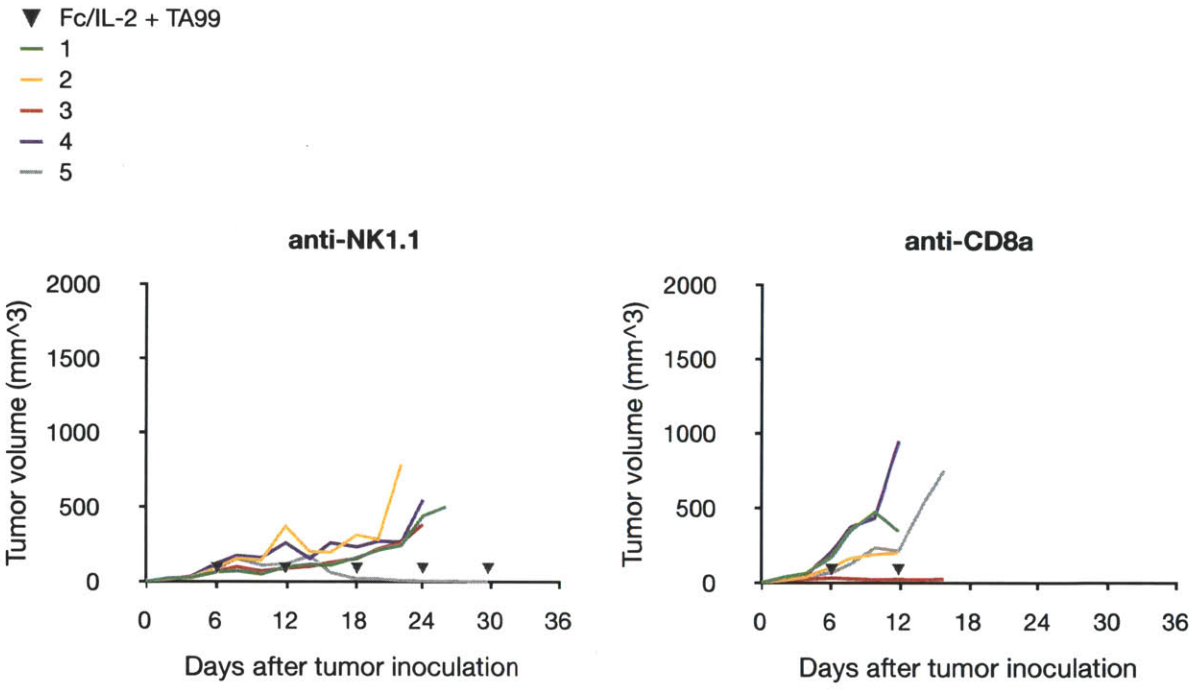

Figure 4-14: NK and CD8⁺ T cells contribute to anti-tumor effects of combination Fc/IL-2 and TA99 therapy. C57BL/6 mice (*n* = 5 mice per group) were injected subcutaneously with 10^6 B16-F10 melanoma cells. Four days after tumor inoculation, mice were injected i.p. with 400 µg anti-NK1.1 or anti-CD8a antibody; subsequent doses were administered every four days. Six days after tumor inoculation, mice were injected intravenously with PBS, 25 µg Fc/IL-2 and 100 µg TA99; subsequent doses were administered every 6 days.

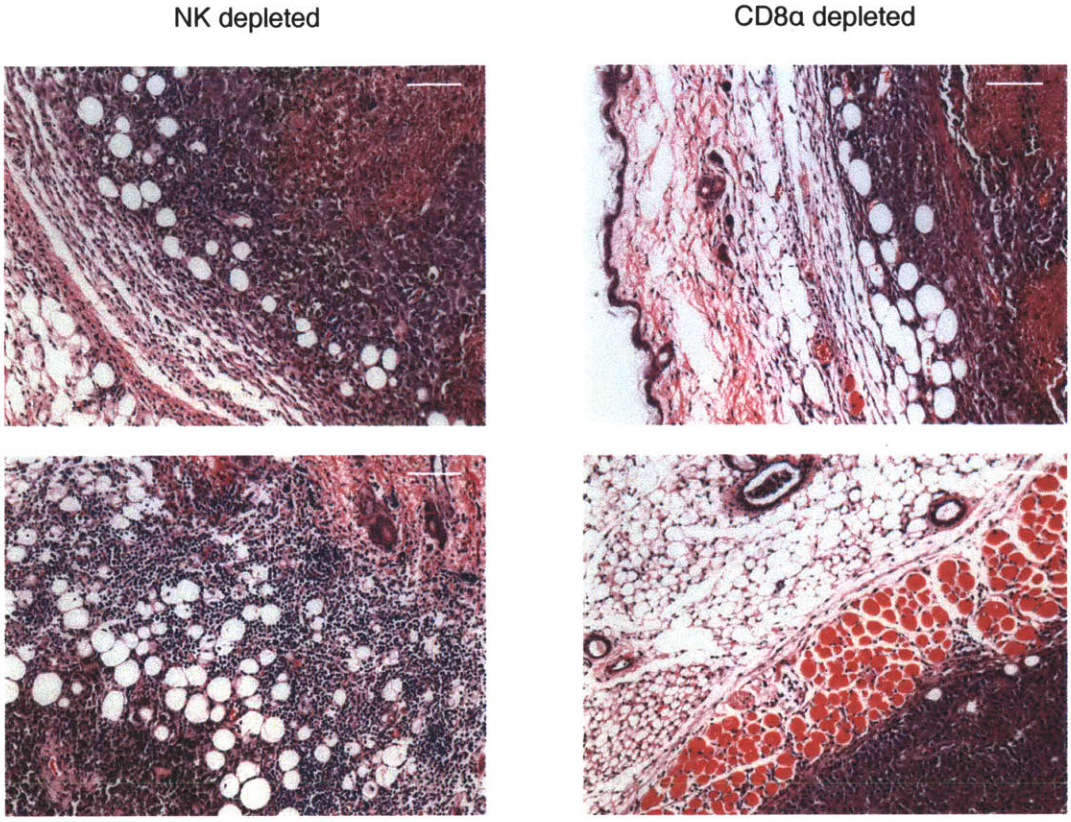

Figure 4-15: NK and CD8⁺ T cells contribute to anti-tumor effects of combination Fc/IL-2 and TA99 therapy. C57BL/6 mice (*n* = 2 mice per group) were injected subcutaneously with 10^6 B16-F10 melanoma cells. Four days after tumor inoculation, mice were injected i.p. with 400 μg anti-NK1.1 or anti-CD8a antibody. Six days after tumor inoculation, mice were injected ly with 25 μg Fc/IL-2 and 100 μg TA99. Four days after Fc/IL-2 and TA99 treatment, tumors sections were stained with H&E. Scale bar represents 100 μm.

4.4. Discussion

The results presented above demonstrate the potent synergy of Fc/IL-2 with anti-tumor antibody TA99 in controlling B16-F10 melanoma. The efficacy of this combination therapy depends on both $CD8^+$ T cells and NK cells, as well as IL-2's interaction with CD25.

As presented in Chapter 3, disruption of CD25 interaction significantly increased the number of $CD8^+$ T cells, NK cells, and $CD4^+$ $CD25^+$ $Foxp3^+$ T_{reg} cells in the spleen, comparable to

the observations of Krieg *et al.* for IL-2Rβγc-directed IL-2 / anti-IL-2 antibody complexes (65). However, ablation of CD25 binding significantly increased IL-2 toxicity and reduced anti-tumor efficacy, in contrast to the observations and conclusions of Krieg *et al.* The differences between our observations may be due to the different behaviors of human IL-2 and mouse IL-2 in mice.

In this study, we employed a mutant Fc with reduced FcγR binding and hence reduced effector function and fused IL-2 to non-lytic Fc monovalently. The significant therapeutic benefit of Fc/IL-2 over free IL-2, therefore, likely results from the extension of IL-2 circulation lifetime. As a monotherapy, the therapeutic benefit of extending IL-2 half-life has already been reported for several IL-2 variants, such as PEGylated IL-2 (97) and IL-2Rβγc -directed IL-2 / anti-IL-2 antibody complexes (101). The extension of half-life is also an essential mechanism for the improved *in vivo* activity of IL-15/IL-15Rα complexes over IL-15 alone (102). These observations, together with our results, suggest that agents capable of prolonged signaling through IL-2Rβγc are therapeutically beneficial and that functional CD25 interaction further improves efficacy.

The critical requirement of the adaptive immune response in anti-tumor antibody therapy was recently reported for two anti-HER2/neu/ErbB-2 antibodies (103, 104). In tumor bearing mice, antibody treatment was found to increase the prevalence of tumor-specific $CD8^+$ T cells, induce $CD8^+$ T cell production of IFN-γ, and promote the development of long-term immunological memory. These effects of antibody therapy may underly the synergy we observe for Fc/IL-2 and TA99. For instance, the long-circulating Fc/IL-2 may support and further expand the activation of tumor-specific $CD8^+$ T cells initiated by antibody therapy. In addition, the IFN-γ secreted by these $CD8^+$ T cells may increase the immunogenicity of B16-F10 tumor cells by increasing their expression of MHC class I, which has been reported to be inducible upon IFN-γ treatment (105). We hypothesize that long-circulating IL-2 would potently synergize with other anti-tumor antibodies for effective cancer immunotherapy.

References

1. Rosenberg SA (2001) Progress in human tumour immunology & immunotherapy. *Nature.* 411:380-384.

2. Woglom WH (1929) Immunity to transplantable tumors. *Cancer Res.* 4:129.

3. Blattman JN & Greenberg PD (2004) Cancer immunotherapy: a treatment for the masses. *Science.* 305(5681):200-205.

4. Schreiber H (2003) Tumor Immunology. *Fundamental Immunology,* ed Paul WE (Lippincott Williams & Wilkins), Vol 5, pp 1557-1592.

5. Sato E, *et al.* (2005) Intraepithelial CD8+ tumor-infiltrating lymphocytes and a high CD8+/ regulatory T cell ratio are associated with favorable prognosis in ovarian cancer. *Proc Natl Acad Sci U S A.* 102(51):18538-18543.

6. Zhang L, *et al.* (2003) Intratumoral T cells, recurrence, and survival in epithelial ovarian cancer. *N Engl J Med.* 348(3):203-213.

7. Schumacher K, Haensch W, Roefzaad C, & Schlag PM (2001) Prognostic significance of activated CD8+ T cell infiltrations within esophageal carcinomas. *Cancer Res.* 61(10): 3932-3936.

8. Dudley ME & Rosenberg SA (2003) Adoptive-cell-transfer therapy for the treatment of patients with cancer. *Nat Rev Cancer.* 3(9):666-675.

9. Hermans IF, Daish A, Yang J, Ritchie DS, & Ronchese F (1998) Antigen expressed on tumor cells fails to elicit an immune response, even in the rresence of increased numbers of tumor-specific cytotoxic T lymphocyte precursors. *Cancer Res.* 58(17):3909-3917.

10. Rosenberg SA (2000) Interleukin-2 and the development of immunotherapy for the treatment of patients with cancer. *Cancer J Sci Am.* 6:S2-7.

11. Lee PP, *et al.* (1999) Characterization of circulating T cells specific for tumor-associated antigens in melanoma patients. *Nat Med.* 5(6):677-685.

12. Zippelius A, *et al.* (2004) Effector function of human tumor-specific CD+8 T cells in melanoma lesions: a state of local functional tolerance. *Cancer Res.* 64(8):2865-2873.

13. Zou W (2005) Immunosuppressive networks in the tumour environment and their therapeutic relevance. *Nat Rev Cancer.* 5(4):263-274.

14. Redmond WL & Sherman LA (2005) Peripheral tolerance of CD8 T lymphocytes. *Immunity.* 22(3):275-284.

15. Sakaguchi S (2005) Naturally arising Foxp3-expressing CD25+CD4+ regulatory T cells in immunological tolerance to self and non-self. *Nat Immunol.* 6(4):345-352.

16. Rosenberg S, *et al.* (1985) Observations on the systemic administration of autologous lymphokine-activated killer cells and recombinant interleukin-2 to patients with metastatic cancer. *N Engl J Med.* 313(23):1485-1492.

17. Fyfe G, *et al.* (1995) Results of treatment of 255 patients with metastatic renal cell carcinoma who received high-dose recombinant interleukin-2 therapy. *J Clin Oncol.* 13(3): 688-696.

18. Atkins MB, *et al.* (1999) High-dose recombinant interleukin 2 therapy for patients with metastatic melanoma: analysis of 270 patients treated between 1985 and 1993. *J Clin Oncol.* 17(7):2105-2116.

19. Fisher RI, Rosenberg SA, & Fyfe G (2000) Long-term survival update for high-dose recombinant interleukin-2 in patients with renal cell carcinoma. *Cancer J Sci Am.* 6 Suppl 1:S55-57.

20. Rosenberg SA & Dudley ME (2004) Cancer regression in patients with metastatic melanoma after the transfer of autologous antitumor lymphocytes. *Proc Natl Acad Sci U S A.* 101(Suppl 2):14639-14645.

21. Taniguchi T, *et al.* (1983) Structure and expression of a cloned cDNA for human interleukin-2. *Nature.* 302(5906):305-310.

22. Brandhuber B, Boone T, Kenney W, & McKay D (1987) Three-dimensional structure of interleukin-2. *Science.* 238(4834):1707-1709.

23. Yamada T, Fujishima A, Kawahara K, Kato K, & Nishimura O (1987) Importance of disulfide linkage for constructing the biologically active human interleukin-2. *Arch Biochem Biophys.* 257(1):194-199.

24. Powell JD, Ragheb JA, Kitagawa-Sakakida S, & Schwartz RH (1998) Molecular regulation of interleukin-2 expression by CD28 co-stimulation and anergy. *Immunol Rev.* 165(1): 287-300.

25. Smith KA (1988) Interleukin-2: inception, impact, and implications. *Science.* 240(4856): 1169-1176.

26. Cheng LE, Öhlén C, Nelson BH, & Greenberg PD (2002) Enhanced signaling through the IL-2 receptor in CD8+ T cells regulated by antigen recognition results in preferential proliferation and expansion of responding CD8+ T cells rather than promotion of cell death. *Proc Natl Acad Sci U S A.* 99(5):3001-3006.

27. Yang-Snyder JA & Rothenberg EV (1998) Spontaneous expression of interleukin-2 in vivo in specific tissues of young mice. *Dev Immunol.* 5(4):223–245.

28. Gaffen SL, Wang S, & Koshland ME (1996) Expression of the immunological J chain in a murine B lymphoma is driven by autocrine production of interleukin-2. *Cytokine.* 8(7): 513-524.

29. Granucci F, *et al.* (2001) Inducible IL-2 production by dendritic cells revealed by global gene expression analysis. *Nat Immunol.* 2(9):882-888.

30. Bazan JF & McKay DB (1992) Unraveling the structure of IL-2. *Science.* 257(5068):410-413.

31. Nelson BH & Willerford DM (1998) Biology of the Interleukin-2 Receptor. *Advances in Immunology,* ed Frank JD (Academic Press), Vol 70, pp 1-81.

32. Kovanen PE & Leonard WJ (2004) Cytokines and immunodeficiency diseases: critical roles of the gamma(c)-dependent cytokines interleukins 2, 4, 7, 9, 15, and 21, and their signaling pathways. *Immunol Rev.* 202(1):67-83.

33. Sakaguchi S, Sakaguchi N, Asano M, Itoh M, & Toda M (1995) Immunologic self-tolerance maintained by activated T cells expressing IL-2 receptor alpha-chains (CD25). Breakdown of a single mechanism of self-tolerance causes various autoimmune diseases. *J Immunol.* 155(3):1151-1164.

34. Nakamura Y, *et al.* (1994) Heterodimerization of the IL-2 receptor beta- and gamma-chain cytoplasmic domains is required for signalling. *Nature.* 369(6478):330-333.

35. Nelson BH, Lord JD, & Greenberg PD (1994) Cytoplasmic domains of the interleukin-2 receptor beta and gamma chains mediate the signal for T-cell proliferation. *Nature.* 369(6478):333-336.

36. Gaffen SL (2001) Signaling domains of the interleukin-2 receptor. *Cytokine.* 14(2):63-77.

37. Yoshimura A, *et al.* (1995) A novel cytokine-inducible gene CIS encodes an SH2-containing protein that binds to tyrosine-phosphorylated interleukin 3 and erythropoietin receptors. *EMBO J.* 14(12):2816–2826.

38. Van Parijs L, *et al.* (1999) Uncoupling IL-2 signals that regulate T Cell proliferation, survival, and Fas-mediated activation-induced cell death. *Immunity.* 11(3):281-288.

39. Assier E, *et al.* (2004) NK cells and polymorphonuclear neutrophils are both critical for IL-2-induced pulmonary vascular leak syndrome. *J Immunol.* 172(12):7661-7668.

40. Yang JC, *et al.* (2003) Randomized study of high-dose and low-dose interleukin-2 in patients with metastatic renal cancer. *J Clin Oncol.* 21(16):3127-3132.

41. Konrad MW, *et al.* (1990) Pharmacokinetics of recombinant interleukin 2 in humans. *Cancer Res.* 50(7):2009-2017.

42. Dudley ME, *et al.* (2002) Cancer regression and autoimmunity in patients after clonal repopulation with antitumor lymphocytes. *Science.* 298(5594):850-854.

43. Klebanoff CA, Khong HT, Antony PA, Palmer DC, & Restifo NP (2005) Sinks, suppressors and antigen presenters: how lymphodepletion enhances T cell-mediated tumor immunotherapy. *Trends Immunol.* 26(2):111-117.

44. Rosenberg S, *et al.* (1990) Gene transfer into humans--immunotherapy of patients with advanced melanoma, using tumor-infiltrating lymphocytes modified by retroviral gene transduction. *N Engl J Med.* 323(9):570-578.

45. Dudley ME, *et al.* (2001) Adoptive transfer of cloned melanoma-reactive T lymphocytes for the treatment of patients with metastatic melanoma. *J Immunother.* 24(4):363-373.

46. Yee C, *et al.* (2002) Adoptive T cell therapy using antigen-specific CD8+ T cell clones for the treatment of patients with metastatic melanoma: in vivo persistence, migration, and antitumor effect of transferred T cells. *Proc Natl Acad Sci U S A.* 99(25):16168-16173.

47. Robbins PF, *et al.* (2004) Cutting edge: persistence of transferred lymphocyte clonotypes correlates with cancer regression in patients receiving cell transfer therapy. *J Immunol.* 173(12):7125-7130.

48. Overwijk WW, *et al.* (2003) Tumor regression and autoimmunity after reversal of a functionally tolerant state of self-reactive CD8+ T cells. *J Exp Med.* 198(4):569-580.

49. Liu K & Rosenberg SA (2001) Transduction of an IL-2 gene into human melanoma-reactive lymphocytes results in their continued growth in the absence of exogenous IL-2 and maintenance of specific antitumor activity. *J Immunol.* 167(11):6356-6365.

50. Teague RM, *et al.* (2006) Interleukin-15 rescues tolerant CD8+ T cells for use in adoptive immunotherapy of established tumors. *Nat Med.* 12(3):335-341.

51. Klebanoff CA, *et al.* (2004) IL-15 enhances the in vivo antitumor activity of tumor-reactive CD8+ T Cells. *Proc Natl Acad Sci U S A.* 101(7):1969-1974.

52. Klebanoff CA, *et al.* (2005) Central memory self/tumor-reactive CD8+ T cells confer superior antitumor immunity compared with effector memory T cells. *Proc Natl Acad Sci U S A.* 102(27):9571-9576.

53. Grabstein K, *et al.* (1994) Cloning of a T cell growth factor that interacts with the beta chain of the interleukin-2 receptor. *Science.* 264(5161):965-968.

54. Giri JG, *et al.* (1994) Utilization of the beta and gamma chains of the IL-2 receptor by the novel cytokine IL-15. *EMBO J.* 13(12):2822–2830.

55. Giri JG, *et al.* (1995) Identification and cloning of a novel IL-15 binding protein that is structurally related to the alpha chain of the IL-2 receptor. *EMBO J.* 14(15):3654–3663.

56. Bulfone-Paus S, *et al.* (1999) Death deflected: IL-15 inhibits TNF-alpha-mediated apoptosis in fibroblasts by TRAF2 recruitment to the IL-15Ralpha chain. *FASEB J.* 13(12):1575-1585.

57. Lodolce JP, *et al.* (1998) IL-15 receptor maintains lymphoid homeostasis by supporting lymphocyte homing and proliferation. *Immunity.* 9(5):669-676.

58. Kennedy MK, *et al.* (2000) Reversible defects in natural killer and memory CD8 T Cell lineages in interleukin 15-deficient mice. *J Exp Med.* 191(5):771-780.

59. Fehniger TA, Cooper MA, & Caligiuri MA (2002) Interleukin-2 and interleukin-15: immunotherapy for cancer. *Cytokine Growth Factor Rev.* 13(2):169-183.

60. Dubois S, Mariner J, Waldmann TA, & Tagaya Y (2002) IL-15Ralpha recycles and presents IL-15 in trans to neighboring cells. *Immunity.* 17(5):537-547.

61. Eicher DM & Waldmann TA (1998) IL-2R alpha on one cell can present IL-2 to IL-2R beta/ gamma(c) on another cell to uugment IL-2 signaling. *J Immunol.* 161(10):5430-5437.

62. Fujii M, *et al.* (1986) High-affinity receptor-mediated internalization and degradation of interleukin 2 in human T cells. *J Exp Med.* 163(3):550–562.

63. Kobayashi H, Carrasquillo JA, Paik CH, Waldmann TA, & Tagaya Y (2000) Differences of biodistribution, pharmacokinetics, and tumor targeting between interleukins 2 and 15. *Cancer Res.* 60(13):3577-3583.

64. Tagaya Y, Burton JD, Miyamoto Y, & Waldmann TA (1996) Identification of a novel receptor/signal transduction pathway for IL-15/T in mast cells. *EMBO J.* 15(18):4928–4939.

65. Krieg C, Létourneau S, Pantaleo G, & Boyman O (2010) Improved IL-2 immunotherapy by selective stimulation of IL-2 receptors on lymphocytes and endothelial cells. *Proc Natl Acad Sci U S A.* 107(26):11906-11911.

66. Rao BM, Girvin AT, Ciardelli T, Lauffenburger DA, & Wittrup KD (2003) Interleukin-2 mutants with enhanced alpha-receptor subunit binding affinity. *Protein Eng.* 16(12): 1081-1087.

67. Rao BM, Driver I, Lauffenburger DA, & Wittrup KD (2004) Interleukin 2 (IL-2) variants engineered for increased IL-2 receptor alpha-subunit affinity exhibit increased potency arising from a cell surface ligand reservoir effect. *Mol Pharmacol.* 66(4):864-869.

68. Rao BM, Driver I, Lauffenburger DA, & Wittrup KD (2005) High-affinity CD25-binding IL-2 mutants potently stimulate persistent T cell growth. *Biochemistry.* 44(31):10696-10701.

69. Hori T, *et al.* (1987) Establishment of an interleukin 2-dependent human T cell line from a patient with T cell chronic lymphocytic leukemia who is not infected with human T cell leukemia/lymphoma virus. *Blood.* 70(4):1069-1072.

70. Mestas J & Hughes CCW (2004) Of mice and not men: differences between mouse and human immunology. *J Immunol.* 172(5):2731-2738.

71. Mosmann T, *et al.* (1987) Species-specificity of T cell stimulating activities of IL 2 and BSF-1 (IL 4): comparison of normal and recombinant, mouse and human IL 2 and BSF-1 (IL 4). *J Immunol.* 138(6):1813-1816.

72. Boder ET & Wittrup KD (1997) Yeast surface display for screening combinatorial polypeptide libraries. *Nat Biotechnol.* 15(6):553-557.

73. Gai SA & Wittrup KD (2007) Yeast surface display for protein engineering and characterization. *Curr Opin Struct Biol.* 17(4):467-473.

74. Chao G, *et al.* (2006) Isolating and engineering human antibodies using yeast surface display. *Nat Protoc.* 1(2):755-768.

75. Schwede T, Kopp J, Guex N, & Peitsch MC (2003) SWISS-MODEL: an automated protein homology-modeling server. *Nucleic Acids Res.* 31(13):3381-3385.

76. Wang X, Rickert M, & Garcia KC (2005) Structure of the quaternary complex of interleukin-2 with its alpha, beta, and gamma_c receptors. *Science.* 310(5751):1159-1163.

77. Hackel BJ (2009) Fibronectin Domain Engineering. Ph.D. (Massachusetts Institute of Technology).

78. Rakestraw JA, Sazinsky SL, Piatesi A, Antipov E, & Wittrup KD (2009) Directed evolution of a secretory leader for the improved expression of heterologous proteins and full-length antibodies in Saccharomyces cerevisiae. *Biotechnol Bioeng.* 103(6):1192-1201.

79. Shusta EV, Raines RT, Pluckthun A, & Wittrup KD (1998) Increasing the secretory capacity of Saccharomyces cerevisiae for production of single-chain antibody fragments. *Nat Biotech.* 16(8):773-777.

80. Cho BK, Wang C, Sugawa S, Eisen HN, & Chen J (1999) Functional differences between memory and naive CD8 T cells. *Proc Natl Acad Sci U S A.* 96(6):2976-2981.

81. Bai A, Higham E, Eisen HN, Wittrup KD, & Chen J (2008) Rapid tolerization of virus-activated tumor-specific CD8+ T cells in prostate tumors of TRAMP mice. *Proc Natl Acad Sci U S A.* 105(35):13003-13008.

82. Higham EM, Shen C-H, Wittrup KD, & Chen J (2010) Cutting edge: delay and reversal of T cell tolerance by intratumoral injection of antigen-loaded dendritic cells in an autochthonous tumor model. *J Immunol.* 184(11):5954-5958.

83. Schreier PH, Bothwell AL, Mueller-Hill B, & Baltimore D (1981) Multiple differences between the nucleic acid sequences of the IgG2aa and IgG2ab alleles of the mouse. *Proc Natl Acad Sci U S A.* 78(7):4495-4499.

84. Geiser M, Cebe R, Drewello D, & Schmitz R (2001) Integration of PCR fragments at any specific site within cloning vectors without the use of restriction enzymes and DNA ligase. *Biotechniques.* 31(1):88-90, 92.

85. Popp MW, Antos JM, Grotenbreg GM, Spooner E, & Ploegh HL (2007) Sortagging: a versatile method for protein labeling. *Nat Chem Biol.* 3(11):707-708.

86. Stephan MT, Moon JJ, Um SH, Bershteyn A, & Irvine DJ (2010) Therapeutic cell engineering with surface-conjugated synthetic nanoparticles. *Nat Med.* 16(9):1035-1041.

87. Moore MW, Carbone FR, & Bevan MJ (1988) Introduction of soluble protein into the class I pathway of antigen processing and presentation. *Cell.* 54(6):777-785.

88. Roopenian DC & Akilesh S (2007) FcRn: the neonatal Fc receptor comes of age. *Nat Rev Immunol.* 7(9):715-725.

89. Baudino L, *et al.* (2008) Crucial role of aspartic acid at position 265 in the CH2 domain for murine IgG2a and IgG2b Fc-associated effector functions. *J Immunol.* 181(9):6664-6669.

90. Cho BK, Rao VP, Ge Q, Eisen HN, & Chen J (2000) Homeostasis-stimulated proliferation drives naive T cells to differentiate directly into memory T cells. *J Exp Med.* 192(4):549-556.

91. McDermott DF & Atkins MB (2004) Application of IL-2 and other cytokines in renal cancer. *Expert Opin Biol Ther.* 4(4):455-468.

92. Alvarez E (2011) B16 Murine Melanoma: Historical Perspective on the Development of a Solid Tumor Model. *Tumor Models in Cancer Research,* ed Teicher BA (Humana Press, New York, NY), 2 Ed, pp 79-95.

93. Fidler IJ (1973) Selection of successive tumour lines for metastasis. *Nat New Biol.* 242(118): 148-149.

94. Fidler IJ (1975) Biological behavior of malignant melanoma cells correlated to their survival in vivo. *Cancer Res.* 35(1):218-224.

95. Houghton AN (1983) The serological analysis of human cancer. Identification of differentiation antigens on melanoma and melanocytes. *Prog Clin Biol Res.* 119:199-205.

96. Hara I, Takechi Y, & Houghton AN (1995) Implicating a role for immune recognition of self in tumor rejection: passive immunization against the brown locus protein. *J Exp Med.* 182(5):1609-1614.

97. Zimmerman RJ, Aukerman SL, Katre NV, Winkelhake JL, & Young JD (1989) Schedule dependency of the antitumor activity and toxicity of polyethylene glycol-modified interleukin-2 in murine tumor models. *Cancer Res.* 49(23):6521-6528.

98. Levin AM, *et al.* (2012) Exploiting a natural conformational switch to engineer an interleukin-2 'superkine'. *Nature.* 484(7395):529-533.

99. Klebanoff CA, *et al.* (2011) Determinants of successful CD8+ T-Cell adoptive immunotherapy for large established tumors in mice. *Clin Cancer Res.* 17(16):5343-5352.

100. Saenger YM, *et al.* (2008) Improved tumor immunity using anti-tyrosinase related protein-1 monoclonal antibody combined with DNA vaccines in murine melanoma. *Cancer Res.* 68(23):9884-9891.

101. Létourneau S, *et al.* (2010) IL-2/anti-IL-2 antibody complexes show strong biological activity by avoiding interaction with IL-2 receptor alpha subunit CD25. *Proc Natl Acad Sci U S A.* 107(5):2171-2176.

102. Stoklasek TA, Schluns KS, & Lefrançois L (2006) Combined IL-15/IL-15Ralpha immunotherapy maximizes IL-15 activity in vivo. *J Immunol.* 177(9):6072-6080.

103. Park S, *et al.* (2010) The therapeutic effect of anti-HER2/neu antibody depends on both innate and adaptive immunity. *Cancer Cell.* 18(2):160-170.

104. Stagg J, *et al.* (2011) Anti–ErbB-2 mAb therapy requires type I and II interferons and synergizes with anti–PD-1 or anti-CD137 mAb therapy. *Proc Natl Acad Sci U S A.* 108(17): 7142-7147.

105. Seliger B, Wollscheid U, Momburg F, Blankenstein T, & Huber C (2001) Characterization of the major histocompatibility complex class I deficiencies in B16 melanoma cells. *Cancer Res.* 61(3):1095-1099.

Appendix

Plasmids for expressing D265A mouse IgG2a Fc / IL-2 fusion proteins in HEK293 cells.

Inserts were cloned into gWIZ between PstI and SalI restriction sites.

>gWIZ (5063 bp)

TCGCGCGTTTCGGTGATGACGGTGAAAACCTCTGACACATGCAGCTCCCGGAGACGGTCACAGCTTGTCTGTAAGCG
GATGCCGGGAGCAGACAAGCCCGTCAGGGCGCGTCAGCGGGTGTTGGCGGGTGTCGGGGCTGGCTTAACTATGCGGC
ATCAGAGCAGATTGTACTGAGAGTGCACCATATGCGGTGTGAAATACCGCACAGATGCGTAAGGAGAAAATACCGCA
TCAGATTGGCTATTGGCCATTGCATACGTTGTATCCATATCATAATATGTACATTTATATTGGCTCATGTCCAACAT
TACCGCCATGTTGACATTGATTATTGACTAGTTATTAATAGTAATCAATTACGGGGTCATTAGTTCATAGCCCATAT
ATGGAGTTCCGCGTTACATAACTTACGGTAAATGGCCCGCCTGGCTGACCGCCCAACGACCCCCGCCCATTGACGTC
AATAATGACGTATGTTCCCATAGTAACGCCAATAGGGACTTTCCATTGACGTCAATGGGTGGAGTATTTACGGTAAA
CTGCCCACTTGGCAGTACATCAAGTGTATCATATGCCAAGTACGCCCCCTATTGACGTCAATGACGGTAAATGGCCC
GCCTGGCATTATGCCCAGTACATGACCTTATGGGACTTTCCTACTTGGCAGTACATCTACGTATTAGTCATCGCTAT
TACCATGGTGATGCGGTTTTGGCAGTACATCAATGGGCGTGGATAGCGGTTTGACTCACGGGGATTTCCAAGTCTCC
ACCCCATTGACGTCAATGGGAGTTTGTTTTGGCACCAAAATCAACGGGACTTTCCAAAATGTCGTAACAACTCCGCC
CCATTGACGCAAATGGGCGGTAGGCGTGTACGGTGGGAGGTCTATATAAGCAGAGCTCGTTTAGTGAACCGTCAGAT
CGCCTGGAGACGCCATCCACGCTGTTTTGACCTCCATAGAAGACACCGGGACCGATCCAGCCTCCGCGGCCGGGAAC
GGTGCATTGGAACGCGGATTCCCCGTGCCAAGAGTGACGTAAGTACCGCCTATAGACTCTATAGGCACACCCCTTTG
GCTCTTATGCATGCTATACTGTTTTTGGCTTGGGGCCTATACACCCCCGCTTCCTTATGCTATAGGTGATGGTATAG
CTTAGCCTATAGGTGTGGGTTATTGACCATTATTGACCACTCCCCTATTGGTGACGATACTTTCCATTACTAATCCA
TAACATGGCTCTTTGCCACAACTATCTCTATTGGCTATATGCCAATACTCTGTCCTTCAGAGACTGACACGGACTCT
GTATTTTTACAGGATGGGGTCCCATTTATTATTTACAAATTCACATATACAACAACGCCGTCCCCCGTGCCCGCAGT
TTTTATTAAACATAGCGTGGGATCTCCACGCGAATCTCGGGTACGTGTTCCGGACATGGGCTCTTCTCCGGTAGCGG
CGGAGCTTCCACATCCGAGCCCTGGTCCCATGCCTCCAGCGGCTCATGGTCGCTCGGCAGCTCCTTGCTCCTAACAG
TGGAGGCCAGACTTAGGCACAGCACAATGCCCACCACCACCAGTGTGCCGCACAAGGCCGTGGCGGTAGGGTATGTG
TCTGAAAATGAGCGTGGAGATTGGGCTCGCACGGCTGACGCAGATGGAAGACTTAAGGCAGCGGCAGAAGAAGATGC
AGGCAGCTGAGTTGTTGTATTCTGATAAGAGTCAGAGGTAACTCCCGTTGCGGTGCTGTTAACGGTGGAGGGCAGTG
TAGTCTGAGCAGTACTCGTTGCTGCCGCGCGCGCCACCAGACATAATAGCTGACAGACTAACAGACTGTTCCTTTCC
ATGGGTCTTTTCTGCAGTCACCGTCGTCGACACGTGTGATCAGATATCGCGGCCGCTCTAGACCAGGCGCCTGGATC
CAGATCACTTCTGGCTAATAAAAGATCAGAGCTCTAGAGATCTGTGTGTTGGTTTTTTGTGGATCTGCTGTGCCTTC
TAGTTGCCAGCCATCTGTTGTTTGCCCCTCCCCCGTGCCTTCCTTGACCCTGGAAGGTGCCACTCCCACTGTCCTTT
CCTAATAAAATGAGGAAATTGCATCGCATTGTCTGAGTAGGTGTCATTCTATTCTGGGGGGTGGGGTGGGGCAGCAC
AGCAAGGGGGAGGATTGGGAAGACAATAGCAGGCATGCTGGGGATGCGGTGGGCTCTATGGGTACCTCTCTCTCTCT
CTCTCTCTCTCTCTCTCTCTCTCTCTCTCGGTACCTCTCTCTCTCTCTCTCTCTCTCTCTCTCTCTCTCTCTCGG
TACCAGGTGCTGAAGAATTGACCCGGTTCCTCCTGGGCCAGAAAGAAGCAGGCACATCCCCTTCTCTGTGACACACC
CTGTCCACGCCCCTGGTTCTTAGTTCCAGCCCCACTCATAGGACACTCATAGCTCAGGAGGGCTCCGCCTTCAATCC
CACCCGCTAAAGTACTTGGAGCGGTCTCTCCCTCCCTCATCAGCCCACCAAACCAAACCTAGCCTCCAAGAGTGGGA
AGAAATTAAAGCAAGATAGGCTATTAAGTGCAGAGGGAGAGAAAATGCCTCCAACATGTGAGGAAGTAATGAGAGAA
ATCATAGAATTTCTTCCGCTTCCTCGCTCACTGACTCGCTGCGCTCGGTCGTTCGGCTGCGGCGAGCGGTATCAGCT
CACTCAAAGGCGGTAATACGGTTATCCACAGAATCAGGGGATAACGCAGGAAAGAACATGTGAGCAAAAGGCCAGCA
AAAGGCCAGGAACCGTAAAAAGGCCGCGTTGCTGGCGTTTTTCCATAGGCTCCGCCCCCCTGACGAGCATCACAAAA
ATCGACGCTCAAGTCAGAGGTGGCGAAACCCGACAGGACTATAAAGATACCAGGCGTTTCCCCCTGGAAGCTCCCTC
GTGCGCTCTCCTGTTCCGACCCTGCCGCTTACCGGATACCTGTCCGCCTTTCTCCCTTCGGGAAGCGTGGCGCTTTC
TCAATGCTCACGCTGTAGGTATCTCAGTTCGGTGTAGGTCGTTCGCTCCAAGCTGGGCTGTGTGCACGAACCCCCCG
TTCAGCCCGACCGCTGCGCCTTATCCGGTAACTATCGTCTTGAGTCCAACCCGGTAAGACACGACTTATCGCCACTG
GCAGCAGCCACTGGTAACAGGATTAGCAGAGCGAGGTATGTAGGCGGTGCTACAGAGTTCTTGAAGTGGTGGCCTAA
CTACGGCTACACTAGAAGGACAGTATTTGGTATCTGCGCTCTGCTGAAGCCAGTTACCTTCGGAAAAAGAGTTGGTA
GCTCTTGATCCGGCAAACAAACCACCGCTGGTAGCGGTGGTTTTTTTGTTTGCAAGCAGCAGATTACGCGCAGAAAA
AAAGGATCTCAAGAAGATCCTTTGATCTTTTCTACGGGGTCTGACGCTCAGTGGAACGAAAACTCACGTTAAGGGAT
TTTGGTCATGAGATTATCAAAAAGGATCTTCACCTAGATCCTTTTAAATTAAAAATGAAGTTTTAAATCAATCTAAA
GTATATATGAGTAAACTTGGTCTGACAGTTACCAATGCTTAATCAGTGAGGCACCTATCTCAGCGATCTGTCTATTT

CGTTCATCCATAGTTGCCTGACTCCGGGGGGGGGGGGCGCTGAGGTCTGCCTCGTGAAGAAGGTGTTGCTGACTCAT
ACCAGGCCTGAATCGCCCCATCATCCAGCCAGAAAGTGAGGGAGCCACGGTTGATGAGAGCTTTGTTGTAGGTGGAC
CAGTTGGTGATTTTGAACTTTTGCTTTGCCACGGAACGGTCTGCGTTGTCGGGAAGATGCGTGATCTGATCCTTCAA
CTCAGCAAAAGTTCGATTTATTCAACAAAGCCGCCGTCCCGTCAAGTCAGCGTAATGCTCTGCCAGTGTTACAACCA
ATTAACCAATTCTGATTAGAAAAACTCATCGAGCATCAAATGAAACTGCAATTTATTCATATCAGGATTATCAATAC
CATATTTTTGAAAAAGCCGTTTCTGTAATGAAGGAGAAAACTCACCGAGGCAGTTCCATAGGATGGCAAGATCCTGG
TATCGGTCTGCGATTCCGACTCGTCCAACATCAATACAACCTATTAATTTCCCCTCGTCAAAAATAAGGTTATCAAG
TGAGAAATCACCATGAGTGACGACTGAATCCGGTGAGAATGGCAAAAGCTTATGCATTTCTTTCCAGACTTGTTCAA
CAGGCCAGCCATTACGCTCGTCATCAAAATCACTCGCATCAACCAAACCGTTATTCATTCGTGATTGCGCCTGAGCG
AGACGAAATACGCGATCGCTGTTAAAAGGACAATTACAAACAGGAATCGAATGCAACCGGCGCAGGAACACTGCCAG
CGCATCAACAATATTTTCACCTGAATCAGGATATTCTTCTAATACCTGGAATGCTGTTTTCCCGGGGATCGCAGTGG
TGAGTAACCATGCATCATCAGGAGTACGGATAAAATGCTTGATGGTCGGAAGAGGCATAAATTCCGTCAGCCAGTTT
AGTCTGACCATCTCATCTGTAACATCATTGGCAACGCTACCTTTGCCATGTTTCAGAAACAACTCTGGCGCATCGGG
CTTCCCATACAATCGATAGATTGTCGCACCTGATTGCCCGACATTATCGCGAGCCCATTTATACCCATATAAATCAG
CATCCATGTTGGAATTTAATCGCGGCCTCGAGCAAGACGTTTCCCGTTGAATATGGCTCATAACACCCCTTGTATTA
CTGTTTATGTAAGCAGACAGTTTTATTGTTCATGATGATATATTTTTATCTTGTGCAATGTAACATCAGAGATTTTG
AGACACAACGTGGCTTTCCCCCCCCCCCCATTATTGAAGCATTTATCAGGGTTATTGTCTCATGAGCGGATACATAT
TTGAATGTATTTAGAAAAATAAACAAATAGGGGTTCCGCGCACATTTCCCCGAAAAGTGCCACCTGACGTCTAAGAA
ACCATTATTATCATGACATTAACCTATAAAAATAGGCGTATCACGAGGCCCTTTCGTC

Insert: human light chain leader | D265A IgG2a Fc | GGGS | FLAG | STOP

>Fc/FLAG
ATGAGGGTCCCCGCTCAGCTCCTGGGGCTCCTGCTGCTCTGGCTCCCAGGTGCACGATGTGAGCCCAGAGTGCCCAT
AACACAGAACCCCTGTCCTCCACTCAAAGAGTGTCCCCCATGCGCAGCTCCAGACCTCTTGGGTGGACCATCCGTCT
TCATCTTCCCTCCAAAGATCAAGGATGTACTCATGATCTCCCTGAGCCCCATGGTCACATGTGTGGTGGTGGCCGTG
AGCGAGGATGACCCAGACGTCCAGATCAGCTGGTTTGTGAACAACGTGGAAGTACACACAGCTCAGACACAAACCCA
TAGAGAGGATTACAACAGTACTCTCCGGGTGGTCAGTGCCCTCCCCATCCAGCACCAGGACTGGATGAGTGGCAAGG
AGTTCAAATGCAAGGTCAACAACAGAGCCCTCCCATCCCCCATCGAGAAAACCATCTCAAAACCCAGAGGGCCAGTA
AGAGCTCCACAGGTATATGTCTTGCCTCCACCAGCAGAAGAGATGACTAAGAAAGAGTTCAGTCTGACCTGCATGAT
CACAGGCTTCTTACCTGCCGAAATTGCTGTGGACTGGACCAGCAATGGGCGTACAGAGCAAAACTACAAGAACACCG
CAACAGTCCTGGACTCTGATGGTTCTTACTTCATGTACAGCAAGCTCAGAGTACAAAAGAGCACTTGGGAAAGAGGA
AGTCTTTTCGCCTGCTCAGTGGTCCACGAGGGTCTGCACAATCACCTTACGACTAAGACCATCTCCCGGTCTCTGGG
TAAAGGTGGCGGATCTGACTACAAGGACGACGATGACAAGTGATAA

MRVPAQLLGLLLLWLPGARCEPRVPITQNPCPPLKECPPCAAPDLLGGPSVFIFPPKIKDVLMISLSPMVTCVVVAV
SEDDPDVQISWFVNNVEVHTAQTQTHREDYNSTLRVVSALPIQHQDWMSGKEFKCKVNNRALPSPIEKTISKPRGPV
RAPQVYVLPPPAEEMTKKEFSLTCMITGFLPAEIAVDWTSNGRTEQNYKNTATVLDSDGSYFMYSKLRVQKSTWERG
SLFACSVVHEGLHNHLTTKTISRSLGKGGGSDYKDDDDK

Insert: human LC leader | D265A IgG2a Fc | GGGS | IL-2 | 6xHis | STOP

>Fc/IL-2
ATGAGGGTCCCCGCTCAGCTCCTGGGGCTCCTGCTGCTCTGGCTCCCAGGTGCACGATGTGAGCCCAGAGTGCCCAT
AACACAGAACCCCTGTCCTCCACTCAAAGAGTGTCCCCCATGCGCAGCTCCAGACCTCTTGGGTGGACCATCCGTCT
TCATCTTCCCTCCAAAGATCAAGGATGTACTCATGATCTCCCTGAGCCCCATGGTCACATGTGTGGTGGTGGCCGTG
AGCGAGGATGACCCAGACGTCCAGATCAGCTGGTTTGTGAACAACGTGGAAGTACACACAGCTCAGACACAAACCCA
TAGAGAGGATTACAACAGTACTCTCCGGGTGGTCAGTGCCCTCCCCATCCAGCACCAGGACTGGATGAGTGGCAAGG
AGTTCAAATGCAAGGTCAACAACAGAGCCCTCCCATCCCCCATCGAGAAAACCATCTCAAAACCCAGAGGGCCAGTA
AGAGCTCCACAGGTATATGTCTTGCCTCCACCAGCAGAAGAGATGACTAAGAAAGAGTTCAGTCTGACCTGCATGAT
CACAGGCTTCTTACCTGCCGAAATTGCTGTGGACTGGACCAGCAATGGGCGTACAGAGCAAAACTACAAGAACACCG
CAACAGTCCTGGACTCTGATGGTTCTTACTTCATGTACAGCAAGCTCAGAGTACAAAAGAGCACTTGGGAAAGAGGA
AGTCTTTTCGCCTGCTCAGTGGTCCACGAGGGTCTGCACAATCACCTTACGACTAAGACCATCTCCCGGTCTCTGGG
TAAAGGAGGGGGCTCCGCACCCACTTCAAGCTCCACTTCAAGCTCTACAGCGGAAGCACAGCAGCAGCAGCAGCAGC
AGCAGCAGCAGCAGCAGCACCTGGAGCAGCTGTTGATGGACCTACAGGAGCTCCTGAGCAGGATGGAGAATTACAGG
AACCTGAAACTCCCCAGGATGCTCACCTTCAAATTTTACTTGCCCAAGCAGGCCACAGAATTGAAAGATCTTCAGTG

CCTAGAAGATGAACTTGGACCTCTGCGGCATGTTCTGGATTTGACTCAAAGCAAAAGCTTTCAATTGGAAGATGCTG
AGAATTTCATCAGCAATATCAGAGTAACTGTTGTAAAACTAAAGGGCTCTGACAACACATTTGAGTGCCAATTCGAT
GATGAGTCAGCAACTGTGGTGGACTTTCTGAGGAGATGGATAGCCTTCTGTCAAAGCATCATCTCAACAAGCCCTCA
ACACCATCACCACCATCACTGATAA

MRVPAQLLGLLLLWLPGARCEPRVPITQNPCPPLKECPPCAAPDLLGGPSVFIFPPKIKDVLMISLSPMVTCVVVAV
SEDDPDVQISWFVNNVEVHTAQTQTHREDYNSTLRVVSALPIQHQDWMSGKEFKCKVNNRALPSPIEKTISKPRGPV
RAPQVYVLPPPAEEMTKKEFSLTCMITGFLPAEIAVDWTSNGRTEQNYKNTATVLDSDGSYFMYSKLRVQKSTWERG
SLFACSVVHEGLHNHLTTKTISRSLGKGGGSAPTSSSTSSSTAEAQQQQQQQQQQQQHLEQLLMDLQELLSRMENYR
NLKLPRMLTFKFYLPKQATELKDLQCLEDELGPLRHVLDLTQSKSFQLEDAENFISNIRVTVVKLKGSDNTFECQFD
DESATVVDFLRRWIAFCQSIISTSPQHHHHHH

>Fc/QQ6210
ATGAGGGTCCCCGCTCAGCTCCTGGGGCTCCTGCTGCTCTGGCTCCCAGGTGCACGATGTGAGCCCAGAGTGCCCAT
AACACAGAACCCCTGTCCTCCACTCAAAGAGTGTCCCCCATGCGCAGCTCCAGACCTCTTGGGTGGACCATCCGTCT
TCATCTTCCCTCCAAAGATCAAGGATGTACTCATGATCTCCCTGAGCCCCATGGTCACATGTGTGGTGGTGGCCGTG
AGCGAGGATGACCCAGACGTCCAGATCAGCTGGTTTGTGAACAACGTGGAAGTACACACAGCTCAGACACAAACCCA
TAGAGAGGATTACAACAGTACTCTCCGGGTGGTCAGTGCCCTCCCCATCCAGCACCAGGACTGGATGAGTGGCAAGG
AGTTCAAATGCAAGGTCAACAACAGAGCCCTCCCATCCCCCATCGAGAAAACCATCTCAAAACCCAGAGGGCCAGTA
AGAGCTCCACAGGTATATGTCTTGCCTCCACCAGCAGAAGAGATGACTAAGAAAGAGTTCAGTCTGACCTGCATGAT
CACAGGCTTCTTACCTGCCGAAATTGCTGTGGACTGGACCAGCAATGGGCGTACAGAGCAAAACTACAAGAACACCG
CAACAGTCCTGGACTCTGATGGTTCTTACTTCATGTACAGCAAGCTCAGAGTACAAAAGAGCACTTGGGAAAGAGGA
AGTCTTTTCGCCTGCTCAGTGGTCCACGAGGGTCTGCACAATCACCTTACGACTAAGACCATCTCCCGGTCTCTGGG
TAAAGGAGGGGGCTCCGCACCCACTTCAAGCTCCACTTCAAGCTCTACAGCGGAAGCACAACAGCAGCAGCAGCAGC
AGCAGCAGCAGCAGCAGCACCTGGAGCAGCTGTTGATGGACCTACAGGAACTCCTGAGTAGGATGGAGGATCACAGG
AACCTGAGACTCCCCAGGATGCTCACCTTCAAATTTTACTTGCCCGAGCAGGCCACAGAATTGGAAGATCTTCAGTG
CCTAGAAGATGAACTTGAACCACTGCGGCAAGTTCTGGATTTGACTCAAAGCAAAAGCTTTCAATTGGAAGATGCTG
AGAATTTCATCAGCAATATCAGAGTAACTGTTGTAAAACTAAAGGGCTCTGACAACACATTTGAGTGCCAATTCGAC
GATGAGCCAGCAACTGTGGTGGACTTTCTGAGGAGATGGATAGCCTTCTGTCAAAGCATCATCTCAACAAGCCCTCA
ACACCATCACCACCATCACTGATAA

MRVPAQLLGLLLLWLPGARCEPRVPITQNPCPPLKECPPCAAPDLLGGPSVFIFPPKIKDVLMISLSPMVTCVVVAV
SEDDPDVQISWFVNNVEVHTAQTQTHREDYNSTLRVVSALPIQHQDWMSGKEFKCKVNNRALPSPIEKTISKPRGPV
RAPQVYVLPPPAEEMTKKEFSLTCMITGFLPAEIAVDWTSNGRTEQNYKNTATVLDSDGSYFMYSKLRVQKSTWERG
SLFACSVVHEGLHNHLTTKTISRSLGKGGGSAPTSSSTSSSTAEAQQQQQQQQQQQQHLEQLLMDLQELLSRMEDHR
NLRLPRMLTFKFYLPEQATELEDLQCLEDELEPLRQVLDLTQSKSFQLEDAENFISNIRVTVVKLKGSDNTFECQFD
DEPATVVDFLRRWIAFCQSIISTSPQHHHHHH

>Fc/E76A
ATGAGGGTCCCCGCTCAGCTCCTGGGGCTCCTGCTGCTCTGGCTCCCAGGTGCACGATGTGAGCCCAGAGTGCCCAT
AACACAGAACCCCTGTCCTCCACTCAAAGAGTGTCCCCCATGCGCAGCTCCAGACCTCTTGGGTGGACCATCCGTCT
TCATCTTCCCTCCAAAGATCAAGGATGTACTCATGATCTCCCTGAGCCCCATGGTCACATGTGTGGTGGTGGCCGTG
AGCGAGGATGACCCAGACGTCCAGATCAGCTGGTTTGTGAACAACGTGGAAGTACACACAGCTCAGACACAAACCCA
TAGAGAGGATTACAACAGTACTCTCCGGGTGGTCAGTGCCCTCCCCATCCAGCACCAGGACTGGATGAGTGGCAAGG
AGTTCAAATGCAAGGTCAACAACAGAGCCCTCCCATCCCCCATCGAGAAAACCATCTCAAAACCCAGAGGGCCAGTA
AGAGCTCCACAGGTATATGTCTTGCCTCCACCAGCAGAAGAGATGACTAAGAAAGAGTTCAGTCTGACCTGCATGAT
CACAGGCTTCTTACCTGCCGAAATTGCTGTGGACTGGACCAGCAATGGGCGTACAGAGCAAAACTACAAGAACACCG
CAACAGTCCTGGACTCTGATGGTTCTTACTTCATGTACAGCAAGCTCAGAGTACAAAAGAGCACTTGGGAAAGAGGA
AGTCTTTTCGCCTGCTCAGTGGTCCACGAGGGTCTGCACAATCACCTTACGACTAAGACCATCTCCCGGTCTCTGGG
TAAAGGAGGGGGCTCCGCACCCACTTCAAGCTCCACTTCAAGCTCTACAGCGGAAGCACAGCAGCAGCAGCAGCAGC
AGCAGCAGCAGCAGCAGCACCTGGAGCAGCTGTTGATGGACCTACAGGAGCTCCTGAGCAGGATGGAGAATTACAGG
AACCTGAAACTCCCCAGGATGCTCACCTTCAAATTTTACTTGCCCAAGCAGGCCACAGAATTGAAAGATCTTCAGTG
CCTAGAAGATGCTCTTGGACCTCTGCGGCATGTTCTGGATTTGACTCAAAGCAAAAGCTTTCAATTGGAAGATGCTG
AGAATTTCATCAGCAATATCAGAGTAACTGTTGTAAAACTAAAGGGCTCTGACAACACATTTGAGTGCCAATTCGAT
GATGAGTCAGCAACTGTGGTGGACTTTCTGAGGAGATGGATAGCCTTCTGTCAAAGCATCATCTCAACAAGCCCTCA
ACACCATCACCACCATCACTGATAA

MRVPAQLLGLLLLWLPGARCEPRVPITQNPCPPLKECPPCAAPDLLGGPSVFIFPPKIKDVLMISLSPMVTCVVVAV
SEDDPDVQISWFVNNVEVHTAQTQTHREDYNSTLRVVSALPIQHQDWMSGKEFKCKVNNRALPSPIEKTISKPRGPV
RAPQVYVLPPPAEEMTKKEFSLTCMITGFLPAEIAVDWTSNGRTEQNYKNTATVLDSDGSYFMYSKLRVQKSTWERG
SLFACSVVHEGLHNHLTTKTISRSLGKGGGSAPTSSSTSSSTAEAQQQQQQQQQQQQHLEQLLMDLQELLSRMENYR
NLKLPRMLTFKFYLPKQATELKDLQCLEDALGPLRHVLDLTQSKSFQLEDAENFISNIRVTVVKLKGSDNTFECQFD
DESATVVDFLRRWIAFCQSIISTSPQHHHHHH

>Fc/E76G
ATGAGGGTCCCCGCTCAGCTCCTGGGGCTCCTGCTGCTCTGGCTCCCAGGTGCACGATGTGAGCCCAGAGTGCCCAT
AACACAGAACCCCTGTCCTCCACTCAAAGAGTGTCCCCCATGCGCAGCTCCAGACCTCTTGGGTGGACCATCCGTCT
TCATCTTCCCTCCAAAGATCAAGGATGTACTCATGATCTCCCTGAGCCCCATGGTCACATGTGTGGTGGTGGCCGTG
AGCGAGGATGACCCAGACGTCCAGATCAGCTGGTTTGTGAACAACGTGGAAGTACACACAGCTCAGACACAAACCCA
TAGAGAGGATTACAACAGTACTCTCCGGGTGGTCAGTGCCCTCCCCATCCAGCACCAGGACTGGATGAGTGGCAAGG
AGTTCAAATGCAAGGTCAACAACAGAGCCCTCCCATCCCCCATCGAGAAAACCATCTCAAAACCCAGAGGGCCAGTA
AGAGCTCCACAGGTATATGTCTTGCCTCCACCAGCAGAAGAGATGACTAAGAAAGAGTTCAGTCTGACCTGCATGAT
CACAGGCTTCTTACCTGCCGAAATTGCTGTGGACTGGACCAGCAATGGGCGTACAGAGCAAAACTACAAGAACACCG
CAACAGTCCTGGACTCTGATGGTTCTTACTTCATGTACAGCAAGCTCAGAGTACAAAAGAGCACTTGGGAAAGAGGA
AGTCTTTTCGCCTGCTCAGTGGTCCACGAGGGTCTGCACAATCACCTTACGACTAAGACCATCTCCCGGTCTCTGGG
TAAAGGAGGGGGCTCCGCACCCACTTCAAGCTCCACTTCAAGCTCTACAGCGGAAGCACAGCAGCAGCAGCAGCAGC
AGCAGCAGCAGCAGCAGCACCTGGAGCAGCTGTTGATGGACCTACAGGAGCTCCTGAGCAGGATGGAGAATTACAGG
AACCTGAAACTCCCCAGGATGCTCACCTTCAAATTTTACTTGCCCAAGCAGGCCACAGAATTGAAAGATCTTCAGTG
CCTAGAAGATGGTCTTGGACCTCTGCGGCATGTTCTGGATTTGACTCAAAGCAAAAGCTTTCAATTGGAAGATGCTG
AGAATTTCATCAGCAATATCAGAGTAACTGTTGTAAAACTAAAGGGCTCTGACAACACATTTGAGTGCCAATTCGAT
GATGAGTCAGCAACTGTGGTGGACTTTCTGAGGAGATGGATAGCCTTCTGTCAAAGCATCATCTCAACAAGCCCTCA
ACACCATCACCACCATCACTGATAA

MRVPAQLLGLLLLWLPGARCEPRVPITQNPCPPLKECPPCAAPDLLGGPSVFIFPPKIKDVLMISLSPMVTCVVVAV
SEDDPDVQISWFVNNVEVHTAQTQTHREDYNSTLRVVSALPIQHQDWMSGKEFKCKVNNRALPSPIEKTISKPRGPV
RAPQVYVLPPPAEEMTKKEFSLTCMITGFLPAEIAVDWTSNGRTEQNYKNTATVLDSDGSYFMYSKLRVQKSTWERG
SLFACSVVHEGLHNHLTTKTISRSLGKGGGSAPTSSSTSSSTAEAQQQQQQQQQQQQHLEQLLMDLQELLSRMENYR
NLKLPRMLTFKFYLPKQATELKDLQCLEDGLGPLRHVLDLTQSKSFQLEDAENFISNIRVTVVKLKGSDNTFECQFD
DESATVVDFLRRWIAFCQSIISTSPQHHHHHH